Dissertations, Theses, and Masters Projects   Theses, Dissertations, & Master Projects

2016

Gas-Phase Thermochemical Properties of Proline-Containing Dipeptides and Fluorinated Alcohols using the Extended Kinetic Method

Kathy Tang Huynh

College of William & Mary - Arts & Sciences

Follow this and additional works at: https://scholarworks.wm.edu/etd

Part of the Physical Chemistry Commons

Gas-Phase Thermochemical Properties of Proline-Containing Dipeptides and
Fluorinated Alcohols Using the Extended Kinetic Method

Kathy Tang Huynh

Falls Church, Virginia

Bachelor of Science, College of William & Mary, 2014

A thesis presented to the Graduate Faculty
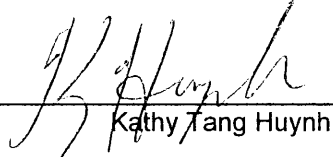of the College of William and Mary in Candidacy for the Degree of
Master of Science

Chemistry Department

The College of William and Mary
January 2016

APPROVAL PAGE

This thesis is submitted in partial fulfillment of the requirements for the degree of

Master of Science

Kathy Tang Huynh
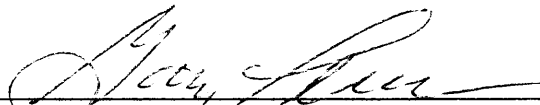
Approved by the Committee, January 2016

Committee Chair
Professor John C. Poutsma, Chemistry
The College of William and Mary

Professor Deborah C. Bebout, Chemistry
The College of William and Mary

Associate Professor Gary W. Rice, Chemistry
The College of William and Mary

ABSTRACT

The proton affinities of ten proline-containing dipeptides and the gas-phase acidities for three fluorinated compounds were determined using the extended kinetic method (EKM) and orthogonal distance regression (ODR) analysis. Kinetic method experiments were performed on a Thermo TSQ Quantum triple quadrupole mass spectrometer and a Thermo LCQ Deca quadrupole ion trap mass spectrometer, both equipped with an electrospray ionization source.

The ten proline-containing dipeptides had experimental proton affinities ranging from 951.7 ± 8.3 kJ/mol to 979.2 ± 20.3 kJ/mol, as determined from the triple quadrupole instrument. The three fluorinated analytes had experimental gas-phase acidities ranging from 1383.2 ± 9.5 kJ/mol to 1459.7 ± 12.0 kJ/mol, as determined from the triple quadrupole and ion trap mass spectrometers.

This is the first time that these thermochemical properties have been obtained for these analytes using the extended kinetic method. Thus, the experimental values were compared to *ab initio* calculations performed on the analytes. Comparison of the theoretical proton affinities to the experimental proton affinities for the proline-containing dipeptides show that the two sets of values are in agreement.

Gas-phase acidity experiments on the fluorinated compounds were carried out on both instruments and compared to the theoretical calculations. Taking into account the uncertainty values associated with each acidity value, the experimental values acquired from the triple quadrupole and ion trap mass spectrometers were in excellent agreement with each other.

TABLE OF CONTENTS

ACKNOWLEDGEMENTS

LIST OF TABLES

LIST OF FIGURES

Chapter 1. Introduction

1.1 Gas-Phase Ion Chemistry

Thermochemical properties are vital in the understanding of chemical compounds, as they affect species' reactivity, structure, and stability. Thermochemical studies can be performed in the solution-phase or in the gas phase. It can be argued that most compounds, especially those that are biologically relevant, are typically found in aqueous solvent therefore, solution-phase studies would be the most appropriate. However, the presence of solvent molecules introduces energetic and reactivity considerations that are not necessarily a result of the intrinsic properties of the compound of interest. As gas-phase studies investigate the intrinsic, or fundamental, properties of a molecule, they can be used to establish limits on reactivity or thermochemistry. In biological systems, gas-phase-like behavior of a species can be observed in places where solvent molecules are absent or in low concentrations. For example, hydrophobic regions of proteins exclude water and have dielectric constants that are far smaller than that of the bulk aqueous solution.[1] Gas-phase systems can also be used as models for understanding complex solvent effects.

Recently, there have been technological advances that have made it easier to study the gas-phase ion chemistry of biological compounds using mass spectrometry. The gas-phase thermochemical properties that can be investigated for a compound include ionization potentials, electron affinities, proton affinities, and gas-phase acidities. In our lab, we concentrate on proton transfer reactions, so the proton affinity and gas-phase acidity are the thermochemical properties of

interest.   In this thesis, proton affinities and gas-phase acidities have been determined for two sets of compounds. The proton affinity (PA) of a species is defined as the negative change in enthalpy of the protonation reaction, shown below. The gas-phase basicity for the reaction is the Gibbs' free energy of the

$$A + H^+ \rightarrow AH^+ \qquad\qquad -\Delta H_{rxn} = PA \qquad (1.1)$$

$$\Delta G_{rxn} = GPB$$
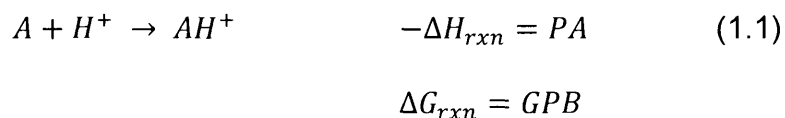
same reaction.[2] Similarly, the gas-phase acidity (GPA) of a species is defined as the Gibbs' free energy of the reaction shown below.

$$AH \rightarrow A^- + H^+ \qquad\qquad \Delta G_{acid} = GPA \qquad (1.2)$$

Fundamental properties such as these have been extensively studied over the decades by many groups using several different techniques, some of which will be described later in this chapter.[3]

1.2 Thermochemistry and Mass Spectrometry

The two projects presented in this thesis investigate the gas-phase properties of various species. As opposed to condensed-phase studies and properties, studying compounds in the gas phase allows us to obtain information about the intrinsic properties of a species. The presence of water or other solvents may interact with the species of interest in such a way that affects or changes the way a species behaves.

One example of conflicting gas-phase and solution-phase trends can be seen in the basicities for a set of methylamines. The gas-phase basicities for a set of methylamines was determined by Brauman et al. in 1971 to be NH_3 < $MeNH_2$ <

Me$_2$NH < Me$_3$N.[4] However, this trend differed from the basicities (pK$_b$) of the methylamines in solution, which was observed to be NH$_3$ < Me$_3$N < MeNH$_2$ < Me$_2$NH. A similar disparity is seen in the acidities of simple alcohols.[5] These examples highlight the importance of studying gas-phase, in addition to solution-phase properties.

Mass spectrometric studies of biological molecules have only been practical for the past few decades. Until the 1980s, all of the ionization sources available were "hard ionization" sources such as electron impact ionization. These sources, due to an excess in energy, would typically fragment the ions of interest upon ionization, making it difficult to study biomolecules as intact molecules.[6] Additionally, thermal lability and low volatility of the biological samples made them difficult to get into the gas phase as neutrals, making electron impact and chemical ionization approaches unsuitable.

In the late 1980s, with the advent of electrospray ionization (ESI)[7] and matrix-assisted laser desorption ionization (MALDI),[8] categorized as "soft ionization" sources, intact biomolecules could be studied using mass spectrometry. ESI, which will be described in detail in a later section, ionizes the species of interest with very little fragmentation, producing mainly protonated, or deprotonated, molecular ions.

1.3 Methods for Determination

Gas-phase thermochemical properties of compounds can be determined through a multitude of methods, influenced by the volatility of the analyte of

interest, purity of the sample, or the presence of competing reactions within the system, among others.[3] Absolute thermochemical properties for ions can be determined through energy-resolved threshold experiments, thermochemical cycles, and appearance potential measurements. These properties have been obtained for many compounds, which can then be used as anchors for the relative measurements described below.[3] However, it is often difficult to experimentally obtain the level of accuracy in appearance potential measurements to determine absolute properties and, as such, the majority of currently available values were obtained using techniques that measure relative thermochemical properties.[99] Fortunately, these techniques are well-developed.[3] The most commonly used methods are ion-molecule equilibrium constant determinations, one- and two-way bracketing reactions, and the kinetic method. Due to the instrumentation available in our lab, only relative measurements are performed.

1.3.1 Equilibrium

Ion-molecule equilibrium experiments are the most accurate of the relative methods for determinations of thermochemical properties.[3] These experiments utilize gas-phase reactions between a neutral molecule and an ion of interest. Equation 1.3 shows an equilibrium reaction that can be used to determine proton affinity.

$$A^+ + B \rightleftharpoons C^+ + D \qquad\qquad (1.3)$$

One introduces known pressures of two neutral molecules, B and D, and a source of protons into the source region of a high pressure mass spectrometer.[10]

When the system has reached equilibrium at a specific temperature, the equilibrium constant can be written in terms of the individual ion intensities and

$$K = \frac{[C^+][P_D]}{[A^+][P_B]} \qquad (1.4)$$

pressures. The equilibrium constant is determined by measuring the ratio of the ion concentrations, $[C^+/A^+]$ using the mass spectrometer, typically ion cyclotron resonance (ICR), high pressure mass spectrometry (HP MS), or flowing afterglow (FA) instruments. Additionally, the neutral species concentrations are acquired using the partial pressures for the species at equilibrium.

Alternatively, one can obtain an equilibrium constant by measuring, in separate experiments, the rate coefficients for the "forward" and "reverse" reactions of Equation 1.3. The equilibrium constant is obtained from Equation 1.5.

$$K = \frac{[C^+][P_D]}{[A^+][P_B]} = \frac{k_f}{k_r} \qquad (1.5)$$

The equilibrium constant can be related to the Gibbs' free energy for Equation 1.5 using the following relationship, $K = e^{-\Delta G/RT}$. If equilibrium constants are determined for the system at varying temperatures, a Van't Hoff plot can be created, $\ln(K_{eq})$ vs. T^{-1}, allowing ΔH and ΔS values for Equation 1.4 to be obtained.

Challenges with this technique arise in the ability to accurately determine the partial pressure of the neutral species and in achieving equilibrium in a timely fashion in the high pressure source. Additionally, an equilibrium constant near unity is normally required in order to obtain a useful ion ratio in HPMS experiments or in order to be able to measure rate coefficients in both directions. The advantage of using equilibrium experiments is the measurement of only a single

5

proton transfer reaction, which is not the case in bracketing and kinetic method studies.

1.3.2 Bracketing

Bracketing experiments have also been utilized for relative determinations of thermochemical properties.[3] Ion-molecule bracketing experiments involve proton transfer reactions between a protonated ion of interest and a set of reference compounds, as shown below in Equation 1.6 for a proton affinity study.

$$AH^+ + B \rightarrow A + BH^+ \tag{1.6}$$
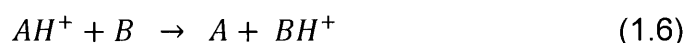
Bracketing experiments, first and foremost, assume that endothermic reactions do not occur in the gas phase, as there are no surrounding medium to provide the energy necessary to drive them. These ion-molecule reactions occur if the system has favorable energetics and if the species involved collide with the correct orientation.

The reference compounds have known thermochemical values and are used to determine the affinity for the analyte of interest. For example, a protonated analyte, AH^+, is reacted with a series of reference bases, B_i, and the occurrence or non-occurrence of proton transfer is noted for each pair. The efficiency of the reaction can also be measured in order to ascertain the proportion of collisions that lead to proton transfer. An efficiency of 50% implies a thermoneutral reaction, where it is equally likely for a colliding pair to proceed to products or to go back to reactants.

To achieve better results, two-way bracketing experiments can also be done. In these experiments, the reference compounds are the ionized species and the analyte of interest is the neutral species. Similarly, the occurrence or non-occurrence of proton transfer and the efficiency of the reaction are recorded. A second bracketing table is constructed and used to determine the proton affinity for the analyte of interest. As the proton affinities of the reference compounds increase, it becomes more likely that proton transfer will occur. An example of an ion-molecule bracketing table is shown below in Figure 1.

AH^+	+	B_1	✗		B_1H^+	+	A	✓
AH^+	+	B_2	✗		B_2H^+	+	A	✓
AH^+	+	B_3	✓		B_3H^+	+	A	✗
AH^+	+	B_4	✓		B_4H^+	+	A	✗
AH^+	+	B_5	✓		B_5H^+	+	A	✗

Figure 1. Ion-molecule bracketing table.

From the table above, proton transfer is observed when AH^+ is reacted with reference compounds B_3, B_4, and B_5, but not for B_1 or B_2. Thus, the experimental proton affinity for the analyte is said to be between those of B_2 and B_3. The experimental ΔH_{acid} value for the analyte is determined by taking the average ΔG_{acid} values of B_2 and B_3 and converting ΔG_{acid} to ΔH_{acid} using the $\Delta H_{acid} = \Delta G_{acid} + T\Delta S_{acid}$ relationship.

It is advantageous to use ion-molecule bracketing experiments if precise ion concentrations or pressure of the involved species cannot be determined. Additionally, this method is often used if equilibrium of a system cannot be reached or if a suitable anchor compound cannot be found.

7

1.3.3 Kinetic Method

The last of the commonly used methods for thermochemical determinations is the kinetic method, which was developed by R. Graham Cooks of Purdue University over thirty-five years ago.[11] The kinetic method uses known thermochemical values of reference compounds in addition to fragmentation data to determine that same thermochemical property of an analyte of interest.

The basis of the kinetic method comes from competitive dissociation of an ion-bound cluster ion. The cluster ions formed in this study are proton-bound heterodimers ions of an analyte and a reference compound. In kinetic method experiments, the heterodimer ion typically can dissociate in two ways, shown below.

$$AH^+ + B \;\leftarrow\; A - H^+ - B \;\rightarrow\; A + BH^+ \tag{1.7}$$
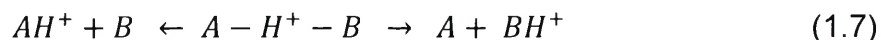
A potential energy surface for this system is shown in Figure 2.
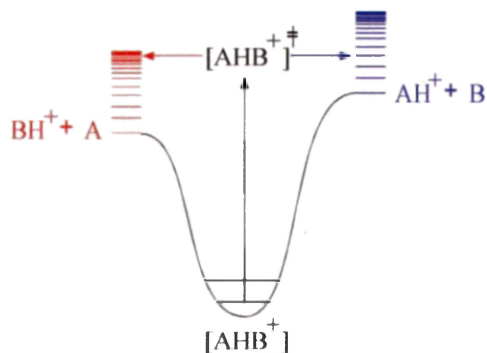
Figure 2. PES for proton-bound heterodimer.

To accurately perform a simple kinetic method experiment, a few assumptions need to be made. These include a negligible entropy difference between the two dissociation reactions, no contributing reverse activation energy barriers, and no interfering isomeric forms of the dimer.[11] If the assumptions are met, the kinetic method yields accurate, robust, and reproducible results.

Applying an activation energy to the heterodimer will result in fragmentation of the dimer as shown in the Equation 1.7 above. Using unimolecular reaction theory, the logarithm of the ratio of rate constants, k and k_i, can be expressed as shown in Equation 1.8,

$$\ln\left(\frac{k_i}{k}\right) = \ln\left(\frac{B_iH^+}{AH}\right) \approx \ln\left(\frac{Q_i^*}{Q^*}\right) + \frac{\Delta\epsilon_o}{RT_{eff}} \qquad (1.8)$$

where Q_i^* and Q^* are the partition functions of the transition states of the two channels, T_{eff} is the "effective temperature" of the reaction, and $\Delta\epsilon_o$ is the difference in critical energies for the two channels. Assuming again that there are no reverse activation barriers results in Equation 1.9.[11]

$$\ln\left(\frac{k_i}{k}\right) = \ln\left(\frac{B_iH^+}{AH}\right) \approx \frac{PA(B_i)-PA(A)}{RT_{eff}} + \frac{\Delta\Delta S}{R} \qquad (1.9)$$

$\Delta(\Delta S)$ refers to the entropy difference of the two fragmentation channels. The $\Delta(\Delta S)/R$ term can be cancelled if the compounds involved are structurally similar. A simple kinetic method analysis requires the construction of a plot of $\ln(k_i/k)$ vs. $PA(B_i)$ (Plot 1). The PA of the analyte is obtained from the x-intercept of Plot 1, i.e. where the $\ln(k_i/k) = 0$.

There are several advantages to using the kinetic method as opposed to the two methods mentioned previously. First, kinetic method determinations can be made quickly and performed on any tandem mass spectrometry system.[11] Second, there is a high degree of sensitivity and reproducibility in kinetic method data when compared to data from other methods. Lastly, non-volatile species and impure compounds can also be used. Limitations of the kinetic method come from the approximations and assumptions needed to apply it.

Modifications from the kinetic method later came from Fenselau,[12] Wesdemiotis,[13] and Armentrout,[14] addressing the structure similarity assumption and attempting to apply the kinetic method to larger biological molecules. The Fenselau and Wesdemiotis groups independently made it possible to accurately utilize the kinetic method in cases where the references were dissimilar in structure to the analyte. Their solution was to choose references that were similar to each other, but dissimilar to the analyte. This would create a non-zero entropy term, but the term would be constant.

In addition, one performs experiments at several varying temperatures and constructs a second kinetic method plot (Plot 2) of the negative of the intercepts vs. the slopes of best fit lines from Plot 1. The slope and intercept of Plot 2 are the enthalpies and protonation entropy of the analyte, respectively. These modifications are known as the "extended" kinetic method, EKM. For the projects in this thesis, the extended kinetic method was exclusively used.

Armentrout developed a modification that addressed the artificial dependency of the slope and intercept of the second kinetic method plot.[14] In this modification, instead of plotting ln(ratio) data versus the PA of the reference bases, one plots the ln(ratio) data vs. PA(Bi) - PA(avg), where PA(avg) is the average proton affinity of the entire set of reference bases. This plotting scheme assures that the y-axis is within the bounds of the fragmentation data and assures independence of the slopes and intercepts of the individual best-fit lines.

Chapter 1.4 Research Goals

Gas-phase thermochemical studies give insight into the intrinsic nature of compounds, without the effects of solvent molecules. Thermochemical properties of biologically relevant compounds have been studied for years in various Ionlab projects.[15-21] These projects include proton affinity[15-17,20,21] and gas-phase acidity determinations[18-21], peptide fragmentation studies[22], and hydrogen-deuterium exchange studies of amino acids analogs and small peptides.[23] Studies of the intrinsic properties of amino acids in the Ionlab have progressed to investigating dipeptides, specifically proline-containing dipeptides.

The goal of this study was to use the extended kinetic method to determine the proton affinities and gas-phase acidities of ten proline-containing dipeptides and three fluorinated alcohols, respectively. Product ion ratios after fragmentation were acquired using a Thermo TSQ Quantum Classic triple quadrupole mass spectrometer and a Thermo LCQ Deca quadrupole ion trap mass spectrometer. After extended kinetic method workup of the fragmentation data, further analysis was performed using orthogonal distance regression theory and experimental values were compared to theoretical calculations or literature values for the analytes, where possible.

Chapter 2. Experimental

The instrumentation used in this thesis included a Thermo TSQ Quantum Classic triple quadrupole mass spectrometer and a Thermo LCQ Deca quadrupole ion trap mass spectrometer. While there are differences among various types of mass spectrometers, all have five main components: a sample introduction inlet; an ionization source; a mass analyzer; a detector; and a way to analyze data, typically through a personal computer. For both mass spectrometers used, direct injection, electrospray ionization, and an electron multiplier were the method of sample introduction, ionization source, and detector, respectively. As the name implies, the Thermo TSQ Quantum Classic uses a triple quadrupole mass filter and the Thermo LCQ Deca uses an ion trap mass analyzer.

2.1 Electrospray Ionization

Both mass spectrometers used in this thesis are equipped with an electrospray ionization (ESI) source. As mentioned earlier, the advent of ESI enabled scientists to study and investigate biological compounds using mass spectrometry. ESI was first developed by John Fenn in 1988[24] and earned him the 2002 Nobel Prize in Chemistry for his contributions to the study of large biomolecules.

In this method of ionization, a high voltage is applied to a liquid sample, forming droplets, which are then desolvated using a drying gas and by passing the droplets through a heated capillary. Shown below is a figure outlining the components of an ESI source.
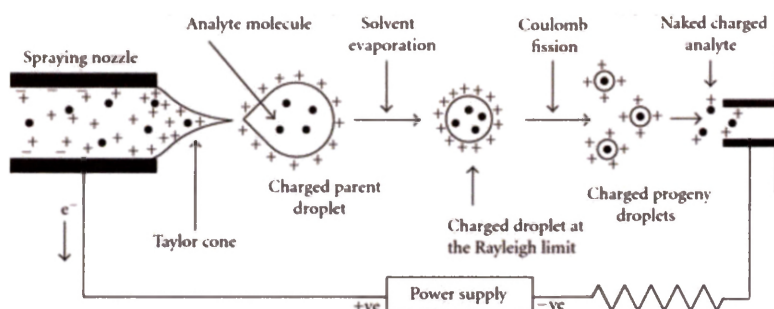
Figure 3. Electrospray Ionization Process. (Figure reprinted from

http://www.hindawi.com/journals/ijac/2012/ 282574/fig6/)

First, the sample is passed through a capillary needle, to which a voltage, typically between 4-5 kV, is applied. Passing through the charged needle nebulizes the sample, forming charged droplets containing the ions of interest. An inert drying gas, typically nitrogen or carbon dioxide, is used to desolvate the droplets. As evaporation occurs and the droplets become smaller in size, the charge density of the droplets increases. The Coulombic repulsion between the like charges increases until the surface tension of the droplet can no longer support the charge density; this point is known as the Rayleigh limit. Once the droplets surpass this limit, they split into smaller charged droplets through a process called Coulombic fission. The desolvation also continues through the heated capillary, which is heated between 75-350°C. Finally, the ions emerge from the heated capillary and proceed toward the mass analyzer.

2.2 Instrumentation

2.2.1 Thermo TSQ Triple Quadrupole Mass Spectrometer

The majority of the experimental data for this thesis was acquired using a Thermo TSQ Quantum Classic triple quadrupole mass spectrometer equipped

with an electrospray ionization source. The triple quadrupole instrument is a tandem mass spectrometer, which performs multiple mass spectrometry experiments "in space." "In space" refers to the spatial difference of the mass analyzers used for ion isolation and fragmentation. The associated software for this instrument is Quantum Tune, run using a desktop computer connected to the mass spectrometer.

Sample introduction is accomplished using a 500µL Hamilton gastight syringe, inserted into the syringe pump of the instrument, which controls the flow rate of the solution into the mass spectrometer. For this project, the flow rate was kept between 7 and 10 µL/min. The solution is passed through PEEK and fused-silica capillary tubing and is introduced into the ESI source and ionized using the process described above. Once ionized, the stream of ions travel through the heated capillary and into the mass spectrometer. The heated capillary, initially set at 125°C, was changed throughout the study to optimize the ion intensity of the heterodimer.

It is necessary for all components of the triple quadrupole system to be under vacuum, which necessitates differential pumping. An external rotary-vane pump brings the pressure of the system down to 10^{-3} Torr and a turbomolecular pump within the instrument brings the pressure down to pressures as low as 10^{-6} Torr. The ions are carried through several sets of focusing lenses until they reach the quadrupole mass analyzers. This instrument uses three quadrupole mass analyzers to scan and filter ions of a specific mass-to-charge (m/z) ratio. A diagram of a triple quadrupole mass analyzer is shown below.
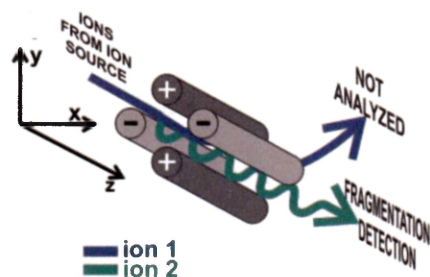
Figure 4.   Triple quadrupole mass analyzer. (Figure reprinted from

http://cdn.intechopen.com/pdfs-wm/44881.pdf)

A quadrupole mass filter consists of four rods organized such that if the center of the rods is the z-axis, two rods lie along the xz-plane while the other two lie along the yz-plane. Radio-frequency (RF) and direct current (DC) potentials are alternately applied to opposing rods and are modified to filter for a specific m/z ratio. For each set of RF and DC voltages, there is an associated mass stability region for which one m/z ratio will maintain a stable trajectory through the rods to reach the detector. All other ions will be unable to maintain a stable trajectory and will not reach the detector. The first and third quadrupoles, termed Q1 and Q3, respectively, are powered by alternating RF and DC potentials while the second quadrupole, Q2, is typically used as a collision cell and, as such, is only subject to an RF potential, which aids in transmitting parent and product ions into Q3.

The triple quadrupole system enables four different scan types: product scan, parent scan, neutral loss scan, and energy-resolved mass spectrometry, ERMS. For kinetic method experiments, data was acquired using the product scan mode. Using this mode, Q1 is fixed to isolate a particular m/z ratio and Q2 is used to fragment the selected ion. Within Q2, argon is used as a neutral collision gas and the selected ions are allowed to undergo collision-induced dissociation (CID)

at varying collisions energies. The third quadrupole then performs a scan, producing a mass spectrum of the fragment ions.

2.2.2 *Thermo LCQ Deca Quadrupole Ion Trap Mass Spectrometer*

Data was also acquired using a Thermo LCQ Deca quadrupole ion trap mass spectrometer equipped with an electrospray ionization source. Unlike the triple quadrupole instrument, ion trap mass spectrometers perform tandem mass spectrometry "in time." In this case, there is a temporal difference for each mass spectrometry experiment, with all experiments being performed in the same physical space. The associated software for the ion trap is LCQ Tune, also run using a desktop computer connected to the mass spectrometer.

Sample introduction for the ion trap is done using a 500µL Hamilton gastight syringe connected to an external syringe pump. Like the triple quadrupole, the solution is passed through PEEK tubing and fused-silica capillary tubing, where it is introduced into the ionization source. The heated capillary for the ion trap was initially set to 125°C and then modified to optimize the heterodimer ion peak intensity. After gas-phase ions are formed, they are focused through various lenses and ion guides until the ions enter the ion trap mass analyzer. Two external rotary-vane pumps bring the pressure of the system down to 10^{-3} Torr and a turbomolecular pump within the instruments brings the pressure down to pressures as low as 10^{-5} Torr.

The ion trap mass analyzer consists of two end cap electrodes and a ring electrode, situated in the configuration shown in the figure below.
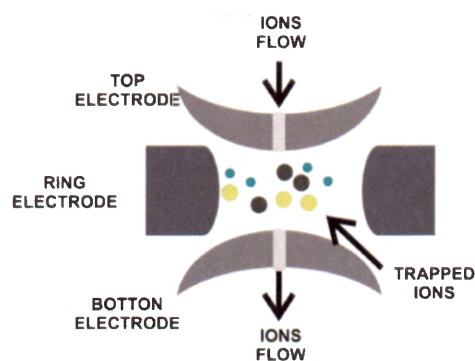
Figure 5. Ion trap mass analyzer. (Figure reprinted from

http://cdn.intechopen.com/pdfs-wm/44881.pdf)

The ions enter and exit the trap through the end cap electrodes, and are "trapped" due to the voltages being applied to the electrodes. In order to detect ions of a particular mass-to-charge ratio, the voltages of the electrodes are modified such that the ion of interest will no longer be stable in the trap. The ions will then exit the trap through the end cap electrode and proceed to the detector. To isolate ions, the electrode voltages are modified such that all ions are unstable except for the desired ion of interest. These ions can then be allowed to undergo CID with the background helium buffer gas and a product ion scan can then be performed.

2.3 Methodology

As experiments using experiments using Cooks' kinetic method have become ubiquitous in determinations of thermochemical properties, a robust protocol has been developed and used by multiple research groups. Ionlab projects involving the kinetic method have followed this procedure, with some modifications for optimized ion count and dimer formation.[25]

As mentioned in Chapter 1, the kinetic method uses reference compounds with a known thermochemical value to determine the relative value for an unknown compound. Thus, the starting point of any kinetic method study is to find appropriate reference compounds to form the proton-bound cluster ions. Predicted values for analytes can be acquired through theoretical calculations or by analyzing trends between groups of compounds. An ideal set of references would be comprised of four to eight reference compounds, each with a known affinity value within 15 kJ/mol above or below the theoretical affinity. Hundreds of gas-phase properties of compounds, including proton affinities and gas-phase acidities, have been cataloged in an online database, available on the National Institute of Standards and Technology (NIST) website, in the Chemistry Webbook.[26] Once the references have been chosen, stock solutions of 10^{-2} M and 10^{-4} M dilutions are created for the analyte and all reference compounds.

The dimer solutions injected into the mass spectrometer are created using 1:1 by volume ratios of the analyte and reference compound with the addition of either formic acid or ammonium hydroxide to promote ion formation. The concentrations used for the analyte and reference compound solutions are 10^{-3} M for negative ion mode studies to 10^{-4} M for positive ion mode studies. For the acidity project, the optimal ammonium hydroxide concentration was found to be between five and ten percent. One percent formic acid was used for the proton affinity project. Additionally, optimization of the instrumentation conditions for each run was done by modifying the heated capillary temperature, flow rate, sheath gas pressure, concentrations of the dimer components, or through the tuning option of

18

the Quantum Tune and LCQ Tune software programs. Optimization was performed with the intention of achieving the highest heterodimer peak ion count possible. An ideal isolated heterodimer ion count is between 10^5 and 10^6 arbitrary units when in positive ion mode whereas negative ion heterodimers are typically an order of magnitude or two lower.

Lastly, the dimer solutions are injected into the mass spectrometers and data is acquired using the two software programs. In the following sections, data acquisition procedures for both the triple quadrupole and ion trap mass spectrometers will be described.

2.4 Data Acquisition

2.4.1 TSQ Quantum Triple Quadrupole

All experimental data for the proton affinity project and a portion of the data for the gas-phase acidity project were obtained from the Thermo TSQ Quantum Classic triple quadrupole mass spectrometer. In the following two sections, data acquisition procedures are described as it applies to proton affinity measurements, with modifications when investigating gas-phase acidities described after. Dimer solutions were prepared using the procedure described above, using concentrations of 10^{-4} M and 1% formic acid when in positive ion mode and 10^{-3} M and 5-10% ammonium hydroxide when in negative ion mode.

In positive ion mode, expected peaks upon injection of the solutions in full scan mode included the heterodimer, protonated analyte, protonated reference, and homodimers comprised of the analyte or reference. Conversely, negative ion mode spectra will include the heterodimer, deprotonated analyte and reference, and homodimers comprised of the analyte or reference. That being said, the only peak of interest is the heterodimer peak, which was optimized and isolated. A spectrum of dimer isolation is shown below, for the proton-bound heterodimer of hexafluoro-2-propanol and ethoxyacetic acid.
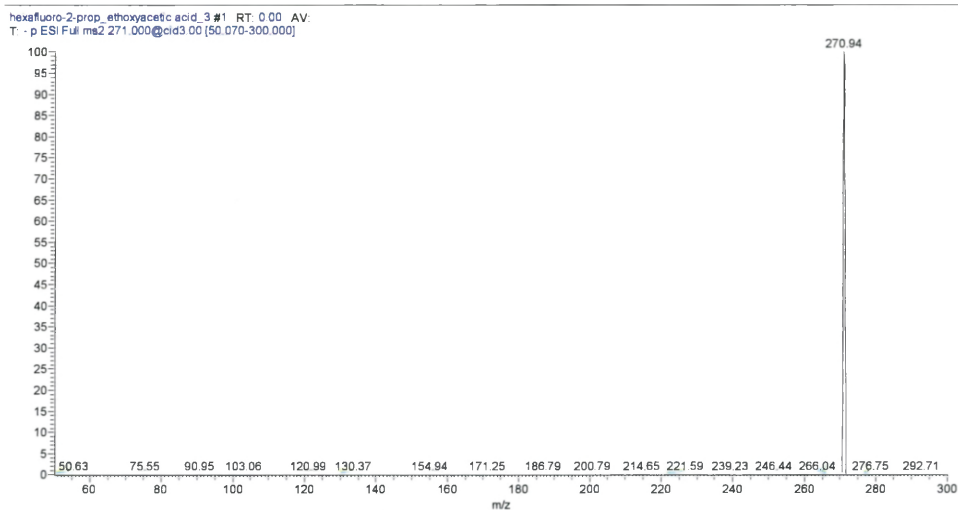

Figure 6. Isolation spectrum for Hexafluoro-2-propanol:Ethoxyacetic acid.

Once successfully isolated, the dimer solution is allowed to fragment via collision-induced dissociation (CID), where an inert gas, argon, is introduced into the stream of gas-phase cluster ions in Q2. The dimer ions are allowed to fragment over a range of collision energies, from 0 - 45 V (lab). Collision energies can be determined using lab frame or center of mass (COM) frame. Lab frame collision energies are instrument-dependent while COM frame energies include the masses of the collision gas and ion of interest. The relationship between the two is shown

20

by the equation below, where M is the mass of the ion and m is the mass of the collision gas.

$$E_{CM} = E_{lab} \left(\frac{m}{M+m} \right) \tag{2.1}$$

The collisions between these molecules result in fragmentation of the dimer ions, spectra for which are obtained for collision energies starting from 0 V, and collected in increments of 3 V. For the proton affinity project, spectra were collected from 0 - 30 V and from 0 - 45 V for the acidity project.

Typically, kinetic method experiments use collision energies from 0 - 30 V. This range resulted in the fragmentation of the heterodimer ions in addition to a ln(ratio) vs. collision energy plot that approached 0, as shown in Figure 7. Recalling the potential energy surface for the proton-bound heterodimer, as the collision energy increases, the density of states increases in both channels and become more alike, yielding a product ion ratio of 1 and a natural log ratio of 0.
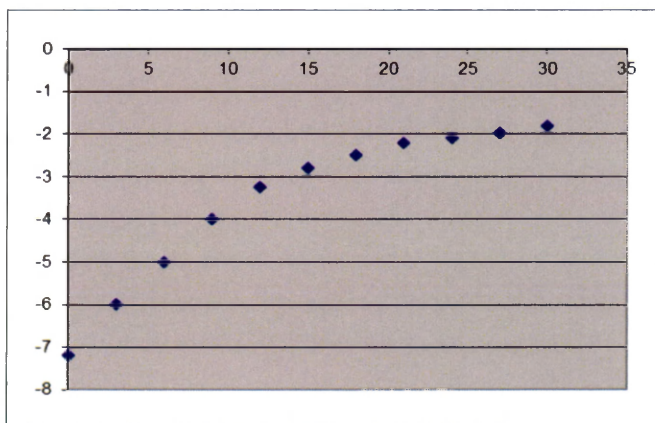

Figure 7. Natural log ratios vs. collision energies.

Plots like the one above were observed for the analytes used in the proton affinity project. However, for the fluorinated alcohols, appropriate ln(ratio) vs.

collision energy plots were achieved when increasing the collision energy range to 45 V.

Additional parameters included: argon CID pressure at 0.3 arbitrary units, Q1 and Q3 peak width at 0.7 amu, and a scan time of 20 scans. All parameters are modified using the Quantum Tune software. Three days of fragmentation data are acquired for each dimer solution, and subsequently averaged and analyzed using the extended kinetic method workup procedure. A fragmentation spectrum for the hexafluoro-2-propanol:ethoxyacetic acid dimer at a collision energy of 45 V is shown below in Figure 8.
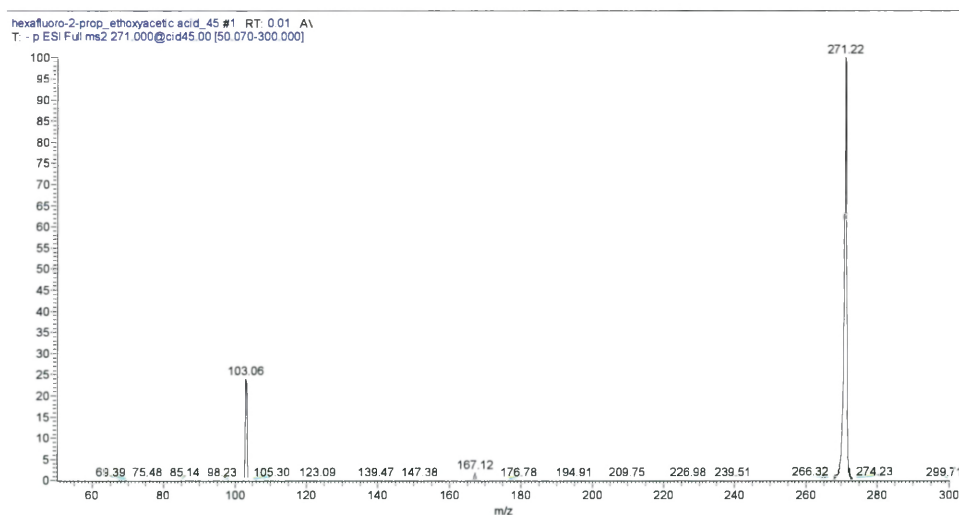

Figure 8. Fragmentation spectrum for Hexafluoro-2-propanol:Ethoxyacetic acid.

2.4.2 LCQ Deca Quadrupole Ion Trap

Additional kinetic method experiments for the acidity project were performed on the Thermo LCQ Deca quadrupole ion trap mass spectrometer. Dimer solutions were made from 10^{-3} M stock solutions and 5-10% ammonium hydroxide. Sample introduction and the expected peaks are identical for the ion

trap compared to the triple quadrupole instrument. Once the solution is injected and present in the full scan, the dimer ion is isolated, using a peak width of 5 m/z. Modifying this parameter will increase or decrease the range of stable m/z ratios that reach the detector. Additional parameters relevant to isolation, which are all modified using the LCQ Tune software, include the activation time, which is set at 30 milliseconds, activation Q at 0.250, and a scan time of 2 microscans with a maximum inject time of 400 milliseconds.

After a sufficient dimer ion count is achieved, the dimer ions are allowed to undergo collision-induced dissociation with helium as the collision gas. Fragmentation data of the cluster ions is acquired by performing a normalized collision energy scan. This type of scan takes into account the mass of the target ion when applying collision energy. Then, a user-specified percentage of the available 5 V is applied to the target ion; in this way, ions with a larger m/z ratio receive a higher, but proportionate amount of collision energy. This allows for sufficient fragmentation of ions over a large m/z range. After inputting the parent and product ions of interest, the dimer ions are fragmented from 0 to 100 arbitrary units, using a step size of two.

The scan outputs a graph, such as the one shown below in Figure 9, plotting the intensity of the product ions of interest as a function of normalized collision energy. For example, three ions of interest (heterodimer, protonated analyte, and protonated reference) are input as ion intensities to be recorded. The ion intensities of any secondary fragments can also be recorded. Multiple scans were obtained and averaged for each dimer solution and three days of fragmentation

23

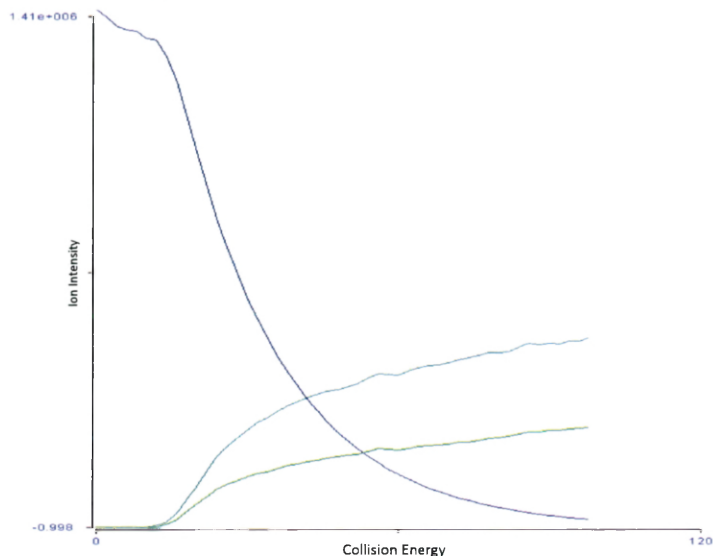data were acquired and analyzed. An example of a normalized collision energy scan is shown below in Figure 9.

Figure 9. Normalized Collision Energy scan.

2.5 Extended Kinetic Method Workup

Workup of the raw experimental data is done using Microsoft Excel and spectra are viewed through Qual Browser. To determine the proton affinity of the analyte, two kinetic method plots are created. The first kinetic method plot for Pro-Asp, shown below, is of $\ln(B_iH^+/AH^+)$ vs. $PA_{Bi} - PA_{avg}$. For gas-phase acidity experiments, the x-axis of the first kinetic method plot is $GPA_{Bi} - GPA_{avg}$.
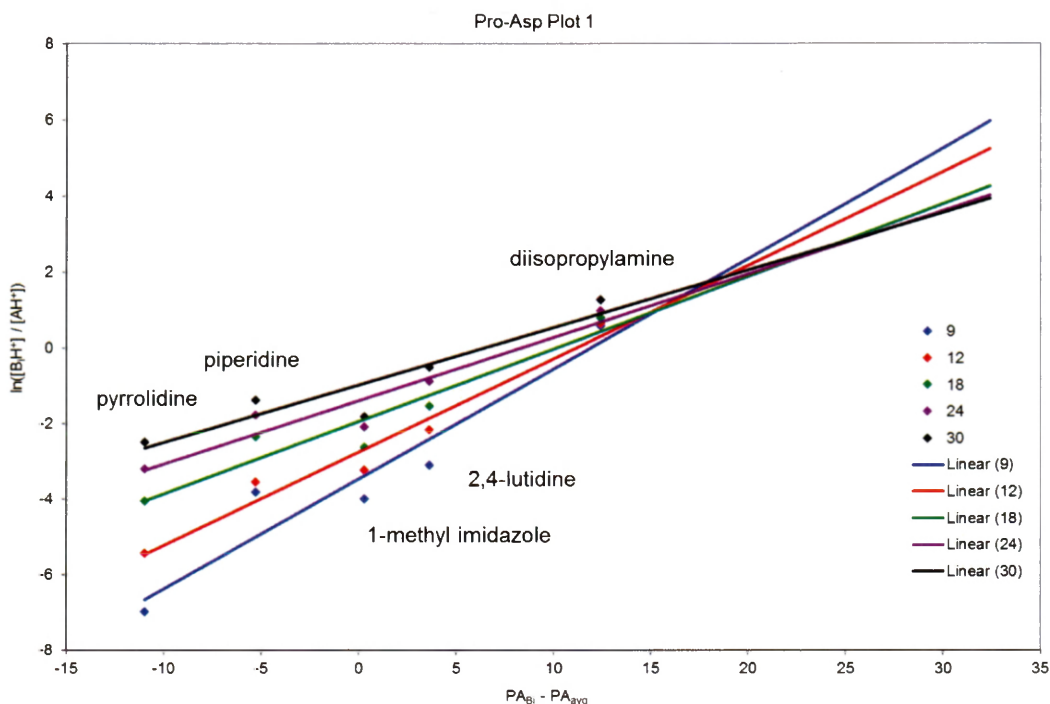
24

Figure 10. Kinetic Method Plot 1 for Pro-Asp.

The key components of kinetic method plot 1 are the lines, clusters of points, and the intersection point of the lines. The lines correspond to a specific collision energy and the clusters of points correspond to the product ion ratios of a specific dimer solution. The intersection point, known as the isothermal point, is the point at which the equilibrium constant is equal for all effective temperatures. A sign of precise data is the presence of an isothermal point in the first kinetic method plot.

In the kinetic method workup, not all of the collision energies are used in the analysis, and even fewer are plotted, for clarity purposes. Finding a useful range of collision energies is done by looking at the effective temperature plot, shown in

25

Figure 11. The region of the plot with the most steeply rising slope is included in the kinetic method workup. In the case of Pro-Asp, that region is from 6 to 30 V.
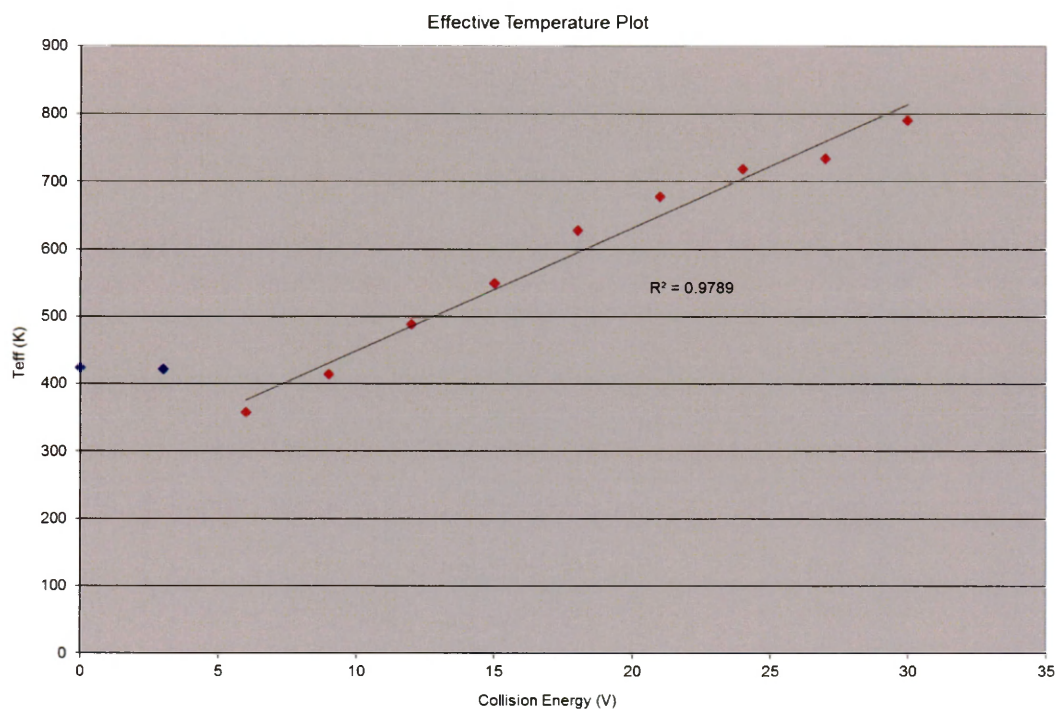

Figure 11. Effective Temperature Plot for Pro-Asp.

Additional plots are created to visualize the robustness of the fragmentation data and references chosen.   The second kinetic method plot for Pro-Asp, shown in Figure 12 below, is of the negative intercept vs. slope of each of the best-fit lines from the first kinetic method plot. This plot is used to obtain the crossing point of those lines, the isothermal point.
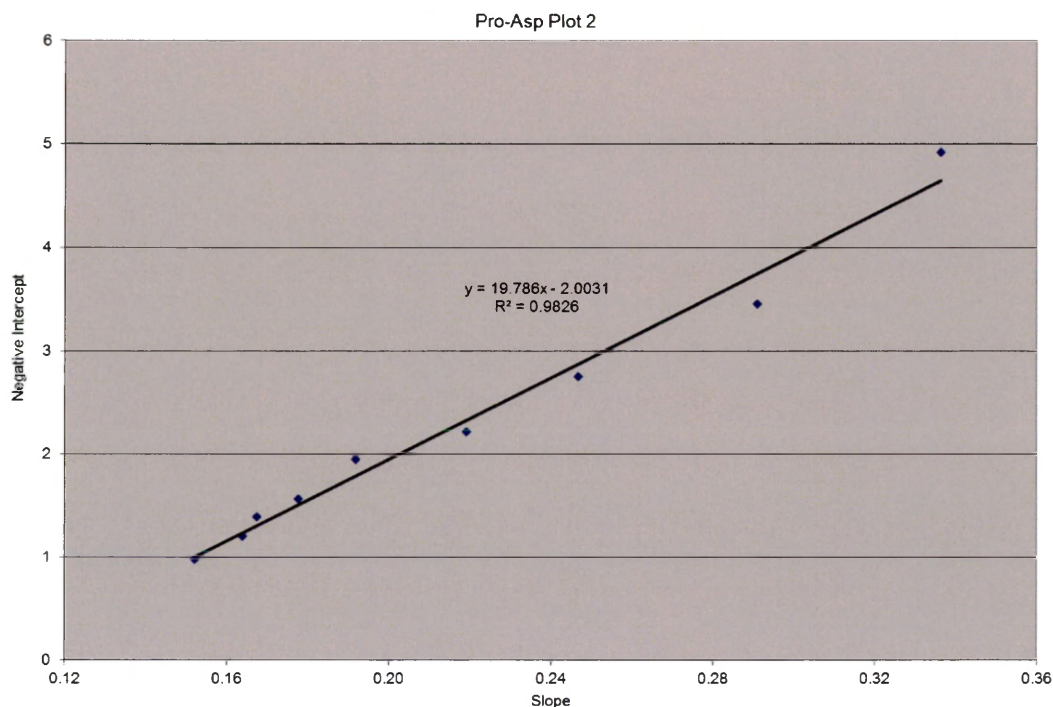
Figure 12. Kinetic Method Plot 2 for Pro-Asp.

2.6 Orthogonal Distance Regression Theory

The final analysis technique utilized in the kinetic method experiments is orthogonal distance regression (ODR) analysis. Developed by Ervin and Armentrout in 2004, ODR analysis removes the dependence of the isothermal point on the individual effective temperature lines.[27] The kinetic method analysis creates best-fit lines for each collision energy and the isothermal point is obtained from the theoretical intersection of these lines. Implemented using the ODRPACK Fortran package, ODR analysis forces all collision energy lines to intersect at the isothermal point.

Lastly, Monte Carlo simulations are performed on the experimental data, to ascertain uncertainty values for the derived thermochemical properties. In these simulations, errors of ± 2 kJ/mol and ± 8 kJ/mol are imposed on the proton affinities

27

or gas-phase acidities of the reference compounds and the ± 0.05 the ln(ratio) measurements. These error values attempt to account for the error in the measurements themselves, resulting in a 95% confident in the experimental results.

After ODR analysis is performed on a set of data, a second KM Plot 1 is created using the values output by the ODR package. Shown below in Figure 13 is the ODR KM Plot 1 for Pro-Asp.
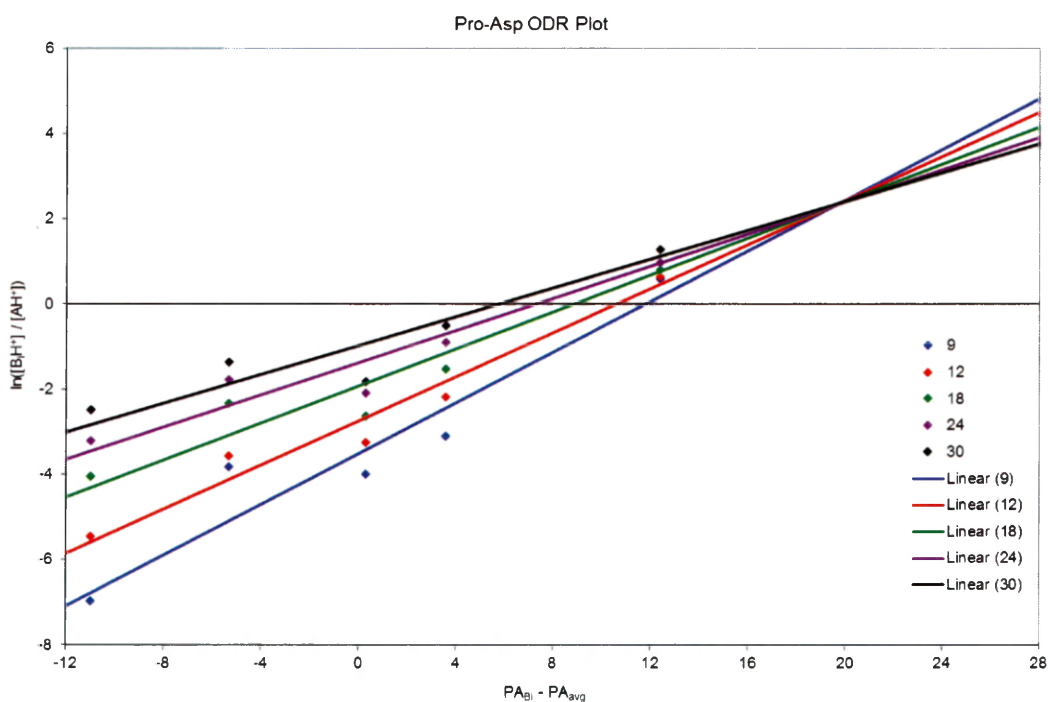

Figure 13. ODR Kinetic Method Plot 1 for Pro-Asp.

2.7 Computational Theory

In addition to experimental values, theoretical values are extremely helpful in providing validation or additional insight into the acid-base properties of a species. For many Ionlab projects, PCModel[28] and the Gaussian98[29] suite of programs have been used to determine theoretical proton affinities and protonation

sites for the analytes of interest. Similarly, theoretical gas-phase acidities and deprotonation sites have also been determined. While I did not perform any of the theoretical calculations, these predictions guided the choice of reference compounds and supported our comparisons to experimental values.

The GMMX conformation search function of PCModel is initially used to determine the lowest-energy conformers for the neutral, protonated, or deprotonated forms of the analyte. The Gaussian98 suite of programs performs density functional theory (DFT) calculations to determine the vibrational frequencies and single-point energies at a specific basis set. For the proton affinity project, single-point energies were determined at the basis set B3LYP/6-31+G*.[30,31] The gas-phase acidity values were performed at the B3LYP/aug-cc-pVTZ basis set by the Morton group.

Single-point energy values and the vibrational frequencies, in addition to the zero-point energies and thermal enthalpy corrections, are used to determine the proton affinity or gas-phase acidity for the analyte.

Chapter 3. Proton Affinity Project

3.1 Protein Amino Acids

Amino acids have great biological importance as the building blocks of peptides and, ultimately, proteins.[32] They have a variety of functions, from neurotransmitters to intermediates in biochemical species. There are twenty protein amino acids (PAAs) which are used to synthesize proteins in the human body. These PAAs can form dipeptides as a product of a condensation reaction between two amino acids.[33] It is important in the study of proteins and other biologically relevant compounds to understand the properties of smaller amino acids and peptides.

3.1.1 Acid-Base Properties of PAAs

This study is part of a larger project investigating the effects of small structural changes on the thermochemical properties of PAAs and other compounds. These changes include modifying the analyte of interest with the addition of amino acid residues to form small peptides from individual amino acids, or replacing the proline residue with one of its NPAA-analogs, azetidine-2-carboxylic acid (Aze) and pipecolic acid (Pip), proline's four- and six-membered ring analogs.[34] These studies will shed light on how the thermochemical properties of individual amino acids are affected when inserted into small peptides and upon small, systematic structural changes.

Past Ionlab projects have investigated the thermochemistry of the twenty standard amino acids and looking at dipeptides is an extension of this overall

study. In 2007, Poutsma et al. reported gas-phase acidities values for all twenty protein amino acids.[18] Ionlab projects have also investigated intrinsic properties of amino acid homologs using the extended kinetic method.[15,16,19] Additionally, while the standard amino acids have been studied fairly extensively with regard to their thermochemistry, little research has been done on the proton affinities and gas-phase acidities of dipeptides.

Some recent research involves gas-phase basicity determinations for various dipeptides, in some cases, containing proline.[35-38] In 1993, Gorman et al. determining the gas-phase basicities for Pro-Val and Val-Pro to be 928.4 ± 12.1 kJ/mol and 936.0 ± 7.9 kJ/mol, respectively.[35] A few years later, Ewing et al. determined the gas-phase basicities for Pro-Gly and Gly-Pro to be 916 kJ/mol and 898.7 kJ/mol, respectively.[38] Cassady et al. determined the gas-phase basicities of several di- and tripeptides involving alanine and glycine.[37] Lastly, additional gas-phase basicities for Gly-Ser, Ser-Gly, and Ser-Ser were determined by Cassady et al.[36]

Further research into the thermochemical properties of dipeptides, particularly the proline-containing dipeptides, is the main goal of the proton affinity study. More recently, Ionlab studies have focused on proline and proline analogs, especially once incorporated into small peptides. As one of the twenty protein amino acids, a structural feature that sets proline apart is that the amino terminus is within a ring. Figure 14 shows the structure of proline.
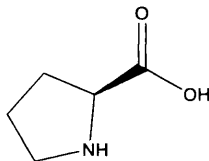
Figure 14. Proline structure.

This feature causes a phenomenon known as the "proline effect,"[39-49] which the Ionlab has also begun to investigate using peptide fragmentation studies.[22] The proline effect has been observed in peptides containing a proline residue, where upon tandem mass spectrometry experiments, enhanced fragmentation at the N-terminal of proline has been observed in the mass spectrum.[39-49]

Studies by Wysocki et al. have observed an over-representation in N-terminus fragments of proline in Xxx-Pro dipeptides, as opposed to Pro-Xxx dipeptides.[48] It has been proposed that this observation is a result of a combination of energetic and structural effects. Proton affinity studies of these proline-containing dipeptides may give insight as to the energetic components of the "proline effect."

Proton affinity measurements using the extended kinetic method involve the most basic site of a molecule, which is also the protonation site. In the case of proline as opposed to other amino acids, that site is a secondary amine, which is more basic than a primary amine. From this, one can infer that the proton affinity for a Pro-Xxx dipeptide to be more basic and have a higher proton affinity, than its analogous Xxx-Pro dipeptide. Similarly, it can also be inferred that Pro-Xxx dipeptides will have overall higher proton affinities than Xxx-Pro dipeptides.

3.1.2 Analytes

Of the thirty-nine total proline-containing dipeptides available for study, proton affinities for ten dipeptides are presented in this thesis: Pro-Ala, Pro-Asp, Pro-Gly, Pro-Leu, Pro-Phe, Pro-Val, Ala-Pro, Gly-Pro, Leu-Pro, and Phe-Pro. Structures for the analytes are shown below in Figures 15 and 16. All analytes are commercially available for purchase and, as such, were the initial analytes investigated. Future work will include solid-phase peptide synthesis and proton affinity determinations by extended kinetic method of the remaining dipeptides unavailable for commercial purchase.

Pro-Ala   Pro-Asp

Pro-Gly   Pro-Leu

Pro-Phe   Pro-Val
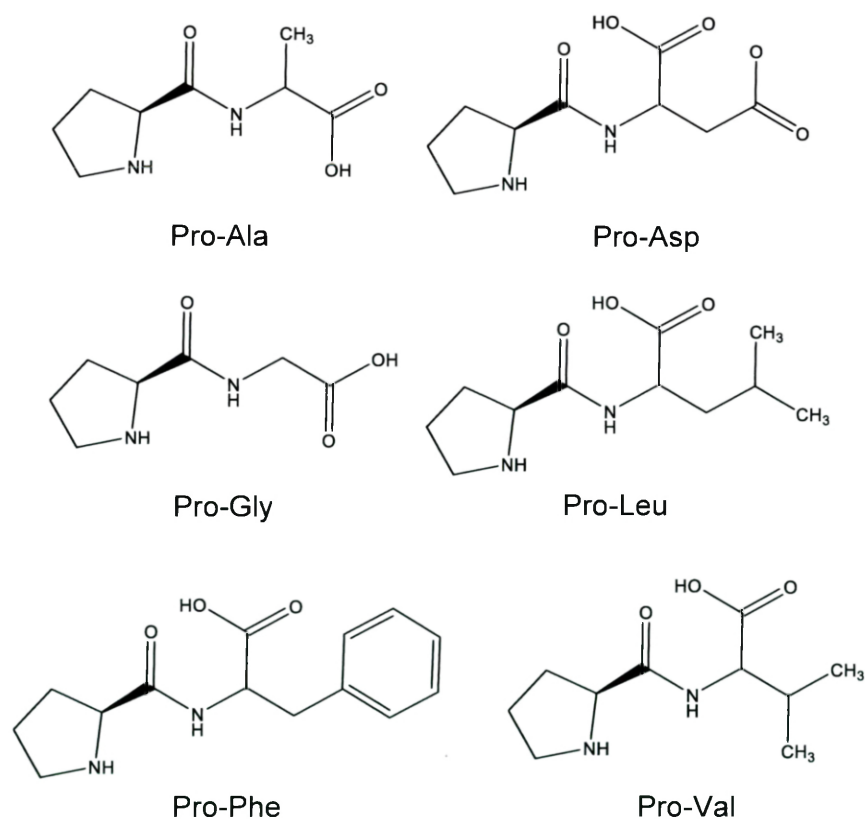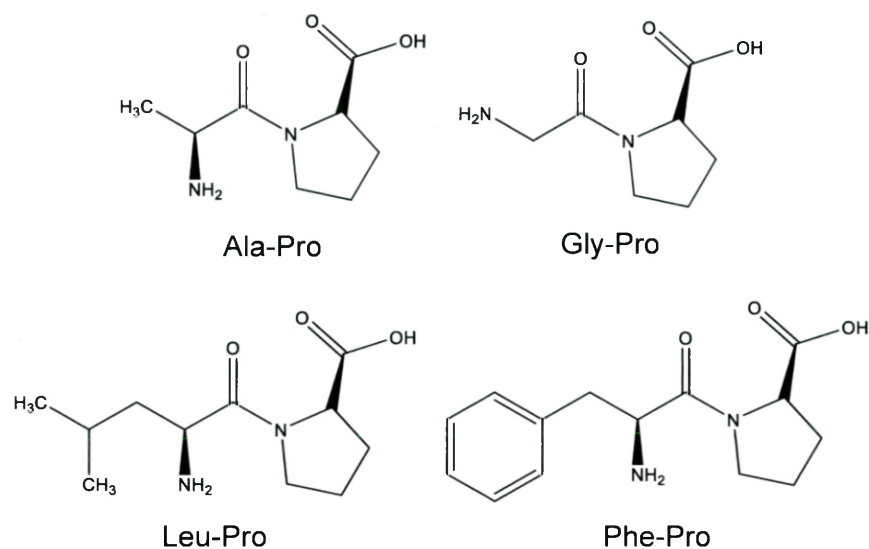
Figure 15. Pro-Xxx structures.

Figure 16. Xxx-Pro structures.

3.2 Reference Bases

An appropriate set of reference bases for the proton affinity study was found using the NIST Chemistry Webbook, and are listed in Tables 1 and 2 below, along with their respective proton affinities.[3] These table show the references used for each analyte. From a cursory glance at the overlap between reference bases and analytes, it can be seen that the analytes will have similar proton affinities.

Reference Base	PA (kJ/mol)[3]	Pro-Gly	Pro-Val	Pro-Ala	Pro-Phe	Pro-Leu	Pro-Asp
Pyrrolidine	948.3	X	X	X	X	X	X
Piperidine	954.0	X	X	X	X	X	X
4-tertbutyl pyridine	957.7			X			
1-methyl imidazole	959.6				X	X	X
N,N-diethylaniline	959.8	X	X				
2,4-lutidine	962.9			X	X	X	X
1-methyl pyrrolidine	965.6	X	X				
1-methyl piperidine	971.1					X	
Diisopropylamine	971.7	X	X	X	X		X

Table 1. Reference Compounds for Pro-Xxx Dipeptides.

34

Reference Base	PA (kJ/mol)[3]	Gly-Pro	Ala-Pro	Leu-Pro	Phe-Pro
Pyridine	930.0	X	X		
Pyrrolidine	948.3	X	X		
Ethylenediamine	951.6			X	
Piperidine	954.0	X	X		X
4-tertbutyl pyridine	957.7			X	
1-methyl imidazole	959.6	X	X		X
2,4-lutidine	962.9		X		X
1-methyl pyrrolidine	965.6			X	
1-methyl piperidine	971.1			X	
Diisopropylamine	971.7			X	X

Table 2. Reference Compounds for Xxx-Pro Dipeptides.

3.3 Results

3.3.1 Experimental Results

Proton affinities for the ten proline-containing dipeptides were analyzed using extended kinetic method workup and orthogonal distance regression theory. Fragmentation data was collected for the triple quadrupole using a range of collision energies from 0 to 30 V. EKM workup involved analysis of the product ion ratios at each collision energy for each dimer solution for determination of the collision energies included in the final analysis. This resulted in collision energies from 6 to 30 V being included in the final EKM and ODR analysis. Tabulated results for each analyte are shown below.

Analyte	Experimental PA (kJ/mol)	Theoretical PA (kJ/mol)[‡]
Pro-Gly	968.7 ± 11.9	966.1
Pro-Val	970.6 ± 12.6	
Pro-Ala	974.7 ± 15.5	973.2
Pro-Phe	975.1 ± 16.0	
Pro-Leu	973.2 ± 17.5	
Pro-Asp	979.2 ± 20.3	
Gly-Pro	951.7 ± 8.3	
Ala-Pro	962.0 ± 9.8	
Leu-Pro	966.8 ± 8.8	
Phe-Pro	968.2 ± 10.8	

[‡] Computations performed by Poutsma, unpublished.

Table 3. Results for Proline-Containing Dipeptides.

In the following sections, kinetic method results for proton affinity determinations of ten proline-containing dipeptides are presented. A detailed explanation of the data and graphs are included for Pro-Asp, and the ODR-analyzed first kinetic method plot and second kinetic method plot are included for the remaining dipeptides. The graphs not included in this chapter are presented in the Appendix.

3.3.1.1 Pro-Asp

Plots for the proton affinity study of Pro-Asp have been shown in Chapter 2, but are repeated in this section. Five reference compounds were utilized for the Pro-Asp kinetic method study, with a proton affinity range of 23.4 kJ/mol. The first and second kinetic method plots are shown below in Figures 17 and 18.
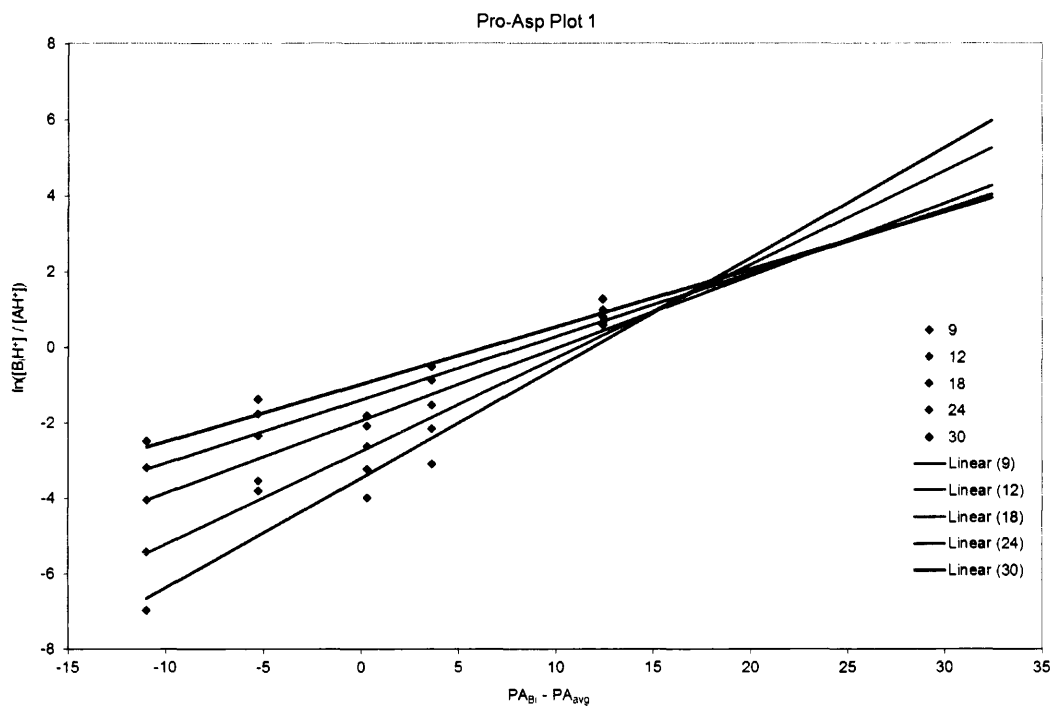
Figure 17. Kinetic Method Plot 1 for Pro-Asp.
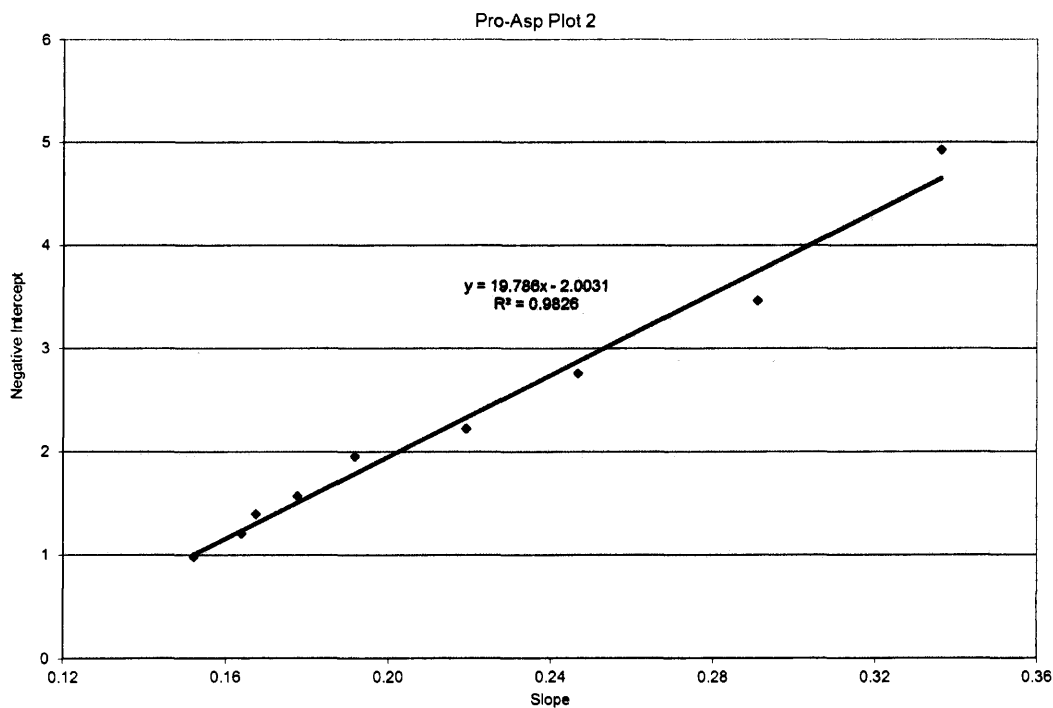
Figure 18. Kinetic Method Plot 2 for Pro-Asp.

The isothermal point is discernable in kinetic method plot 1 and the collision energy lines correspond fairly well to the experimental product ion ratios. Kinetic method plot 2 has a high correlation, with an R^2 value of 0.983. This correlation implies precise data and validates the choice of reference compounds. The proton affinity and ΔS values after the initial kinetic method workup were determined to be 979.1 kJ/mol and 16.7 J/mol·K, respectively.

Collision energies from 6 to 30 V were included in the kinetic method workup. The effective temperature plot, shown in Figure 19, is used to determine the collision energies used in the workup. The region on the graph with the most steeply rising slope, as illustrated with the red data points, shows the range of useful collision energies. This method was used for each dipeptide to determine the collision energies to be included in the workup.
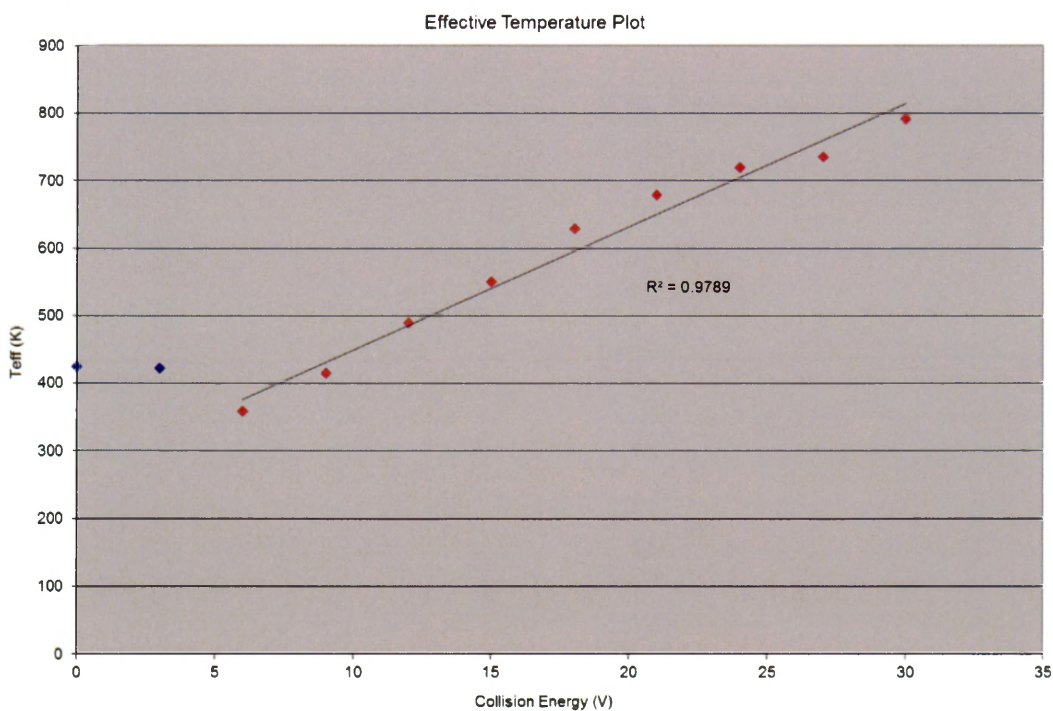
Figure 19. Effective Temperature Plot for Pro-Asp.

After ODR analysis is applied to the raw kinetic method data, a second first kinetic method plot is constructed, shown in Figure 20. In this plot, the lines are converging to a single point, the isothermal point. ODR analysis determined the proton affinity and ΔS values to be 979.2 ± 20.3 kJ/mol and -18.6 ± 29.9 J/mol·K, respectively.
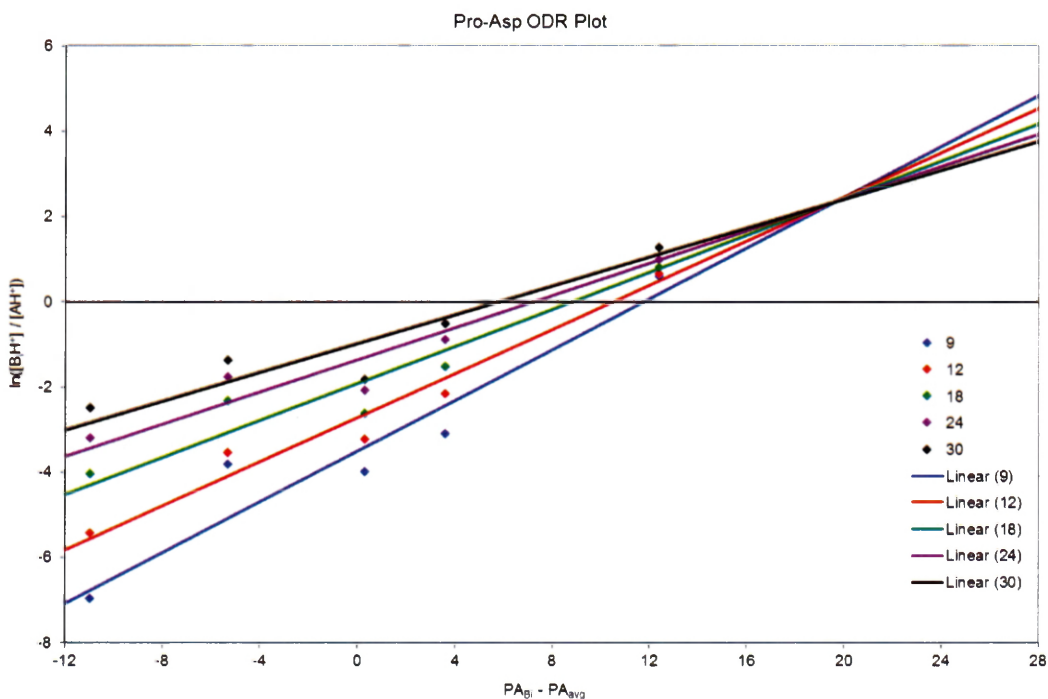
Figure 20. ODR KM Plot for Pro-Asp.

3.3.1.2 Remaining Pro-Xxx Dipeptides

Five reference compounds were used for the Pro-Gly kinetic method study, with an affinity range of 23.4 kJ/mol. Figure 21, shown below, is the ODR-analyzed kinetic method plot 1. ODR analysis determined the proton affinity and ΔS values to be 968.7 ± 11.9 kJ/mol and -22.0 ± 7.6 J/mol·K, respectively.

39
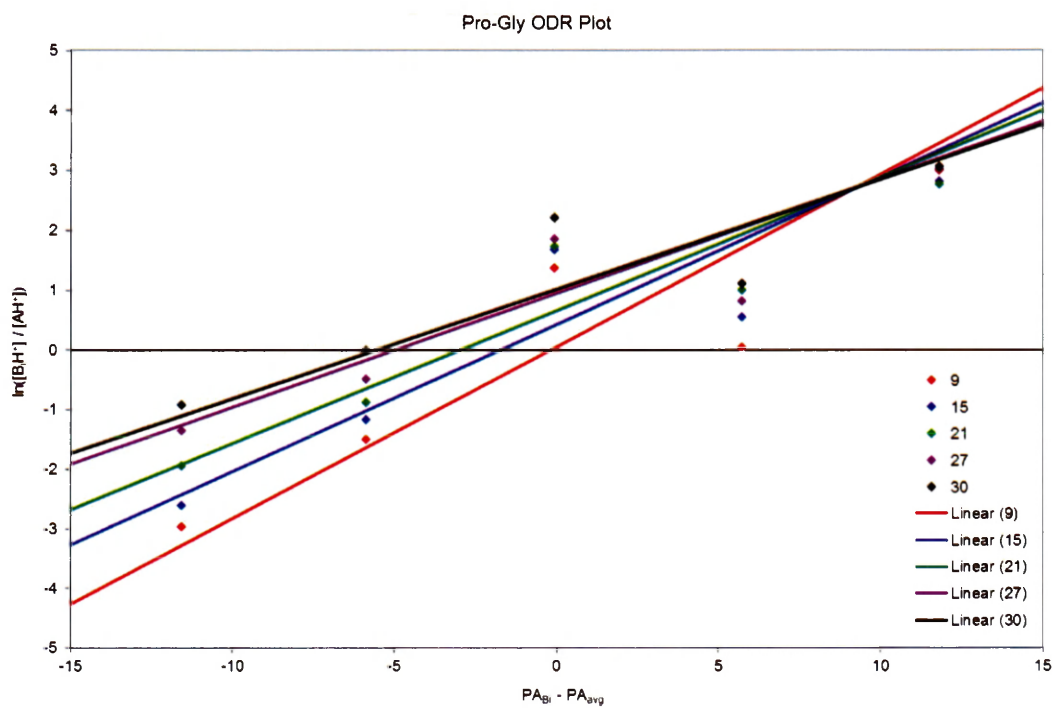
Figure 21. ODR KM Plot for Pro-Gly.

The second kinetic method plot shows an R^2 value of 0.941.

$$y = 11.996x - 2.8483$$
$$R^2 = 0.9413$$
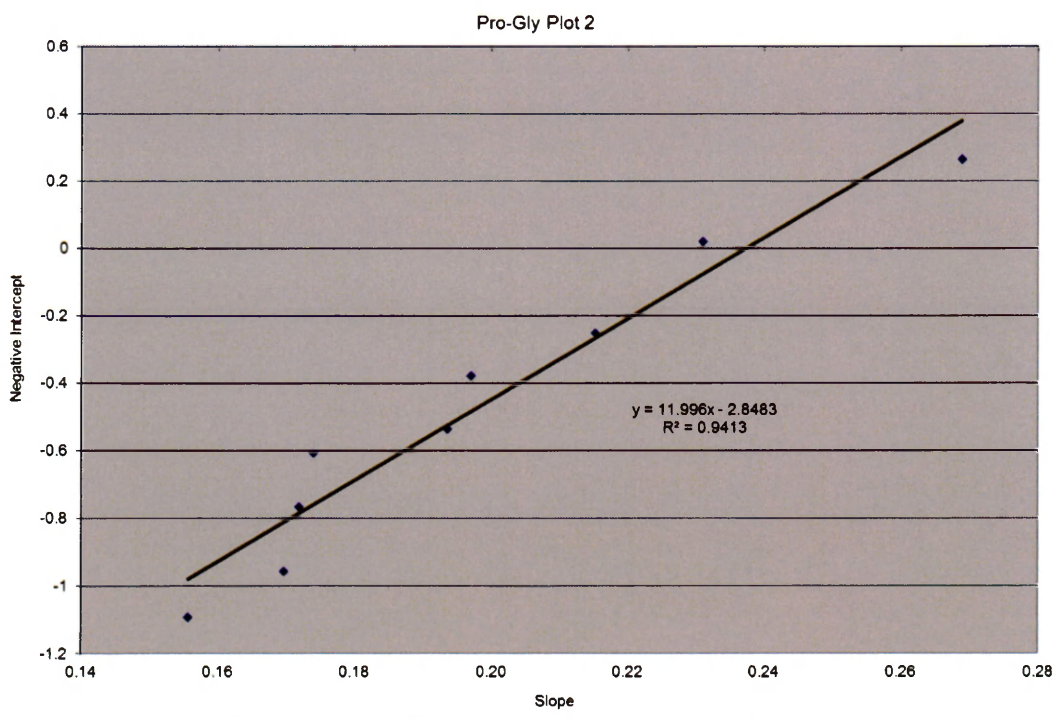
Figure 22. Kinetic Method Plot 2 for Pro-Gly.

40

Kinetic method experiments for Pro-Val utilized the same five reference compounds as for Pro-Gly, which implies very similar affinity values. Figure 23 shows the ODR-analyzed kinetic method plot 1, which determined the proton affinity and ΔS values to be 970.6 ± 12.6 kJ/mol and -6.8 ± 9.5 J/mol·K, respectively.
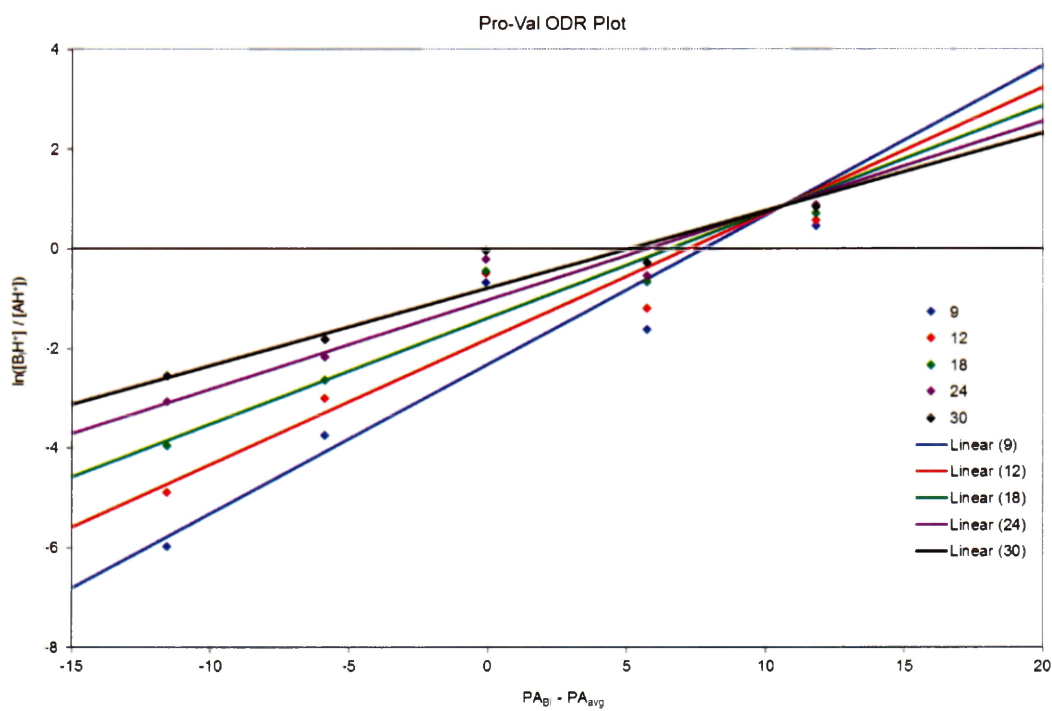
Figure 23. ODR KM Plot for Pro-Val.

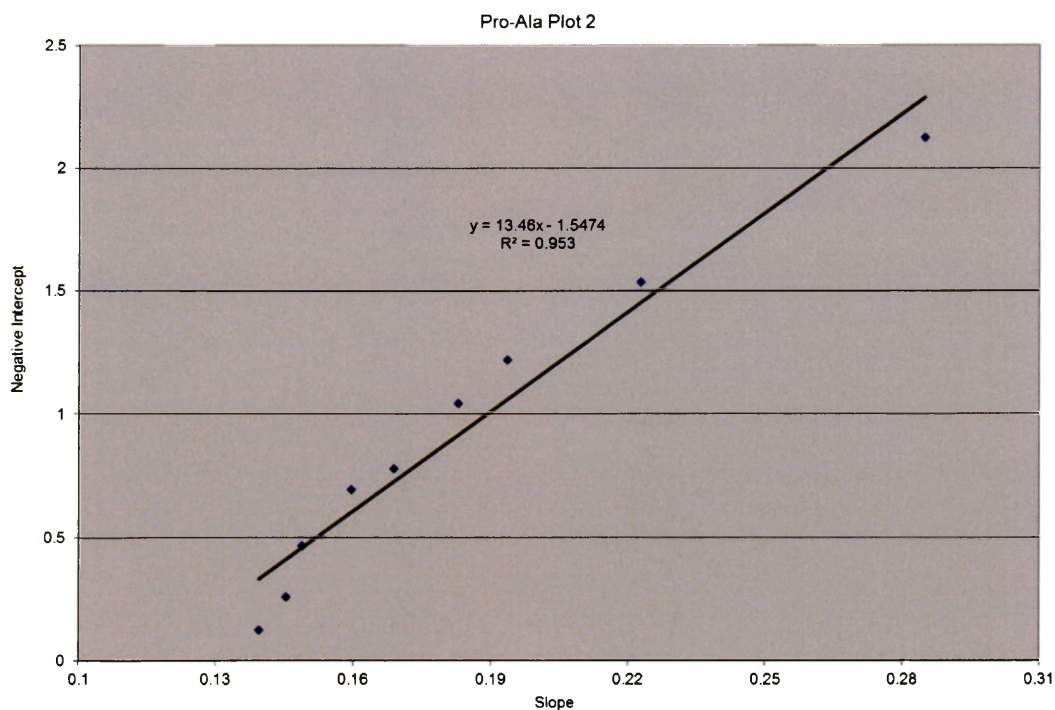Figure 24 shows the second kinetic method plot which has a very high R^2 value of 0.993.
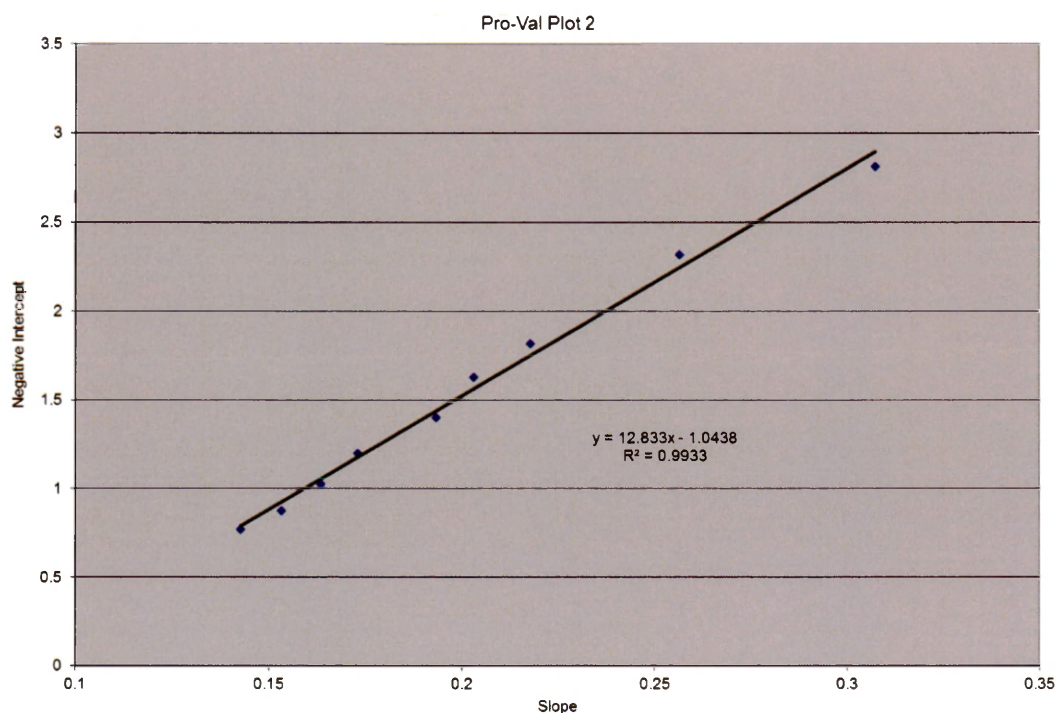
Figure 24. Kinetic Method Plot 2 for Pro-Val.

Five reference compounds were used for the Pro-Ala kinetic method study. These compounds had an affinity range of 23.4 kJ/mol. Shown below in Figure 25 is the ODR-analyzed kinetic method plot 1 for Pro-Ala. ODR analysis determined the proton affinity and ΔS values to be 974.7 ± 15.5 kJ/mol and -16.5 ± 7.5 J/mol·K, respectively.
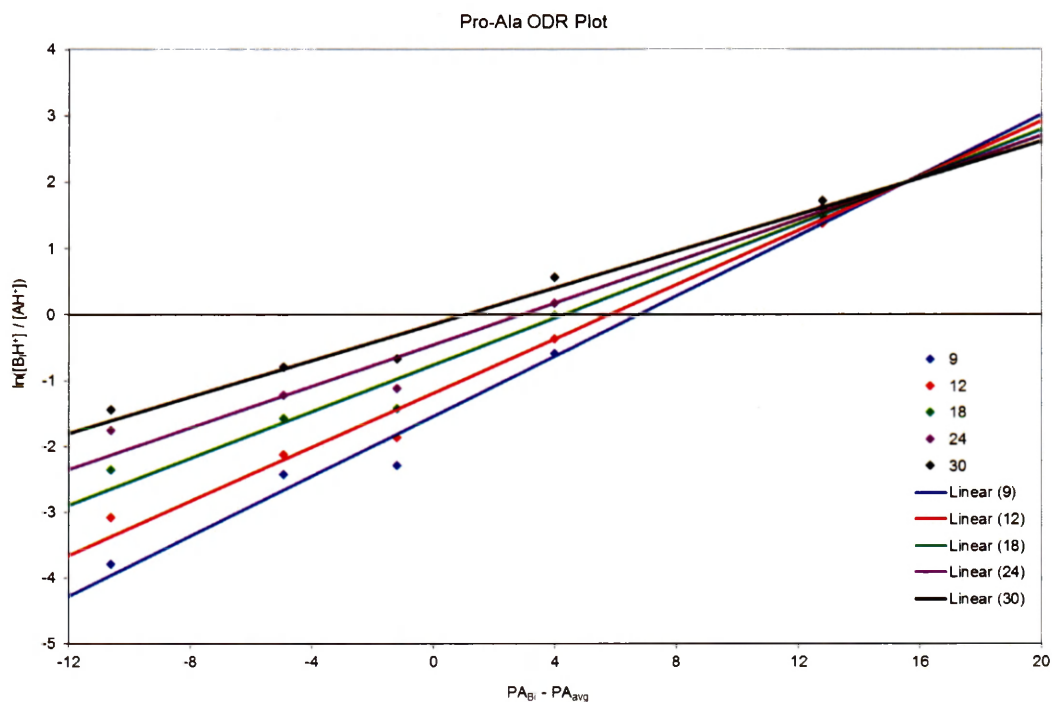
Figure 25. ODR KM Plot for Pro-Ala.

Figure 26 shows the second kinetic method plot with an R^2 value of 0.953.

Figure 26. Kinetic Method Plot 2 for Pro-Ala.

Five reference compounds were used for the Pro-Phe kinetic method study, with an affinity range of 23.4 kJ/mol. The ODR-analyzed kinetic method plot 1 is shown below in Figure 27. ODR analysis determined the proton affinity and ΔS values to be 975.1 ± 16.0 kJ/mol and -7.0 ± 15.4 J/mol·K, respectively.
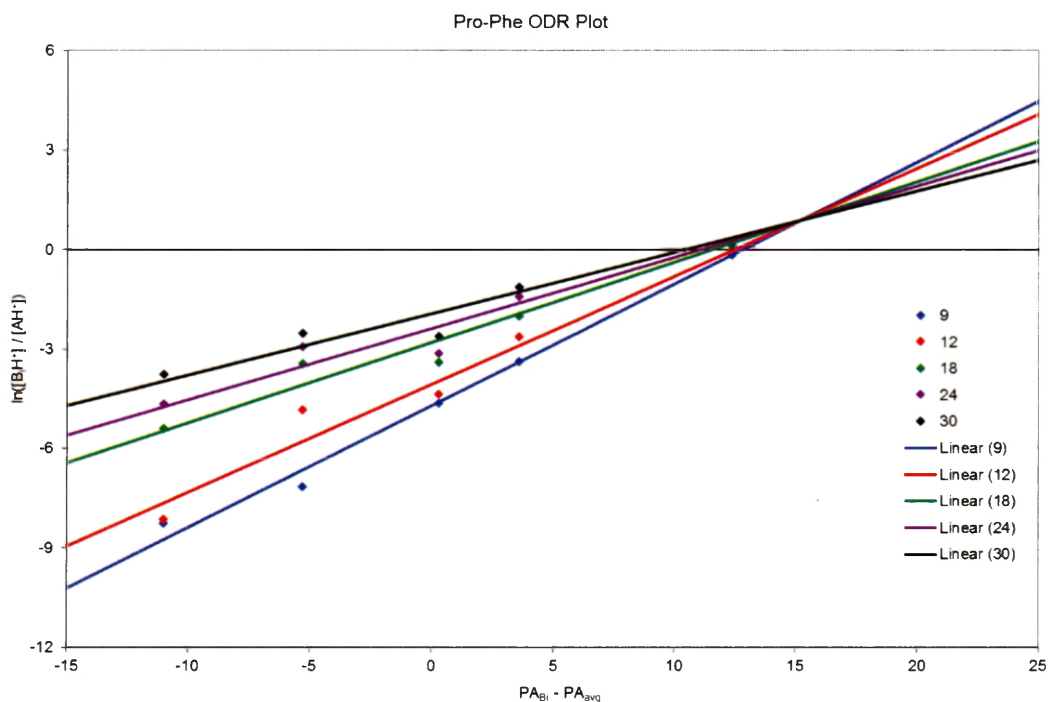
Figure 27. ODR KM Plot for Pro-Phe.

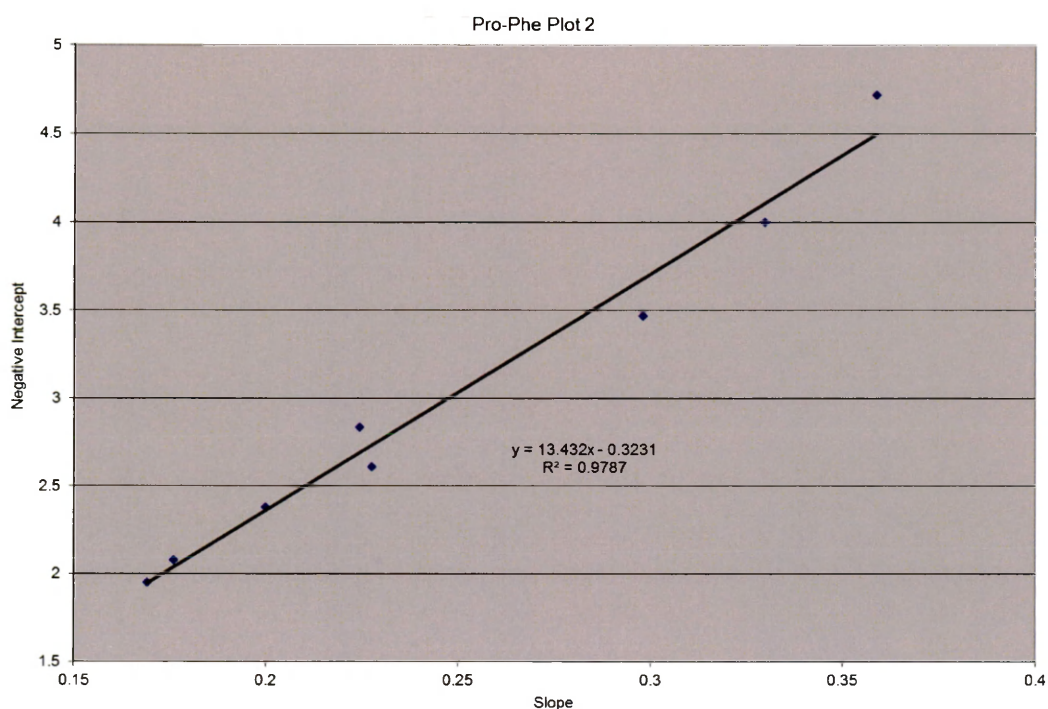The second kinetic method plot, shown in Figure 28, has an R^2 value of 0.970.

Figure 28. Kinetic Method Plot 2 for Pro-Phe.

The Pro-Leu kinetic method experiments utilized five reference compounds, with an affinity range of 22.8 kJ/mol. Figure 29 shows the ODR-analyzed kinetic method plot 1, which determined the proton affinity and ΔS values to be 973.2 ± 17.5 kJ/mol and -2.9 ± 18.8 J/mol·K, respectively.
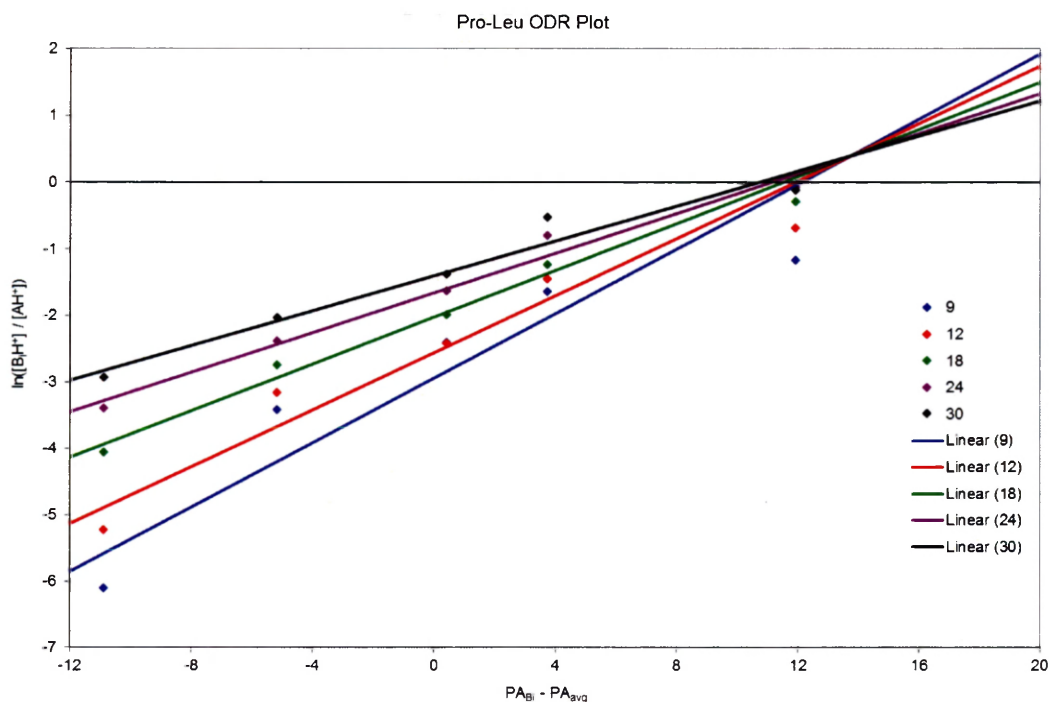
Figure 29. ODR KM Plot for Pro-Leu.

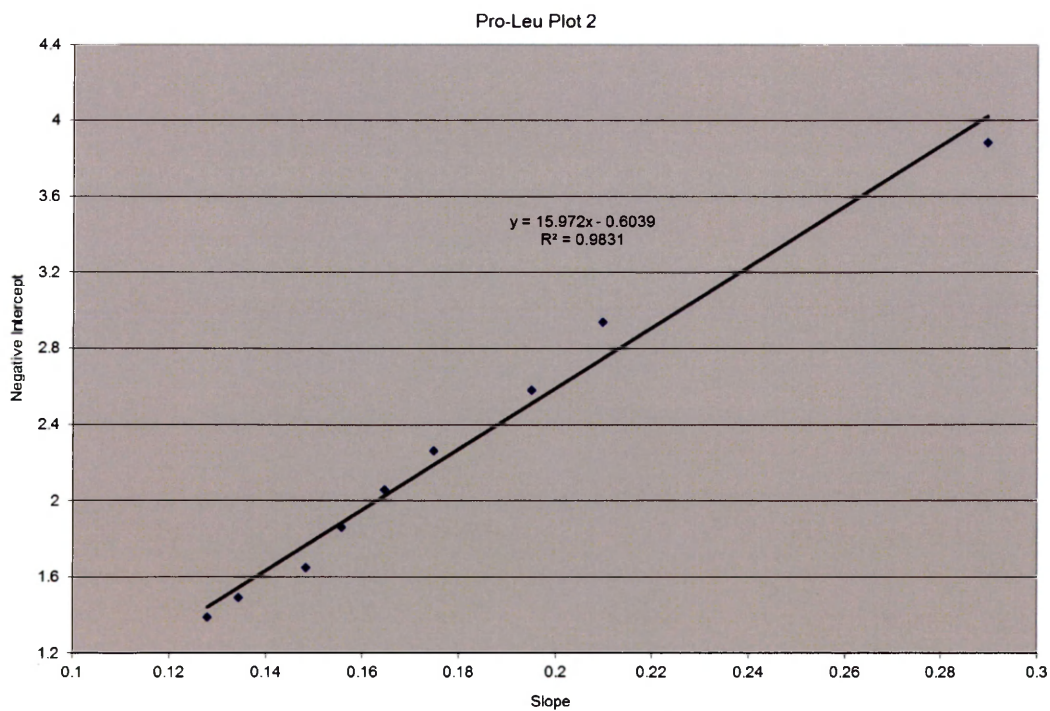The second kinetic method plot shows an R^2 value of 0.983.

Figure 30. Kinetic Method Plot 2 for Pro-Leu.

46

3.3.1.3 Xxx-Pro Dipeptides

Four reference compounds were used in the Gly-Pro proton affinity study, with an affinity range of 29.6 kJ/mol. Shown below in Figure 31 is the ODR-analyzed kinetic method plot 1. ODR analysis determined the proton affinity and ΔS values to be 951.7 ± 8.3 kJ/mol and -15.1 ± 1.2 J/mol·K, respectively.
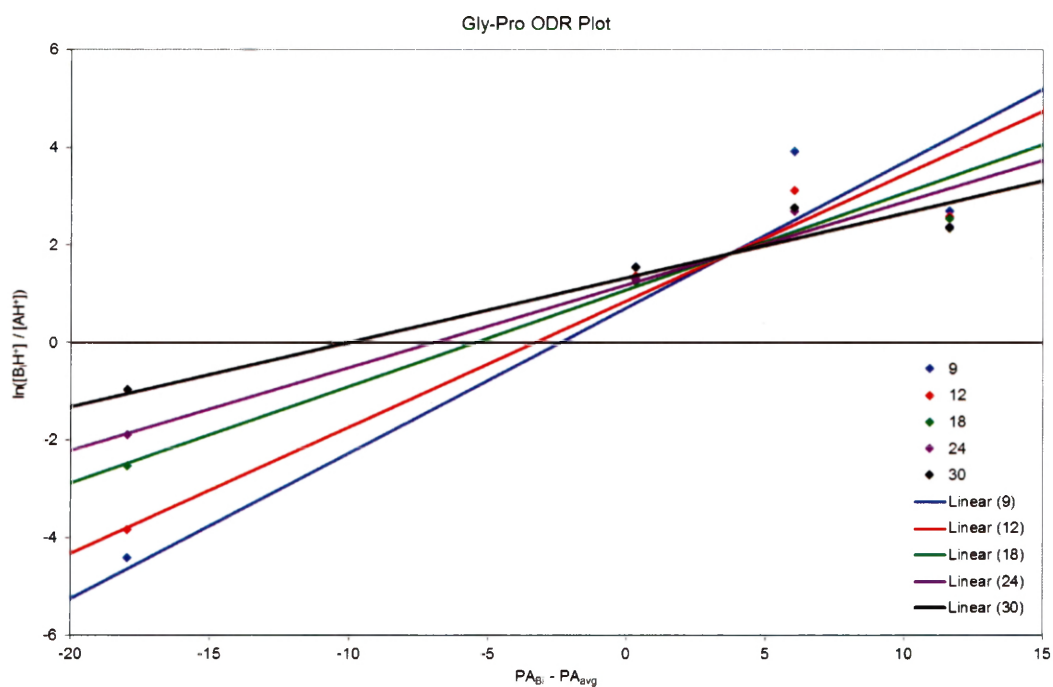

Gly-Pro ODR Plot

Figure 31. ODR KM Plot for Gly-Pro.

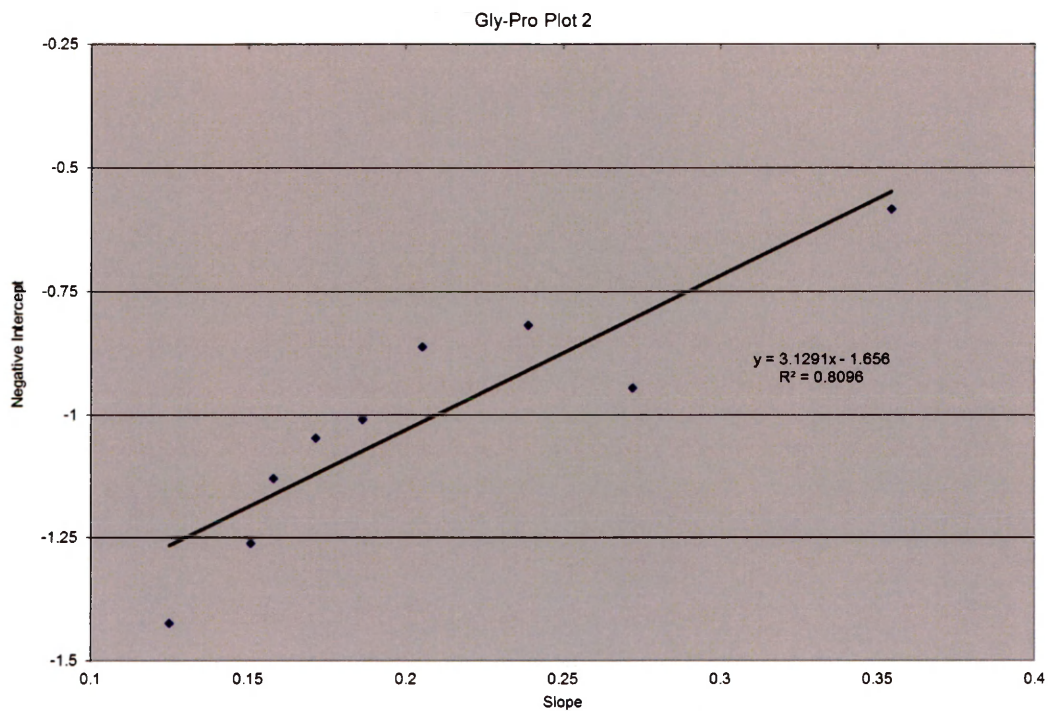The second kinetic method plot shown in Figure 32 has an R^2 value of 0.810.

Figure 32. Kinetic Method Plot 2 for Gly-Pro.

Five reference compounds were used in the Ala-Pro study, with an affinity range of 32.9 kJ/mol. The ODR-analyzed first kinetic method plot is shown below in Figure 33. ODR analysis determined the proton affinity and ΔS values to be 962.0 ± 9.8 kJ/mol and -18.8 ± 3.9 J/mol·K, respectively.
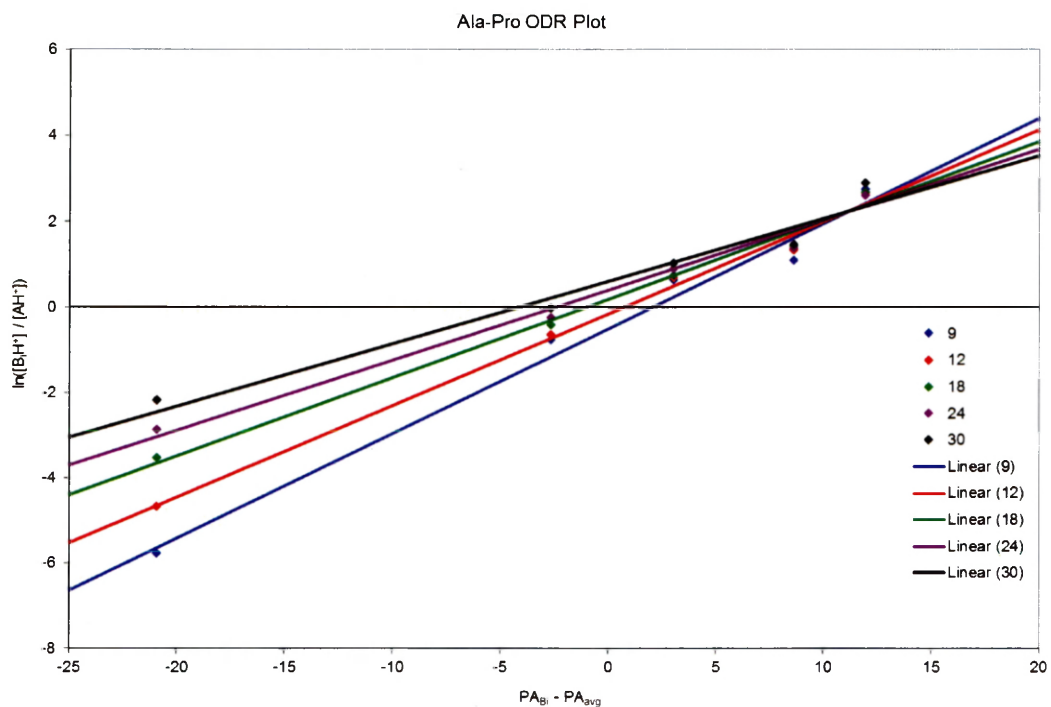
Figure 33. ODR KM Plot for Ala-Pro.

Below is the second kinetic method plot which has an R^2 value of 0.922.
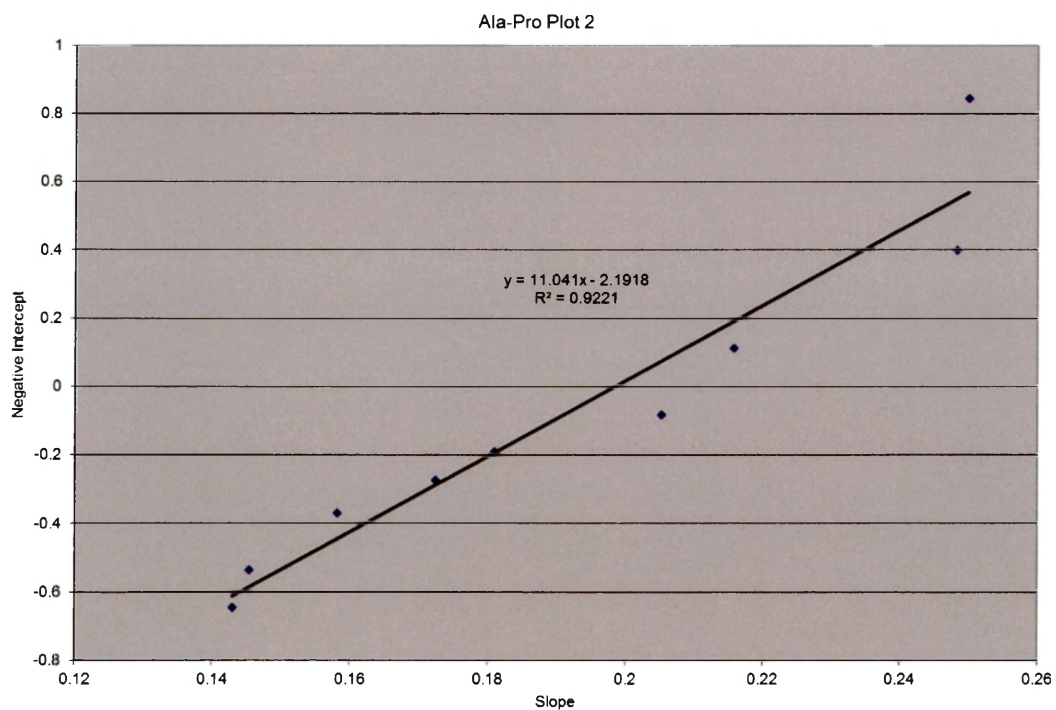

$$y = 11.041x - 2.1918$$
$$R^2 = 0.9221$$

Figure 34. Kinetic Method Plot 2 for Ala-Pro.

49

The proton affinity study for Leu-Pro utilized five reference compounds with an affinity range of 20.1 kJ/mol. Figure 35 shows the ODR-analyzed first kinetic method plot, which determined the proton affinity and ΔS values to be 966.8 ± 8.8 kJ/mol and -9.5 ± 10.9 J/mol·K, respectively.
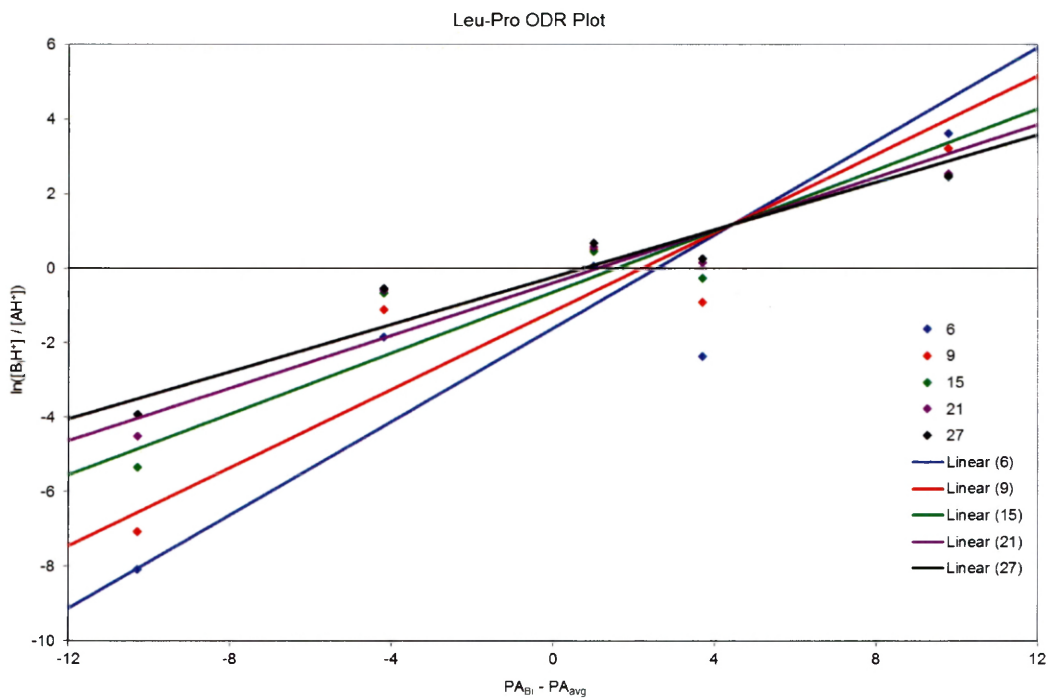

Figure 35. ODR KM Plot for Leu-Pro.

The second kinetic method plot, shown in Figure 36, has an R^2 value of 0.933.
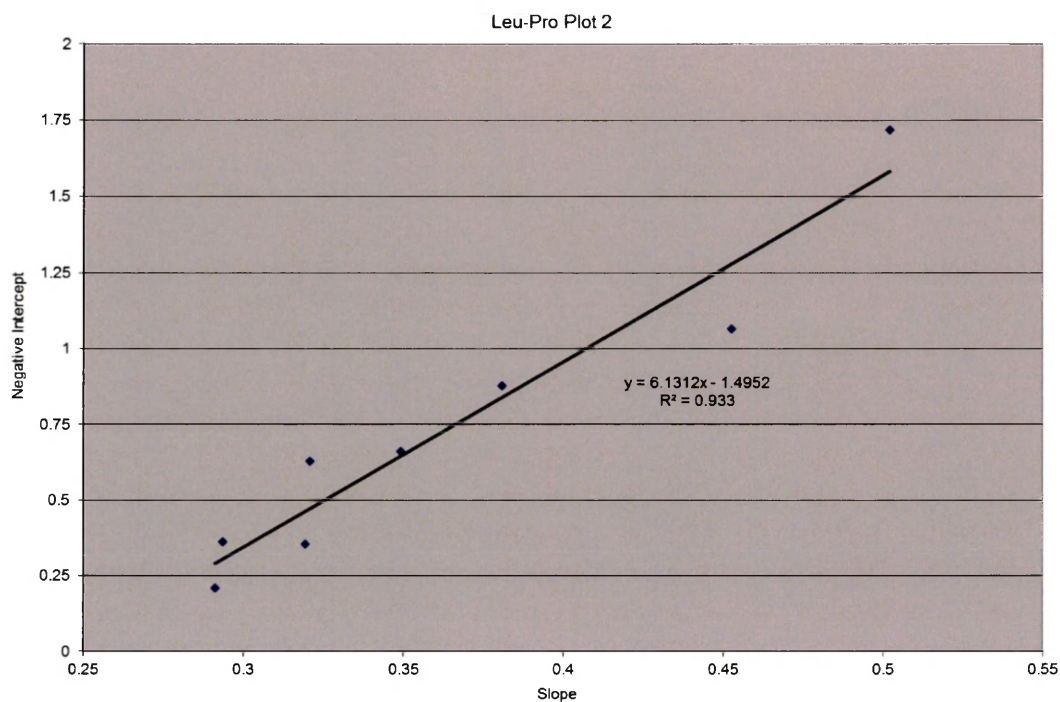
Figure 36. Kinetic Method Plot 2 for Leu-Pro.

Four reference compounds were utilized in the Phe-Pro proton affinity study, with an affinity range of 17.7 kJ/mol. The ODR-analyzed kinetic method plot 1 is shown below in Figure 37. ODR analysis determined the proton affinity and ΔS values to be 968.2 ± 10.8 kJ/mol and -5.5 ± 9.5 J/mol·K, respectively.
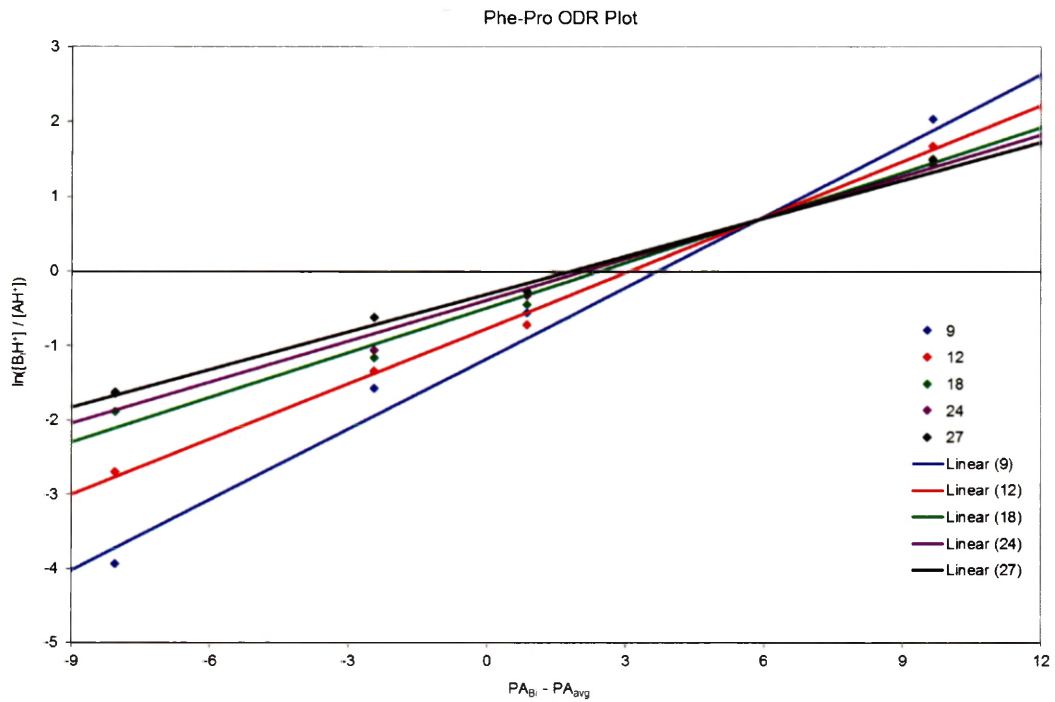
Figure 37. ODR Kinetic Method Plot for Phe-Pro.

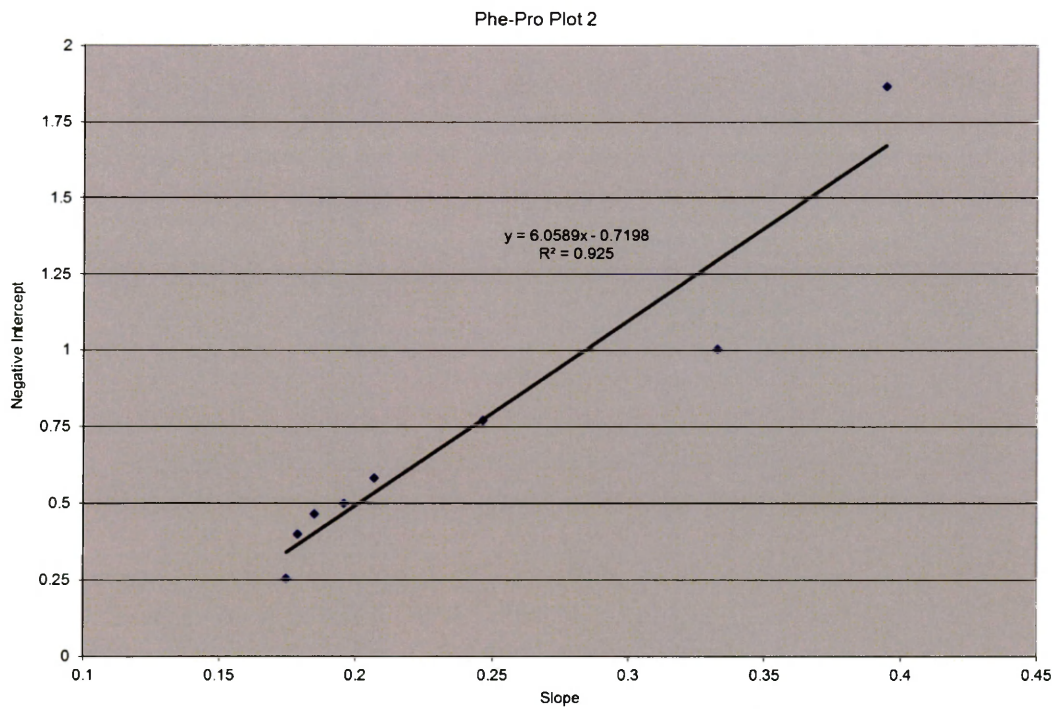Below is the second kinetic method plot which has an R^2 value of 0.925.

Figure 38. Kinetic Method Plot 2 for Phe-Pro.

52

3.3.2 Computational Results

Theoretical calculations are currently being performed on these analytes by the Poutsma group at Old Dominion University. So far, the proton affinities for Pro-Gly and Pro-Ala have been completed and determined to be 966.1 and 973.2 kJ/mol, respectively. These theoretical values are in very good agreement to the experimental values of 968.7 ± 11.9 kJ/mol for Pro-Gly and 974.7 ± 15.5 kJ/mol for Pro-Ala. The lowest-energy structures neutral and protonated structures for Pro-Gly and Pro-Ala are shown below in Figures 39 and 40. These sturctures were obtained after sorting through hundreds of conformers in order to find the lowest energy structure. For both Pro-Gly and Pro-Ala, the protonation site was found to be the nitrogen of the proline ring.
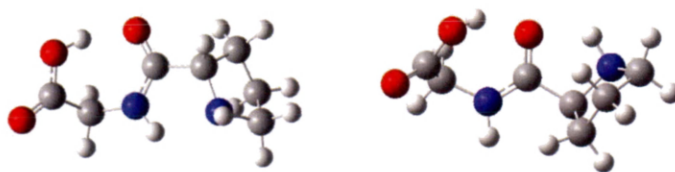

Figure 39. Optimized neutral (left) and protonated (right) Pro-Gly structures.
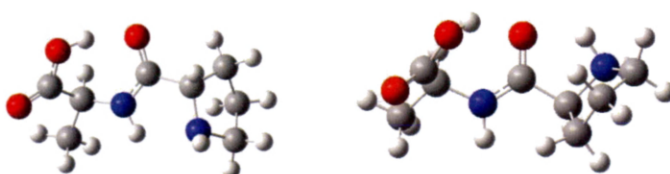

Figure 40. Optimized neutral (left) and protonated (right) Pro-Ala structures.

3.4 Discussion

Proton affinities for proline-containing dipeptides, and dipeptides in general, have not been studied extensively for their gas-phase thermochemical

properties. The gas-phase basicities of several dipeptides have been determined by the Amster and Cassady groups. Overall, the proton affinity trend, in increasing order, for the dipeptides studies was determined to be Pro-Gly < Pro-Val < Pro-Ala < Pro-Phe < Pro-Leu < Pro-Asp for the Pro-Xxx dipeptides. In increasing order, the trend for the Xxx-Pro dipeptides was determined to be Gly-Pro < Ala-Pro < Leu-Pro < Phe-Pro.

As can be seen in the trends and from the particular affinity values, the proton affinity trends generally agree with each other, with Pro-Gly and Gly-Pro having the lowest affinity of the analytes studied. While the dipeptides containing phenylalanine and leucine do not follow the trend exactly, the similarity in affinity values, in addition to the uncertainties associated with that value, show that those dipeptides generally agree with the trend. However, it must also be noted that the uncertainties associated with each proton affinity value results in affinity values that overlap each other greatly.

One explanation for such a large uncertainty for several of the analytes comes from the larger entropy of the analytes. The larger the protonation entropy, the more likely that the isothermal points would lie outside of the reference compounds chosen.

Theoretical calculations have been started by Professor Jennifer Poutsma at Old Dominion University to provide comparison values for the proton affinities. The theoretical values for Pro-Gly and Pro-Ala are in extremely good agreement with our experimental values. For Pro-Gly, the theoretical value was determined to be 966.1 kJ/mol, which agrees with the experimental value of 968.7 ± 11.9

kJ/mol. Similarly, the theoretical value for Pro-Ala was determined to be 973.2 kJ/mol, which is in good agreement with the experimental value of 974.7 ± 15.5 kJ/mol. Additional theoretical calculations are being performed for the remaining dipeptides.

Chapter 4. Gas-Phase Acidity Project

4.1 Fluorinated Alcohols

Scientific collaboration presents an interesting opportunity for research groups to utilize their particular skill sets and instrumentation in addition to expanding their knowledge on areas outside of their current research. The gas-phase acidity study of fluorinated alcohols arose from a collaboration between Professor Poutsma and Professor Thomas Morton at the University of California-Riverside. Professor Morton is studying fluorinated alkoxide ions, particularly looking at vibrational spectra of these ions in the gas-phase, through computational theory and infrared multiple photon dissociation (IRMPD) spectroscopy.[50] It is difficult to obtain vibrational spectra for the ion paired alkoxide anions, thus IRMPD was used to obtain spectra for the anions in the gas phase. In IRMPD spectroscopy, gas-phase ions are subjected to a tunable infrared laser. As the laser is applied over a range of IR wavelengths, resonance occurs between the laser and one of the vibrational modes of a molecule, causing ion dissociation and resulting in a vibrational "action" spectra.

Understanding the stability of these fluorinated alkoxide ions are of interest to us. Stability of anions arises through several ways; inductive effects, resonance, electronegativity properties, or negative hyperconjugation, among others. Professor Morton has performed IRMPD spectroscopy to begin to parse out whether the blue shifts observed in the IRMPD spectra are a result of negative hyperconjugation, electronegativity, or both.[50]

Highly fluorinated alcohols have greater acidities than hydrocarbon alcohols of the same structure; however, geminally fluorinated alcohols larger than CF_3OH are typically unstable due to a spontaneous expulsion of HF.[50] Obtaining acidities of the neutral molecules would allow us to gain insight as to the stability of the analogous anion. An increase in the acidity of a neutral molecule would also lead to an increase in stability of the anion.

4.1.1 Analytes of Interest

The fluorinated alcohols investigated in this thesis include 2,2,2-trifluoroethanol, 1,1,1-trifluoro-2-propanol, 2-trifluoromethyl-2-propanol, 1,1,1,3,3,3-hexafluoro-2-propanol, 1,1,1,3,3,3-hexafluoro-2-methyl-2-propanol, and perfluoro-tert-butyl alcohol. The structures and abbreviated names of these analytes are shown below.
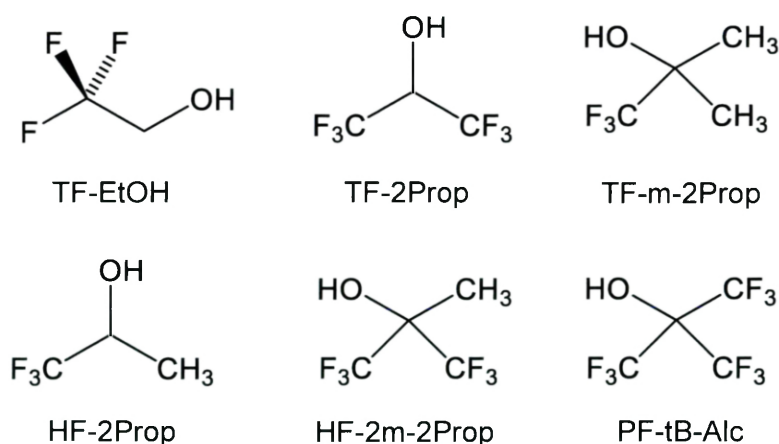

Figure 41. Fluorinated alcohol structures.

Due to the weak acidity of the trifluorinated compounds, I was unable to perform kinetic method experiments as they do not form dimers using electrospray

ionization. Gas-phase acidity values for the last three compounds are presented in this thesis.

4.2 Reference Acids

Reference compounds were found through the NIST Chemistry Webbook and based off of theoretical calculations performed by Professor Tom Morton at UC-Riverside. Many of the references used with the triple quadrupole were not appropriate when using an ion trap, as the product ratios were much higher than desired. Thus, different sets of reference compounds were utilized for the experiments on the two instruments. These references, in addition to the instrument with which they are associated, are shown below in Tables 4 and 5.

Reference Base	GPA (kJ/mol)[26]	PF-tB-Alc	HF-2Prop	HF-2m-2Prop
Dichloroacetic acid	1374	X		
Difluoroacetic acid	1385	X		
2-chlorobenzoic acid	1402	X		
4-fluorobenzoic acid	1410	X	X	
3-hydroxybenzoic acid	1417		X	
2,5-dimethylbenzoic acid	1420		X	X
Benzoic acid	1423		X	X
Phenylacetic acid	1429		X	X
Ethoxyacetic acid	1431		X	
Hexanoic acid	1448		X	X

Table 4. Reference Compounds for Fluorinated Alcohols on TSQ.

Reference Base	GPA (kJ/mol)[26]	PF-tb-Alc	HF-2prop	HF-2m-2prop
Dichloroacetic acid	1374	X		
3-nitrobenzoic acid	1377	X		
Difluoracetic acid	1385	X		
3-nitrophenol	1399	X		
2-chlorobenzoic acid	1402	X		
Phenylacetic acid	1429		X	
Methoxyacetic acid	1431		X	X
4-pentenoic acid	1441		X	X
2-tertbutyl phenol	1446		X	
Hexanoic acid	1448		X	X
4-fluorophenol	1451		X	X
4-methoxyphenol	1466			X

Table 5. Reference Compounds for Fluorinated Alcohols on LCQ.

4.3 Experimental Results

Gas-phase acidities for 1,1,1,3,3,3-hexafluoro-2-propanol, 1,1,1,3,3,3-hexafluoro-2-methyl-2-propanol, and perfluoro-tert-butyl alcohol were determined using extended kinetic method workup and orthogonal distance regression theory. As mentioned previously, kinetic method experiments require a minimum of three days of fragmentation data for each dimer solution. Initially, I had started experiments on the triple quadrupole mass spectrometer, but more than halfway through the project, the triple quadrupole became inoperable. The large majority of the data had been acquired and the remaining data for the analytes on this instrument included the third and last day for a few analyte:reference pairs. Because of this, I worked up and analyzed the data as usual, with the understanding that I did not have three days of data for each reference compound.

Nevertheless, this data is presented in the thesis and will be completed once we have a working triple quadrupole instrument. In the meantime, I re-

performed the project on the ion trap mass spectrometer. While it is possible to obtain accurate thermochemical values on ion trap instruments, it is much more preferable to perform kinetic method experiments on triple quadrupole instruments. The effective temperature range is much larger with the triple quadrupole instrument than with the ion trap instrument and provides more precise results.

Spectra were acquired on the triple quadrupole for collision energies from 0 to 45 V and 0 to 100 arbitrary units on the ion trap. Collision energies used in the final analysis were the fragmentation data from 21 to 45 V for the triple quadrupole and 16 to 28 arbitrary units for the LCQ. Tabulated data for the three analytes for both instruments is shown in Table 6 below. Theoretical predictions performed by the Morton group are also presented in the table.

Analyte	TSQ Experimental GPA (kJ/mol)	LCQ Experimental GPA (kJ/mol)	Theoretical GPA (kJ/mol)[‡]
PF-tb-Alc	1383.2 ± 9.5	1391.6 ± 7.5	1387
HF-2prop	1439.3 ± 10.0	1448.6 ± 10.2	1443
HF-2m-2prop	1458.9 ± 34.5	1459.7 ± 12.0	1457

[‡] Computations performed by Morton, unpublished.

Table 6. Results for Fluorinated Alcohols on TSQ and LCQ.

In the following three sections, triple quadrupole and ion trap results are presented. A detailed explanation of the data and graphs for perfluoro-tert-butyl alcohol are included, and the ODR-analyzed first kinetic method plot and the kinetic method plot 2 are included for the remaining analytes. The graphs not included in the initial results section are presented in the Appendix.

4.3.1 Secondary Fragmentation

A common occurrence upon fragmentation, especially at higher collision energies, is secondary fragmentation. In these situations, the heterodimer, analyte ion, or reference ion may undergo an additional fragmentation due to the excess of energy. Secondary fragmentation in the form of decarboxylation of the carboxylic acid moiety of several reference compounds were observed, indicated by a loss of 44, or CO_2, from the deprotonated reference peak.

Fragmentation was also observed from one of the analytes, perfluoro-tert-butyl alcohol. Deprotonated perfluoro-tert-butyl alcohol has a m/z ratio of 235 and a secondary peak at 186 was also observed when perfluoro-tert-butyl alcohol was allowed to undergo CID at high energies. This loss of 50 is associated with CF_2 expulsion, which is often observed with highly fluorinated ions. Tabulated below are the reference compounds that underwent secondary fragmentation and the peaks observed.

Compound	[MH⁻] m/z	Observed peak (m/z)	Fragment Loss
Benzoic acid	121	77	Decarboxylation (-44)
Dichloroacetic acid	127	83	Decarboxylation (-44)
Phenylacetic acid	135	91	Decarboxylation (-44)
4-aminobenzoic acid	136	92	Decarboxylation (-44)
3-hydroxybenzoic acid	137	93	Decarboxylation (-44)
4-flurobenzoic acid	139	95	Decarboxylation (-44)
2,5-dimethylbenzoic acid	149	105	Decarboxylation (-44)
2-chlorobenzoic acid	155	111	Decarboxylation (-44)
Perfluoro-tert-butyl alcohol	236	186	CF_2 expulsion (-50)

Table 7. Secondary Fragmentation Observed.

If secondary fragment peaks are consistently present and in a sufficient amount, it is necessary to include their contribution to the overall fragmentation

data workup. In order to account for this second peak, it is added to its respective parent ion. For example, a peak was observed at 77 m/z, which was determined to be a secondary fragment peak from benzoic acid. The ion intensity for the peak at 77 m/z was then added to the ion intensity for the reference compound when calculating product ion ratios.

4.3.2 Perfluoro-tert-butyl alcohol

4.3.2.1 TSQ Results

Four reference compounds were used for the perfluoro-tert-butyl alcohol kinetic method experiments on the triple quadrupole mass spectrometer. The range of gas-phase acidities for the references was 36.1 kJ/mol. The first and second kinetic method plots are shown below in Figures 42 and 43.
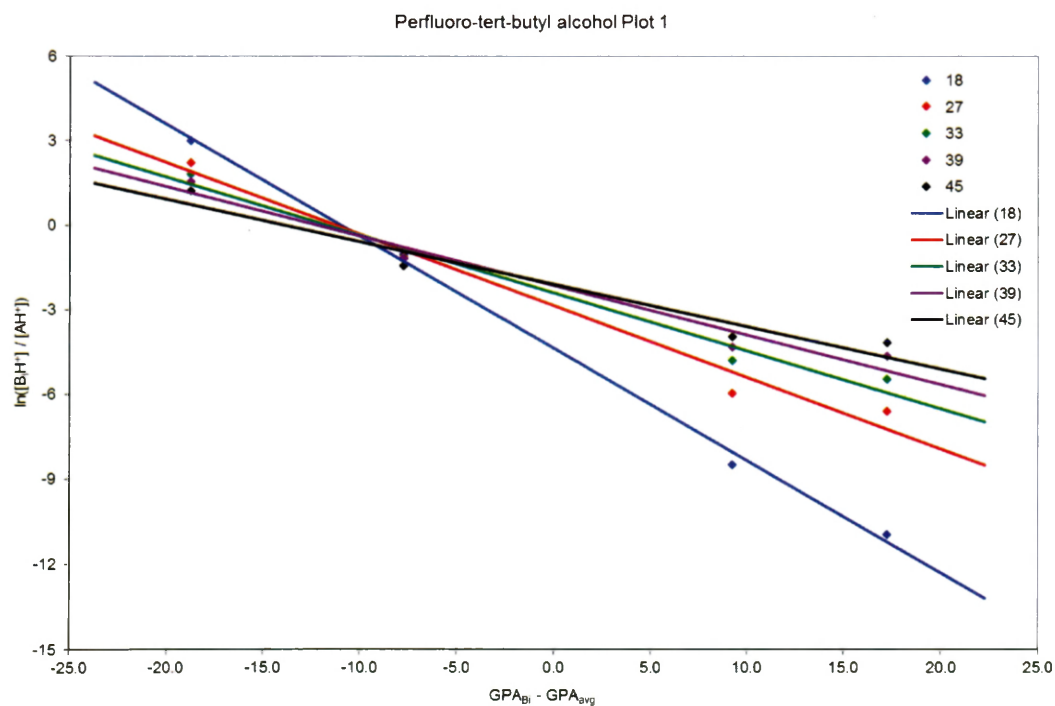
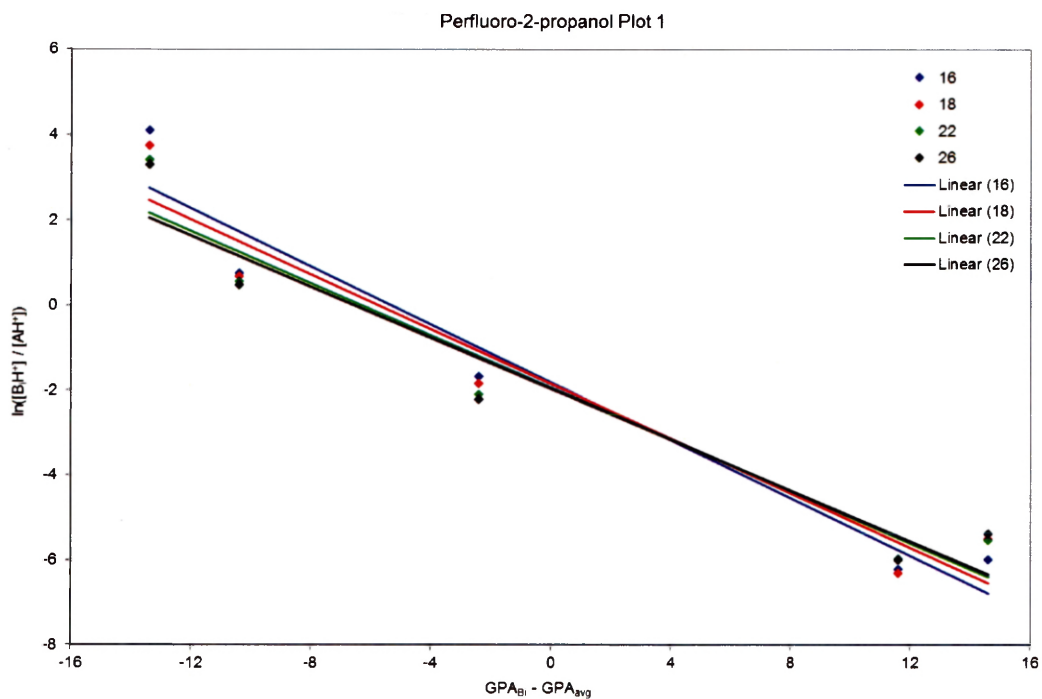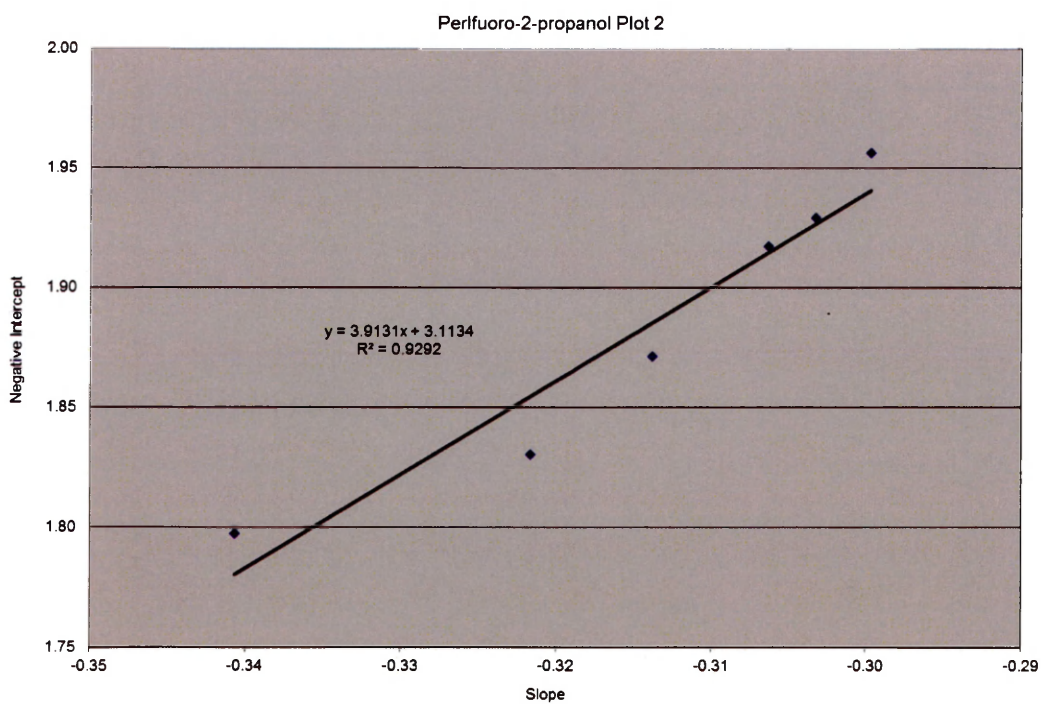Figure 42. Kinetic Method Plot 1 for Perfluoro-tert-butyl alcohol on TSQ.
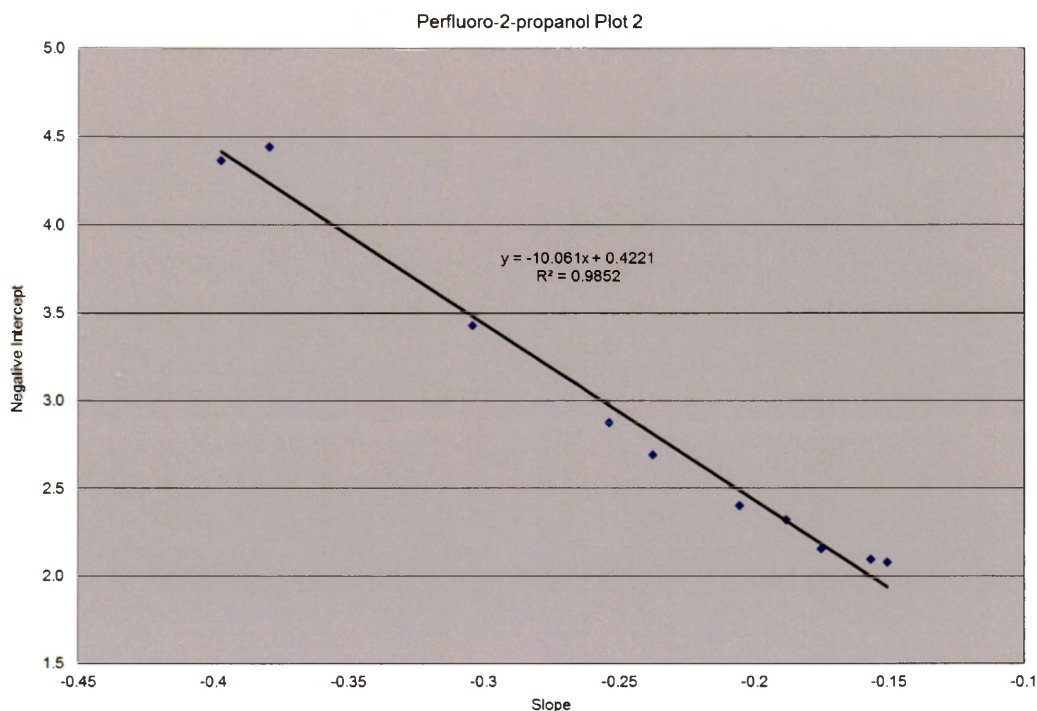
Figure 43. Kinetic Method Plot 2 for Perfluoro-tert-butyl alcohol on TSQ.

The isothermal point is clearly visible in the first kinetic method plot and the collision energy lines correspond well to the experimental product ion ratios. The second kinetic method plot has a very high correlation, with an R^2 value of 0.985. The gas-phase acidity and ΔS values after initial kinetic method workup were determined to be 1382.7 kJ/mol and -3.5 J/mol·K, respectively.

Collision energies from 18 to 45 V were included in the kinetic method workup. Looking at the effective temperature plot, shown below in Figure 44, that range of collision energies was the best choice. That region of the graph, indicated by the red data points, has the most steeply rising slope, which provides a steadily increasing range of effective temperatures. This method was used for each analyte to determine the collision energies included in the kinetic method workup. Additionally, the effective temperature plot validates increasing the

collision energy range to 45 V, as the original maximum of 30 V does not provide

a sufficient set of data points to include in the workup.
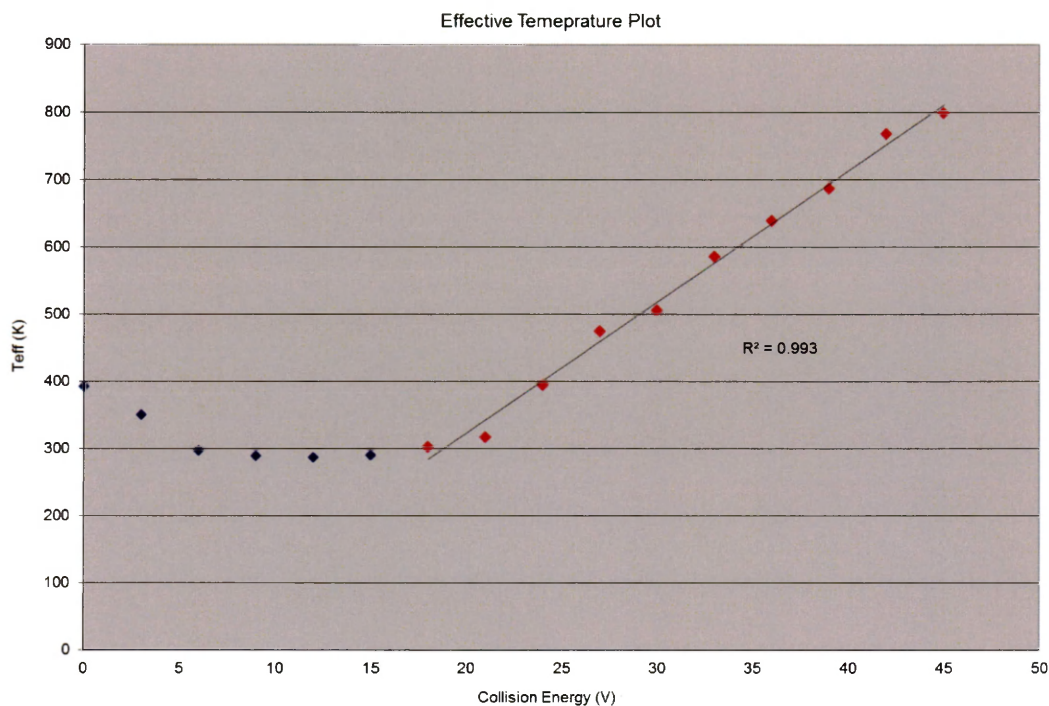
Figure 44. Effective Temperature Plot for Perfluoro-tert-butyl alcohol on TSQ.

Lastly, the ODR KM Plot 1, shown below in Figure 45, shows the lines

intersecting at the isothermal point. ODR analysis determined the gas-phase

acidity and ΔS values to be 1383.2 ± 9.5 kJ/mol and 4.0 ± 3.4 J/mol·K, respectively.

Perfluoro-tert-butyl alcohol ODR Plot
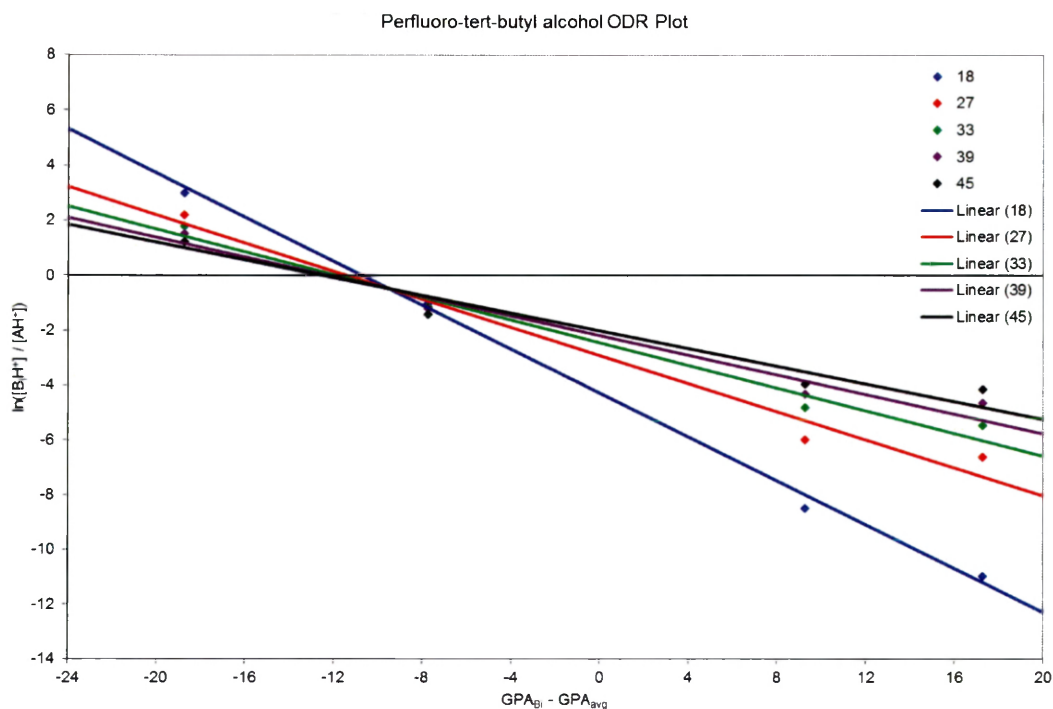
Figure 45. ODR KM Plot for Perfluoro-tert-butyl alcohol on TSQ.

4.3.2.2 LCQ Results

When repeating the kinetic method experiments on the ion trap mass spectrometer, not all of the reference compounds were able to be used. Five reference compounds were used in the perfluoro-tert-butyl alcohol experiments on the ion trap mass spectrometer, with a range of 28.0 kJ/mol. The first and second kinetic method plots are shown below in Figures 46 and 47.

Figure 46. Kinetic Method Plot 1 for Perfluoro-tert-butyl alcohol on LCQ.

Figure 47. Kinetic Method Plot 2 for Perfluoro-tert-butyl alcohol on LCQ.

The isothermal point is very visible in the first kinetic method plot, even though the collision energy lines do not correspond well to the experimental product ion ratios. After the initial kinetic method workup, the gas-phase acidity and ΔS values were determined to be 1391.3 kJ/mol and 25.9 J/mol·K, respectively. The second kinetic method plot is very linear, with an R^2 value of 0.929.

Activation amplitudes from 16 to 26 units were included in the kinetic method analysis. These values were determined by looking at the effective temperature plot, shown below in Figure 48.
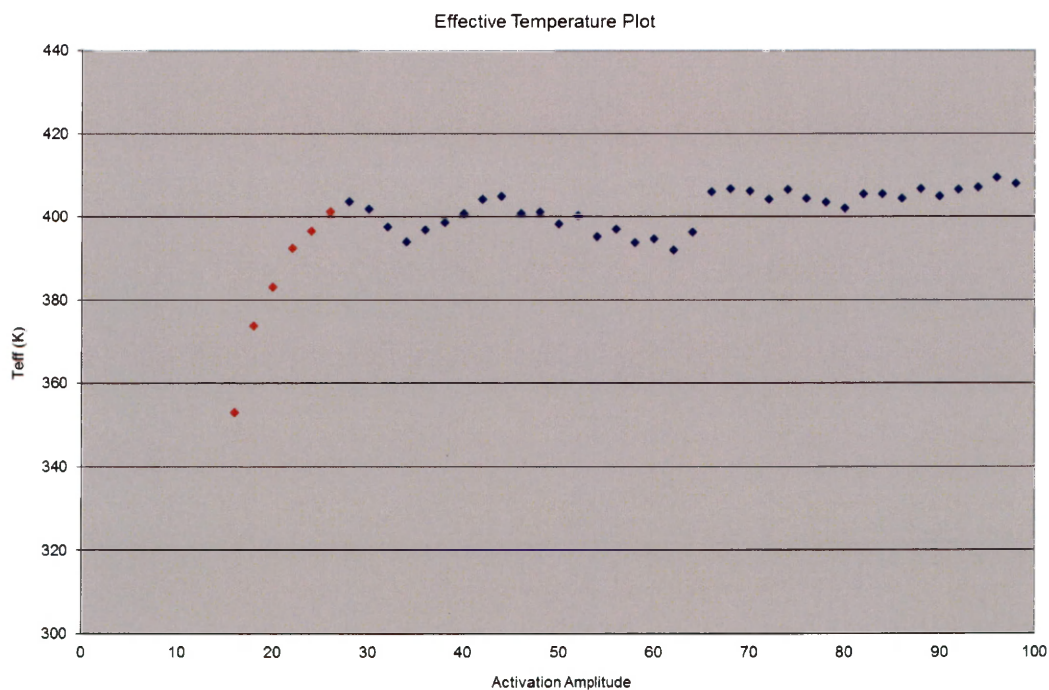
Figure 48. Effective Temperature Plot for Perfluoro-tert-butyl alcohol on LCQ.

The blue data points indicate all of the effective temperature values calculated using the fragmentation data. The data points included in the kinetic method

workup were the amplitudes in the region with the most steeply rising slope. This method was used to determine the activation amplitudes included in the kinetic method workup for all ion trap experiments.

Shown in Figure 49 is the ODR KM Plot 1, which is similar to the initial kinetic method plot 1. The gas-phase acidity and ΔS values determined after ODR analysis were 1391.6 ± 7.5 kJ/mol and 27.7 ± 7.0 J/mol·K, respectively.
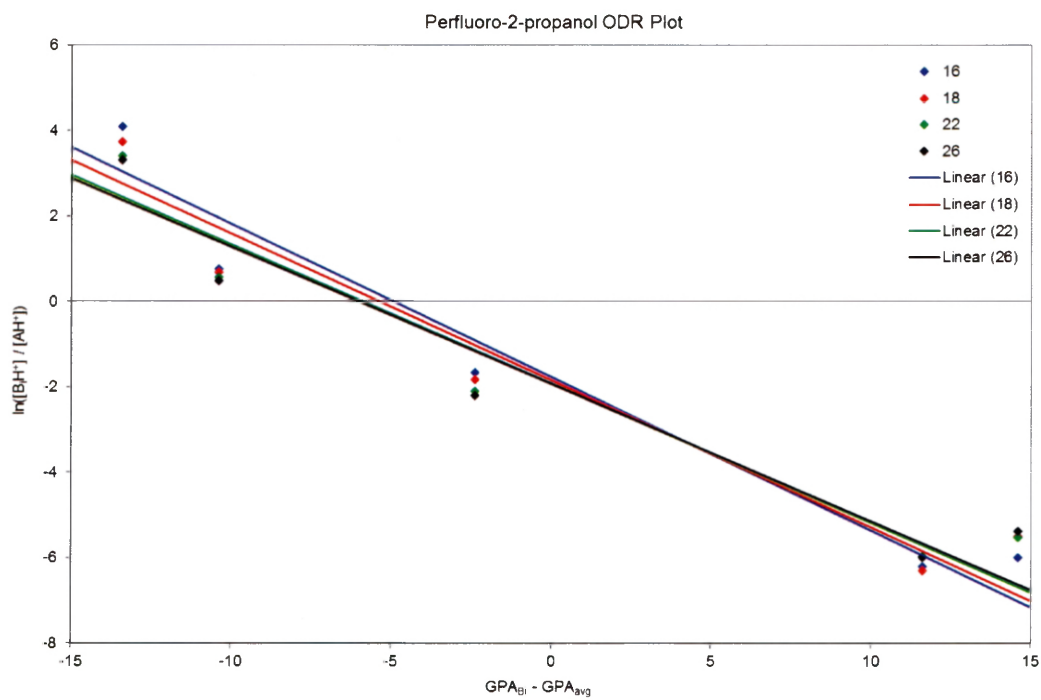
Figure 49. ODR KM Plot for Perfluoro-tert-butyl alcohol on LCQ.

4.3.3 Hexafluoro-2-propanol

4.3.3.1 TSQ Results

Seven references were found to produce a sufficient dimer count in addition to appreciable product ion peaks. The range of gas-phase acidities for the references used was 38.0 kJ/mol. Figure 50 shows the ODR-analyzed kinetic method plot 1 for hexafluoro-2-propanol. ODR analysis determined the gas-phase

acidity and ΔS values to be 1439.3 ± 10.0 kJ/mol and -14.3 ± 5.9 J/mol·K, respectively.
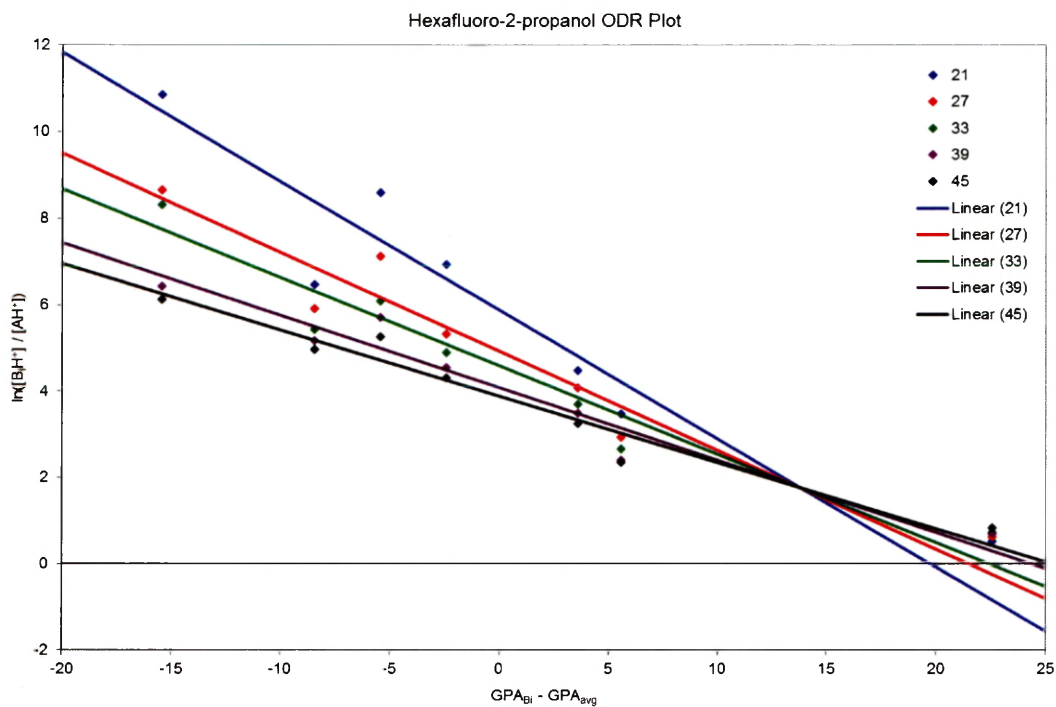
Figure 50. ODR KM Plot for Hexafluoro-2-propanol on TSQ.
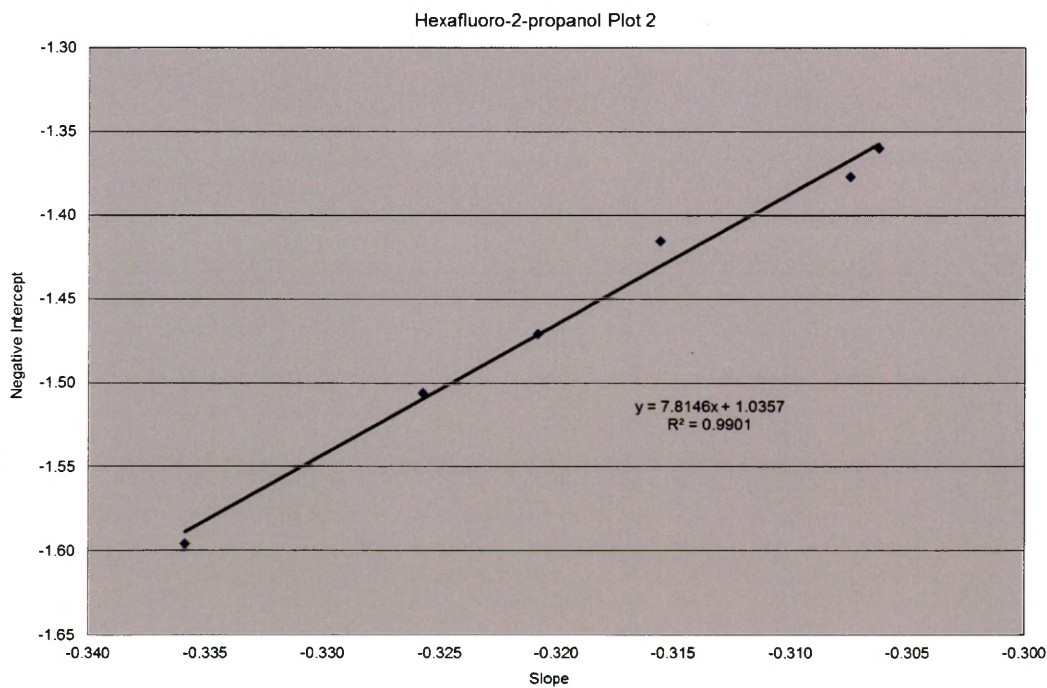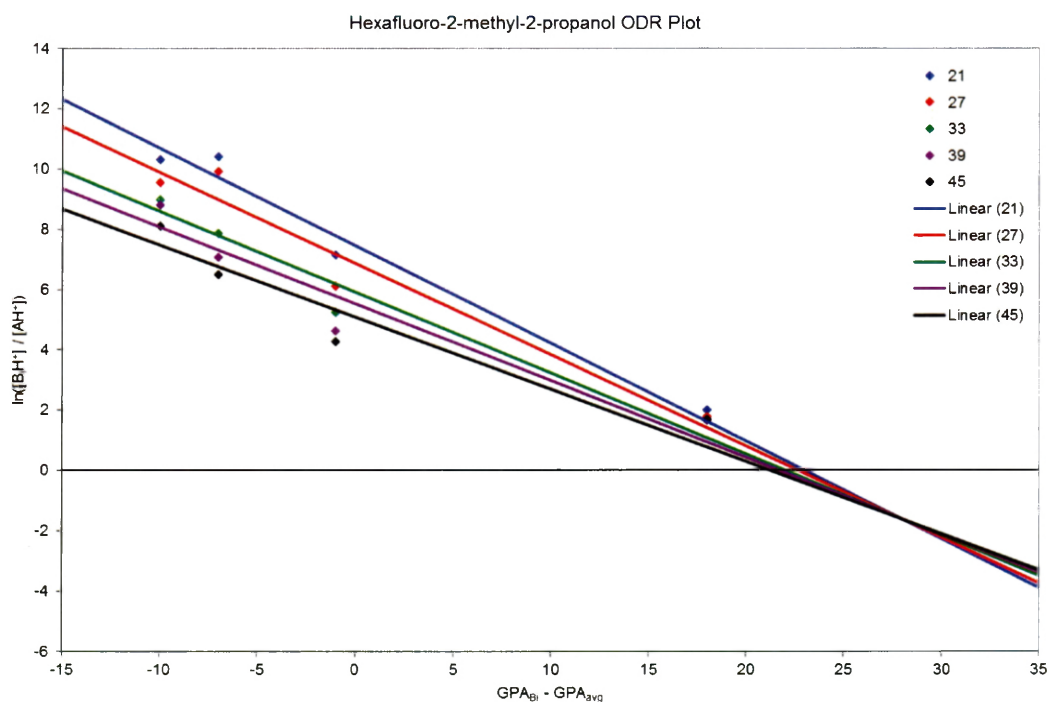
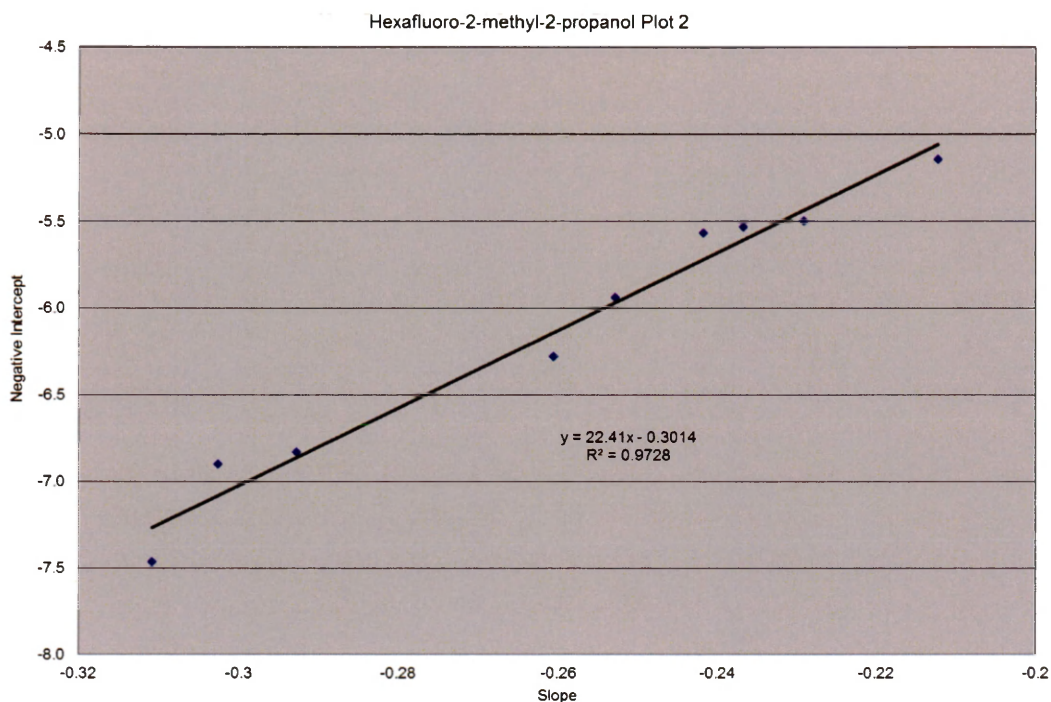The second kinetic method plot has an R^2 value of 0.980, which validates our choices in reference compounds.
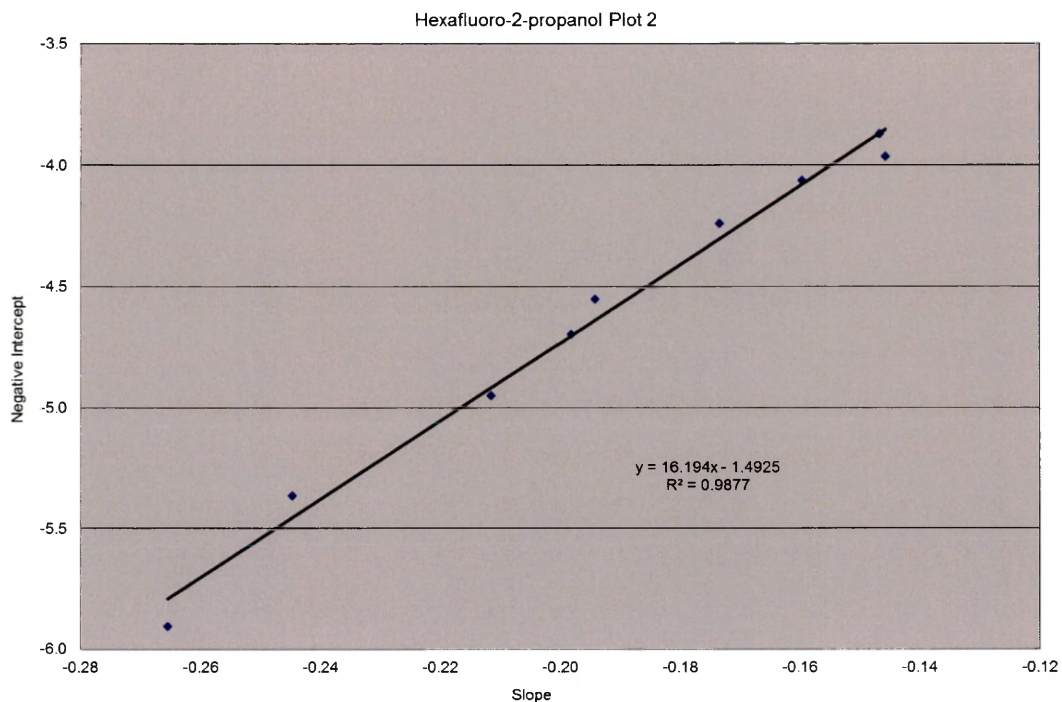
Figure 51. Kinetic Method Plot 2 for Hexafluoro-2-propanol on TSQ.

4.3.3.2 LCQ Results

Six reference compounds were used in the hexafluoro-2-propanol study on the ion trap mass spectrometer. The range of gas-phase acidities for the references was 24.0 kJ/mol. Shown below in Figure 52 is the ODR kinetic method plot 1, which determined the gas-phase acidity and ΔS values to be 1448.6 ± 10.2 kJ/mol and 8.4 ± 15.5 J/mol·K, respectively.
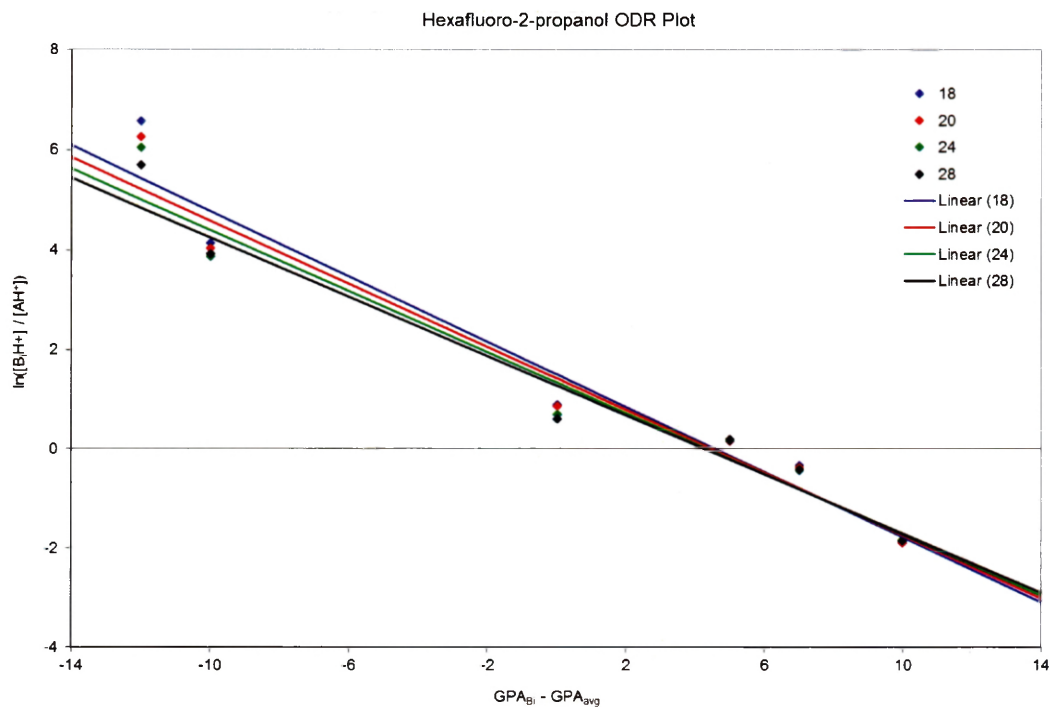
Figure 52. ODR KM Plot for Hexafluoro-2-propanol on LCQ.

Kinetic method plot 2, shown below, has an R^2 value of .990.

Figure 53. Kinetic Method Plot 2 for Hexafluoro-2-propanol on LCQ.

4.3.4 Hexafluoro-2-methyl-2-propanol

4.3.4.1 TSQ Results

Four reference acids were utilized in the hexafluoro-2-methyl-2-propanol study on the triple quadrupole. The range of the gas-phase acidities for the references was 28.0 kJ/mol. The ODR KM Plot 1 is shown below in Figure 54. ODR analysis for the gas-phase acidity and ΔS values yielded 1458.9 ± 34.5 kJ/mol and 14.2 ± 63.1 J/mol·K, respectively.

Figure 54. ODR KM Plot for Hexafluoro-2-methyl-2-propanol on TSQ.

The second kinetic method plot has an R^2 value of 0.973, which validates our choices in reference compounds.

Figure 55. KM Plot 2 for Hexafluoro-2-propanol on TSQ.

4.3.4.2 LCQ Results

Five reference compounds were used in the hexafluoro-2-methyl-2-propanol study on the ion trap mass spectrometer, with a range of 35.0 kJ/mol for the gas-phase acidity values. Shown below in Figure 56 is the ODR kinetic method plot 1, which determined the gas-phase acidity and ΔS values to be 1459.7 ± 12.0 kJ/mol and 24.0 ± 20.4 J/mol·K, respectively.
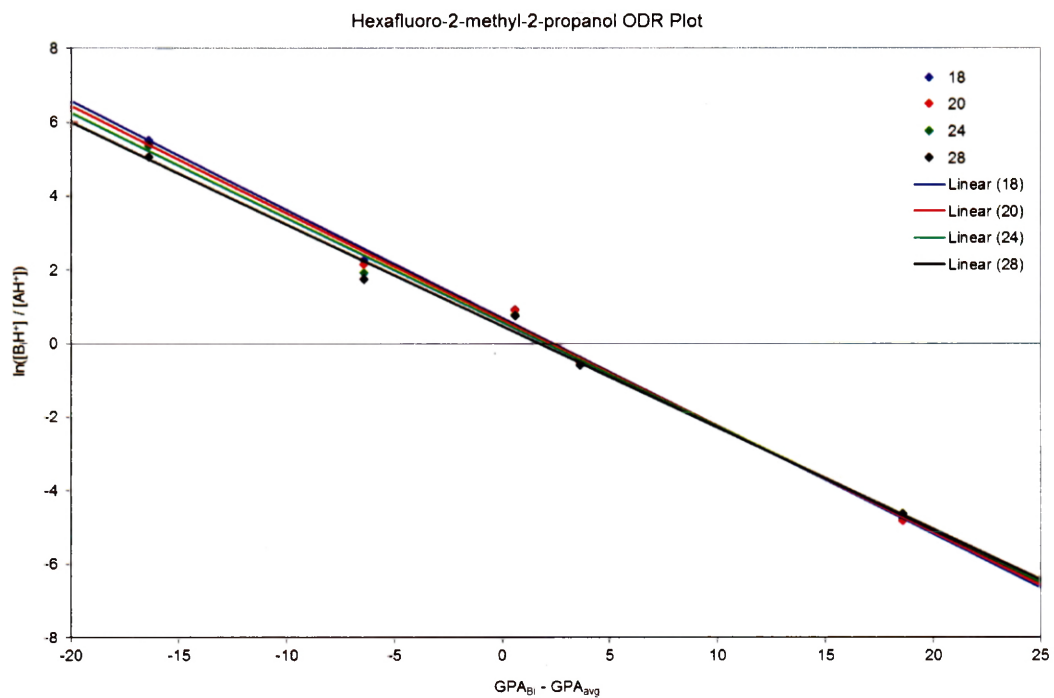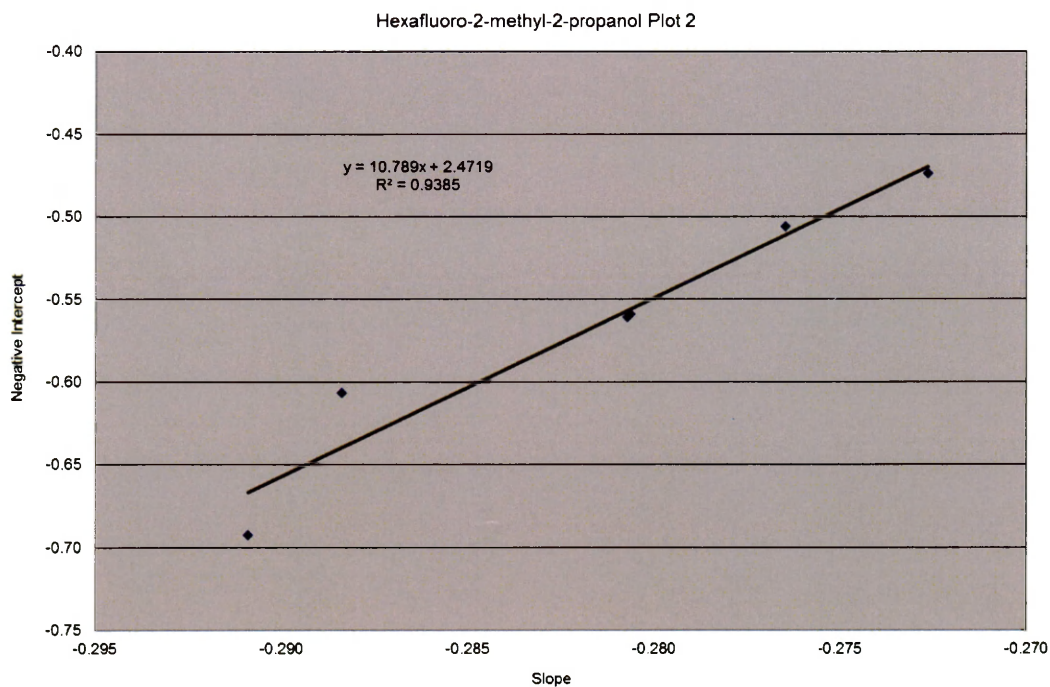
Figure 56. ODR KM Plot for Hexafluoro-2-methyl-2-propanol on LCQ.

Kinetic method plot 2, shown below, has an R^2 value of 0.939.

Figure 57. Kinetic Method Plot 2 for Hexafluoro-2-methyl-2-propanol on LCQ.

4.4 Discussion

While there are no known gas-phase acidity values for hexafluoro-2-methyl-2-propanol and perfluoro-tert-butyl alcohol, the acidity value for hexafluoro-2-propanol has been determined by Taft et al.[51] Using ion-molecule bracketing experiments, they determined the acidity for hexafluoro-2-propanol to be 1443. ± 8.8 kJ/mol. After uncertainty values are taken into account, the experimental values determined using the kinetic method were in very good agreement with the literature value. The gas-phase acidity values using the triple quadrupole and ion trap mass spectrometers were determined to be 1439.3 ± 10.0 and 1448.6 ± 10.2 kJ/mol, respectively.

The experimental values from both the triple quadrupole and ion trap mass spectrometers were in agreement to the theoretical values determined. Comparisons were also made between the two sets of experimental values and particularly for hexafluoro-2-methyl-2-propanol, the experimental values were very much identical, at 1458.9 ± 34.5 and 1459.7 ± 12.0 kJ/mol, for the triple quadrupole and ion trap, respectively. However, the uncertainty for the triple quadrupole was much higher than ideal. This could be due to the extrapolation that occurred in the analysis. If additional reference acids were used in the 1460-1470 kJ/mol range, the uncertainty would be lower and the data would be more robust. This issue was not as apparent for the ion trap, as a reference acid with an acidity of 1466 kJ/mol was used.

The kinetic method experiments performed on the trifluorinated species were not very successful. The theoretical acidity values for the species were

between 1500-1520 kJ/mol. It was difficult to produce a sufficient amount of dimer ions to isolate and fragment because of the weak acidity of those compounds. It seems that further modifications to the experimental conditions or setup should be done in order to be successful with the trifluorinated compounds.

Chapter 5. Conclusions and Future Work

Proton affinities were determined for ten proline-containing dipeptides using the extended kinetic method and orthogonal distance regression analysis in this thesis, as part of a larger study investigating the relationship between structure and gas-phase properties of protein amino acids. The proton affinity trend for the Pro-Xxx and Xxx-Pro dipeptides were Pro-Gly < Pro-Val < Pro-Ala < Pro-Phe < Pro-Leu < Pro-Asp and Gly-Pro < Ala-Pro < Leu-Pro < Phe-Pro, respectively. With respect to the trend, one must recognize that the uncertainties associated with each value result in a large overlap of proton affinities.

The entropy of the Pro-Xxx analytes affected the quality of the experimental data, shown by the large uncertainty values and extrapolation present in the first kinetic method plots. Overall, it was determined that the Pro-Xxx dipeptides had higher entropy values than the Xxx-Pro dipeptides.

Secondly, our assumption that Pro-Xxx dipeptides would have overall higher proton affinity values than their analogous Xxx-Pro dipeptides was proven. As proline-containing dipeptides have not been largely investigated for their gas-phase properties, the experimental results were compared to theoretical calculations, done by the Poutsma group at Old Dominion University. So far, the experimental and theoretical values are in excellent agreement.

Acidity values for three fluorinated alcohols, determined using the extended kinetic method and ODR analysis, were also presented in this thesis. Values were acquired on both the triple quadrupole and ion trap mass spectrometers and were in very good agreement, after taking into account the uncertainties associated with

each value. This consistency between instruments, in addition to comparisons with literature values, validates the experimental values presented. However, a major source of error in this study is the extrapolation that was required for the hexafluoro-2-methyl-2-propanol study on the triple quadrupole instrument. The large amount of extrapolation resulted in an uncertainty value of 34.5 kJ/mol.

For the proton affinity project, there is still much to be done. Proton affinities for only ten of the proline-containing dipeptides were investigated in this thesis. As mentioned, the majority of the commercially available proline-containing dipeptides were studied. In the future, the remaining analytes are to be synthesized using solid-phase peptide synthesis and studied using the extended kinetic method. Additionally, the Ionlab has been studying the proline analogs, azetidine-2-carboxylic acid and pipecolic acid, and intend to perform proton affinity measurements on the analogous dipeptides.

Regarding the gas-phase acidity project, changing experimental conditions like ionization source or other experimental parameters may be helpful. While the gas-phase acidities for three of the six fluorinated alcohols have been determined, extended kinetic method measurements for all six compounds on the same instrument is the most ideal option.
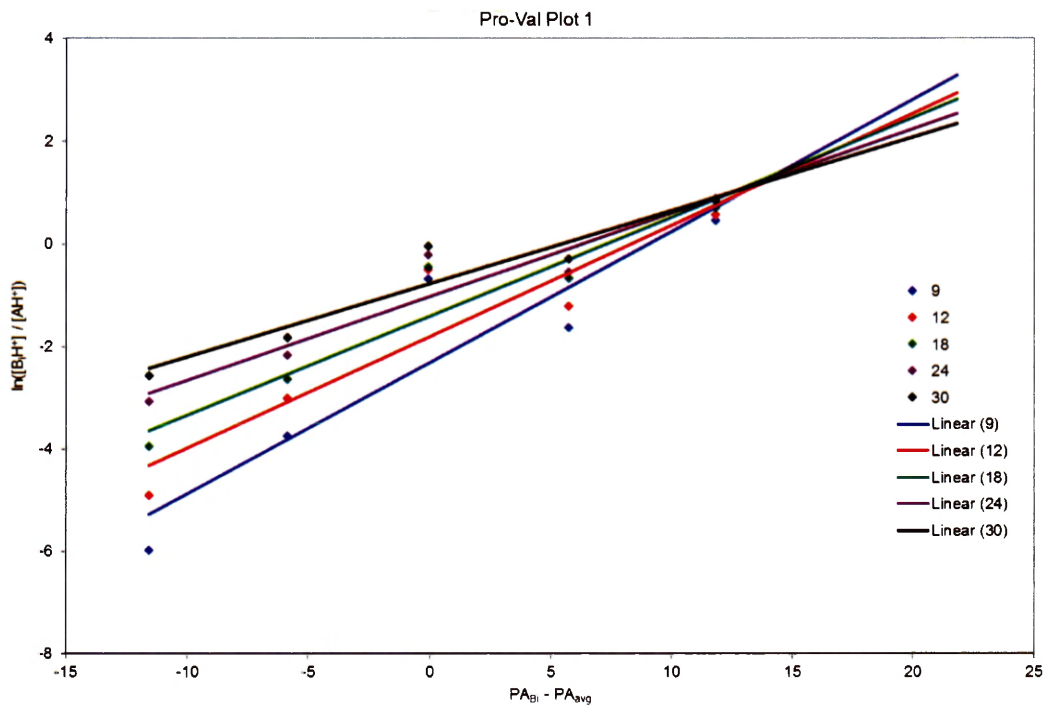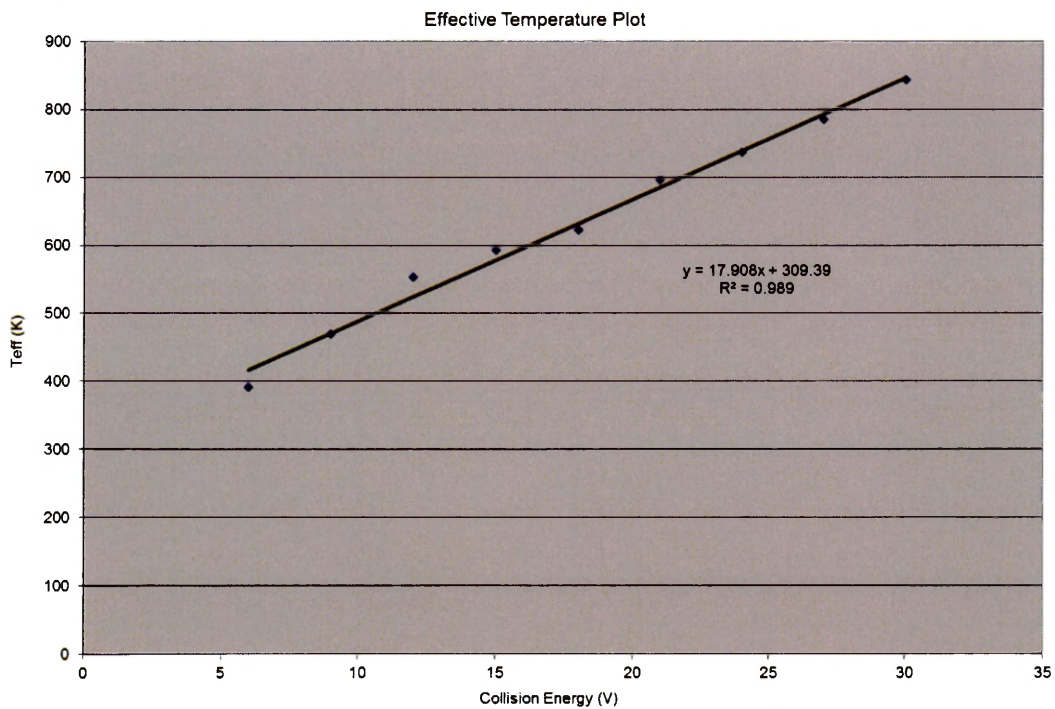
Appendix
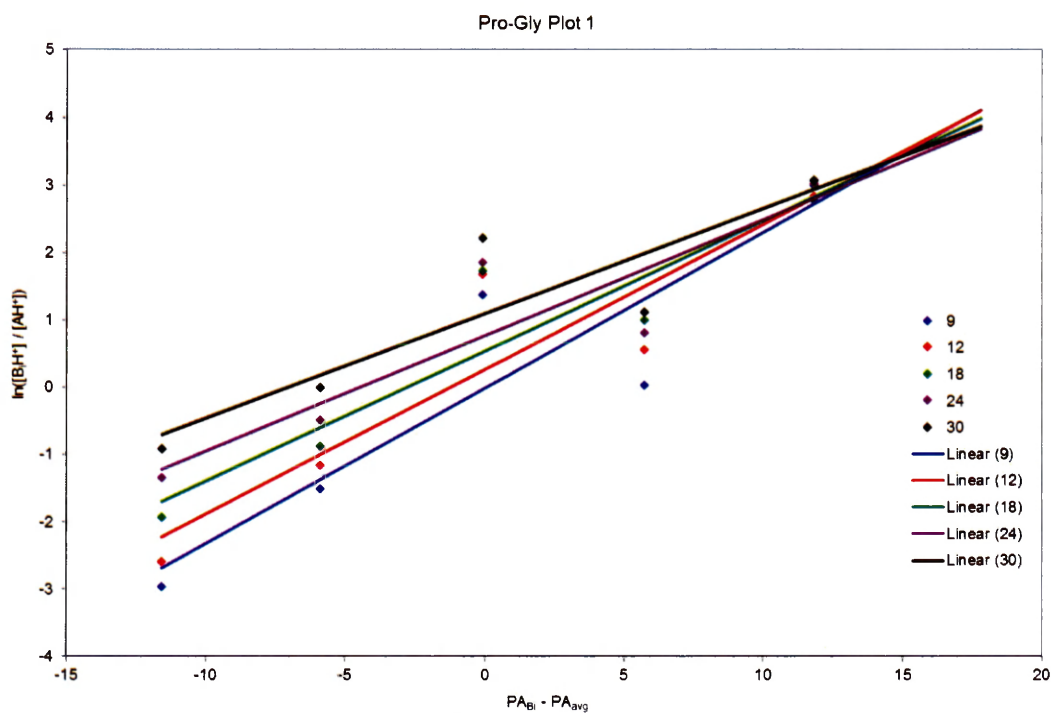
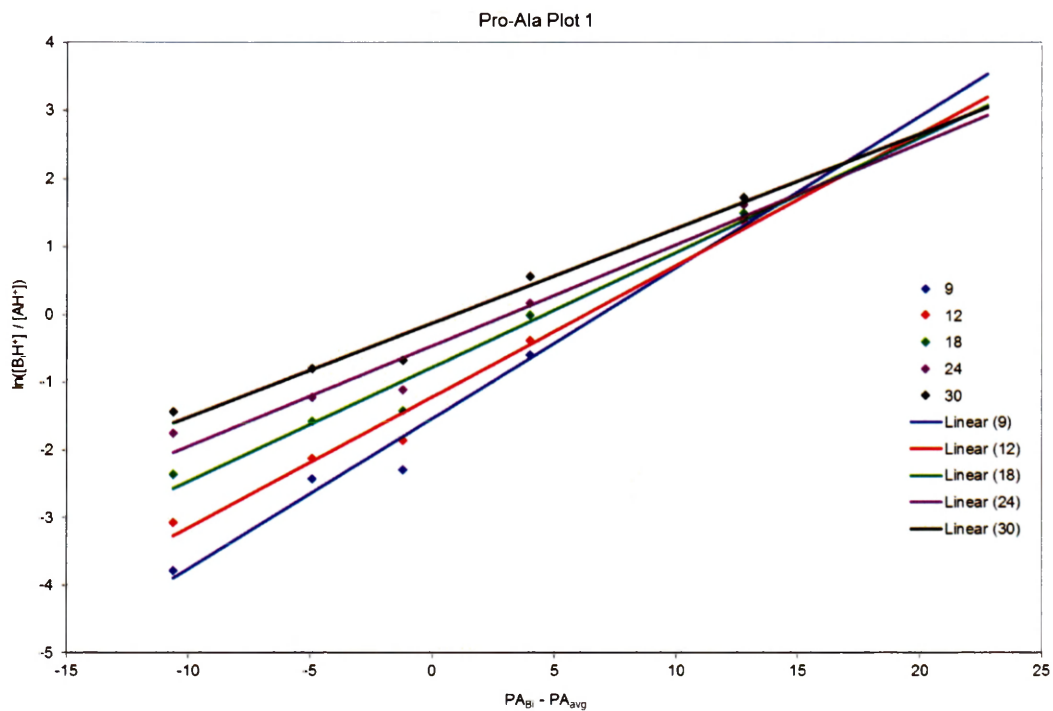*Kinetic Method Plot 1 for Pro-Gly.*
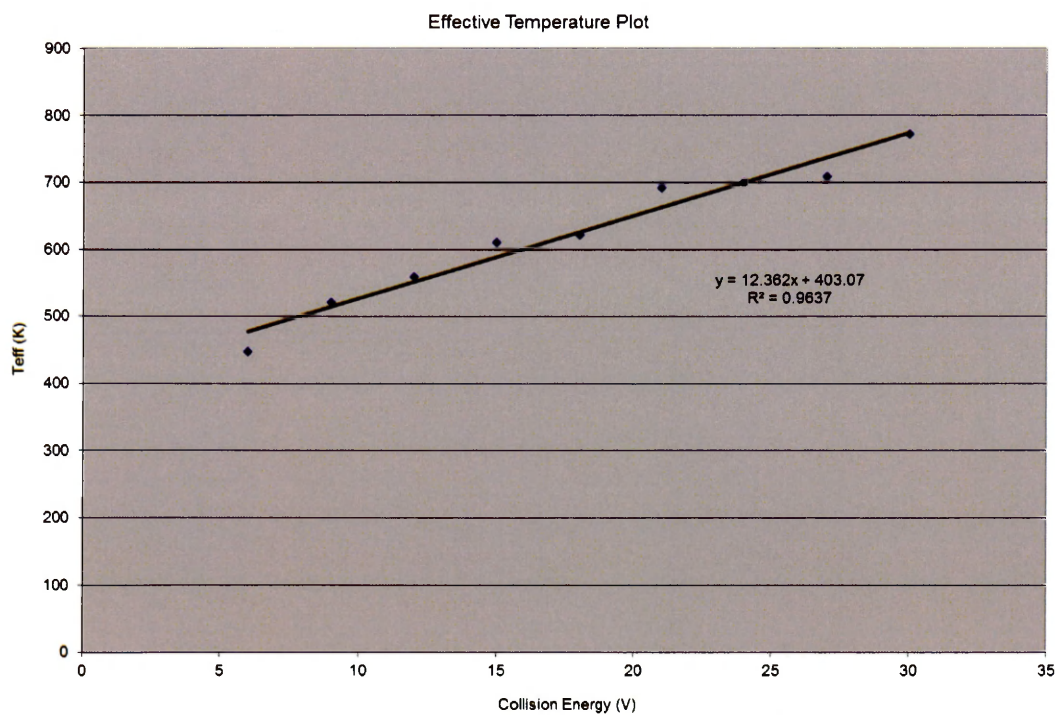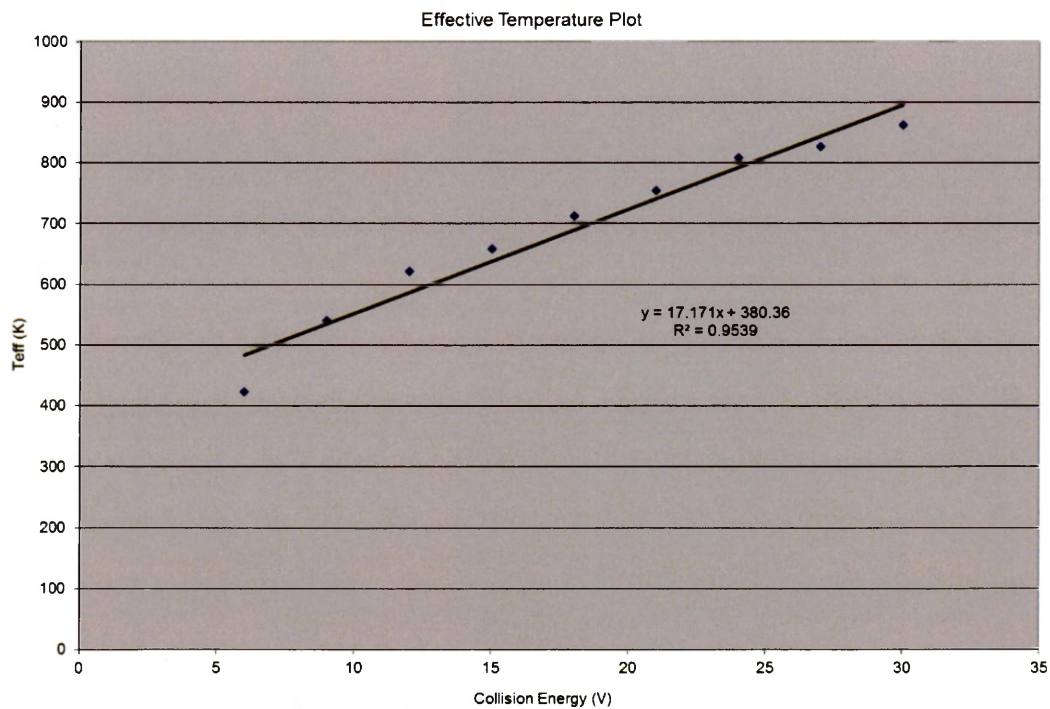

Effective Temperature Plot for Pro-Gly.

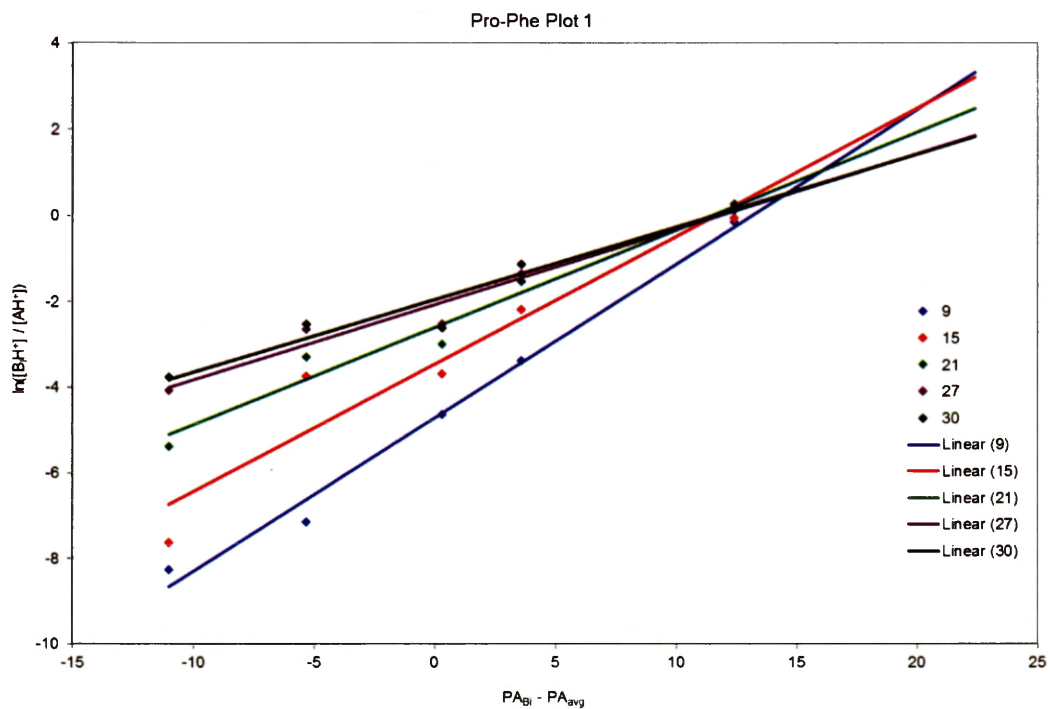*Kinetic Method Plot 1 for Pro-Val.*

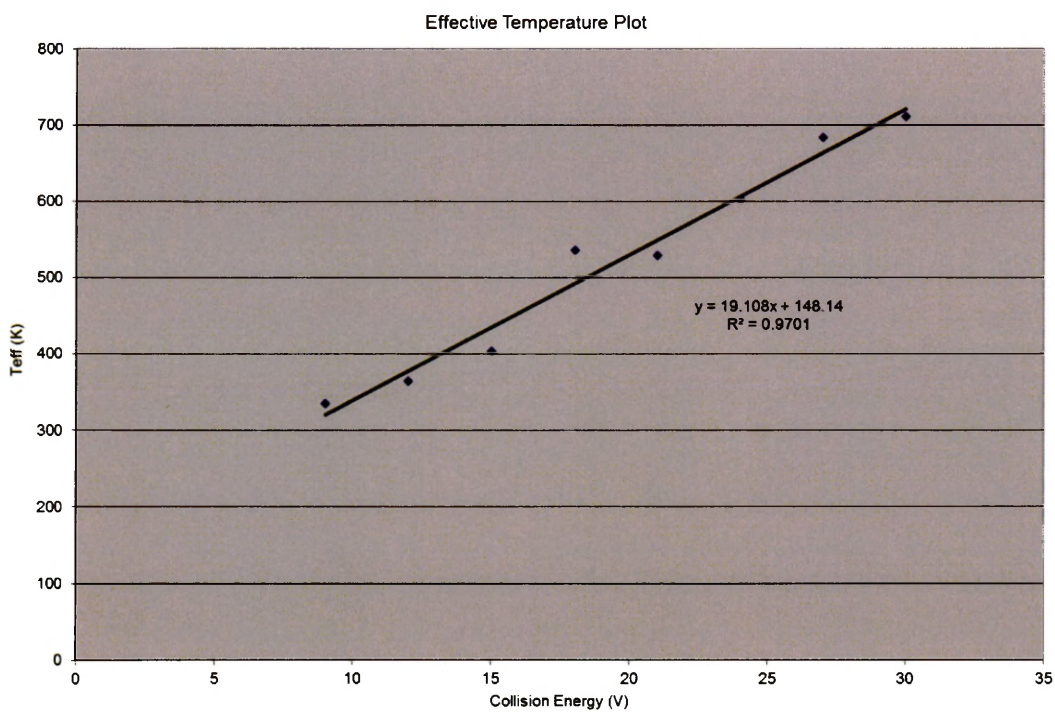

Effective Temperature Plot for Pro-Val.

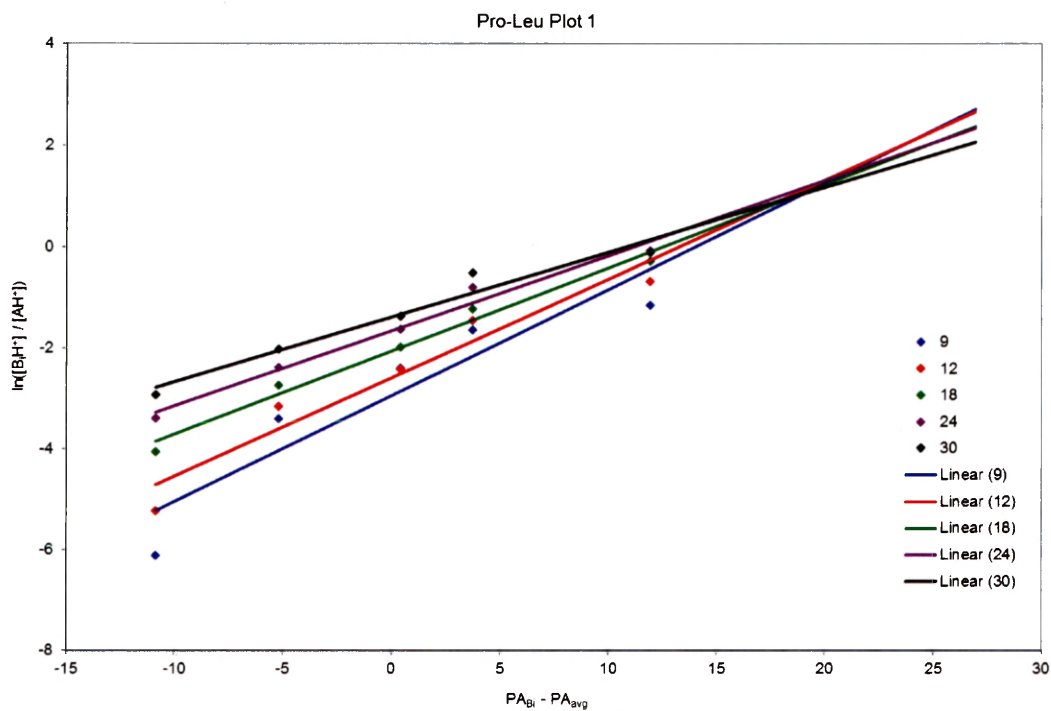*Kinetic Method Plot 1 for Pro-Ala.*

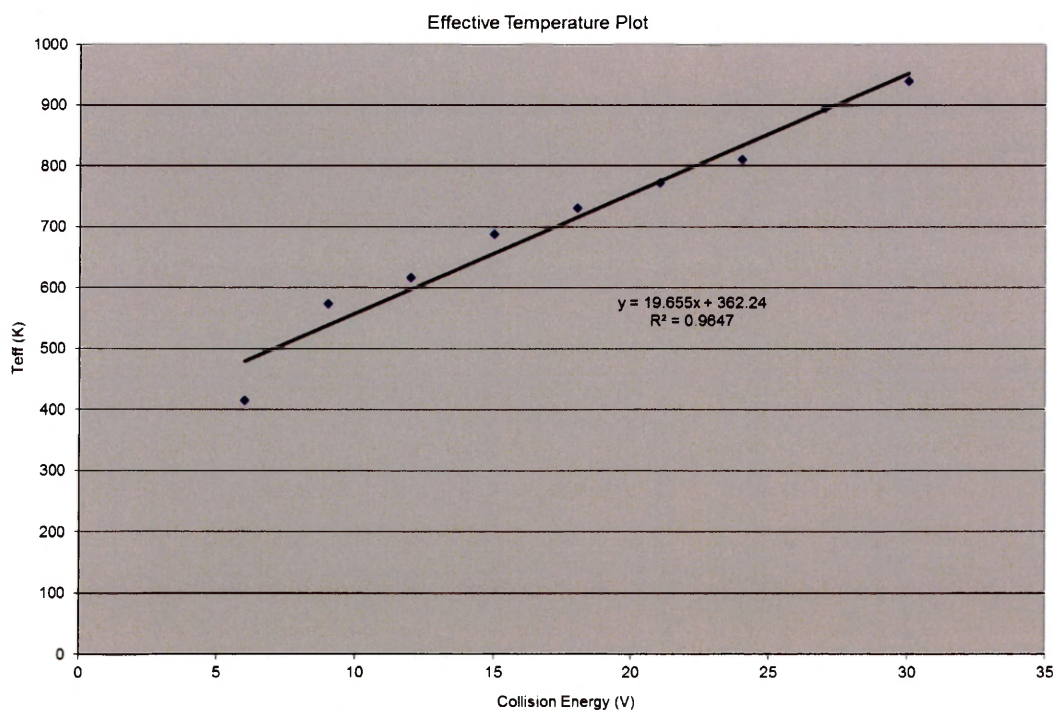*Effective Temperature Plot for Pro-Ala.*
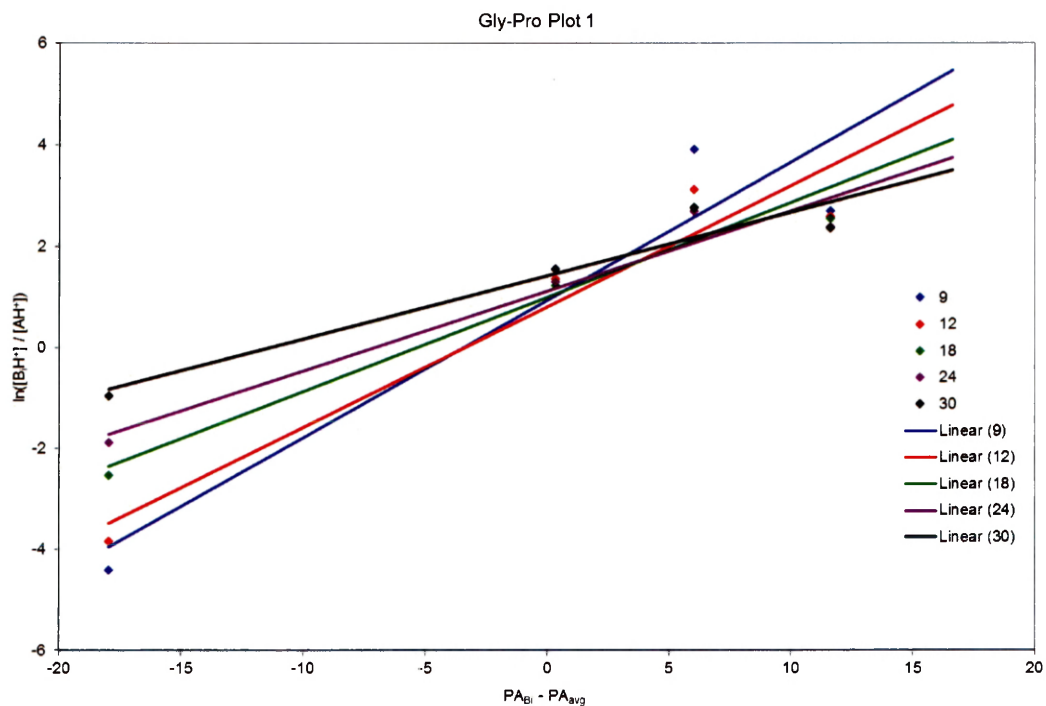
Kinetic Method Plot 1 for Pro-Phe.

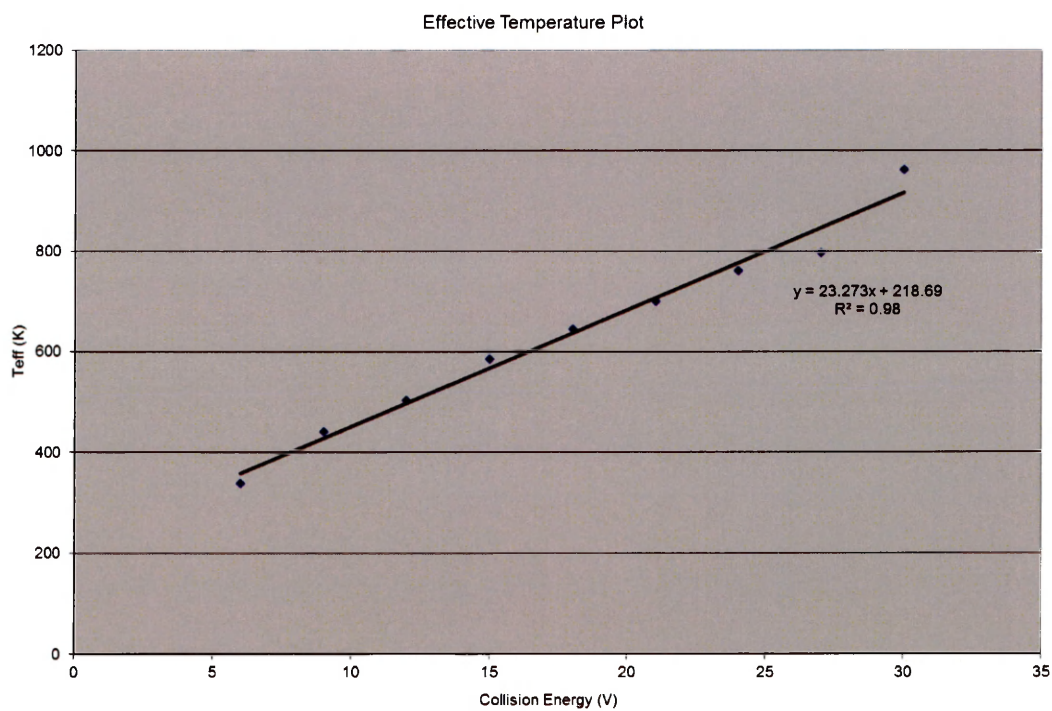*Effective Temperature Plot for Pro-Phe.*

Kinetic Method Plot 1 for Pro-Leu.

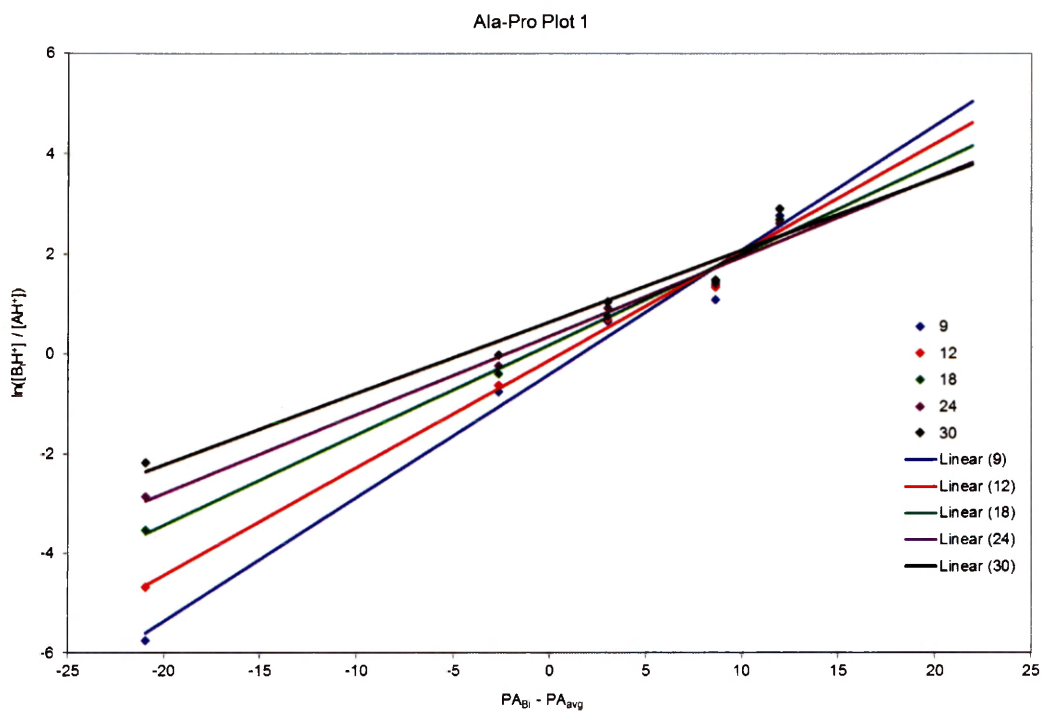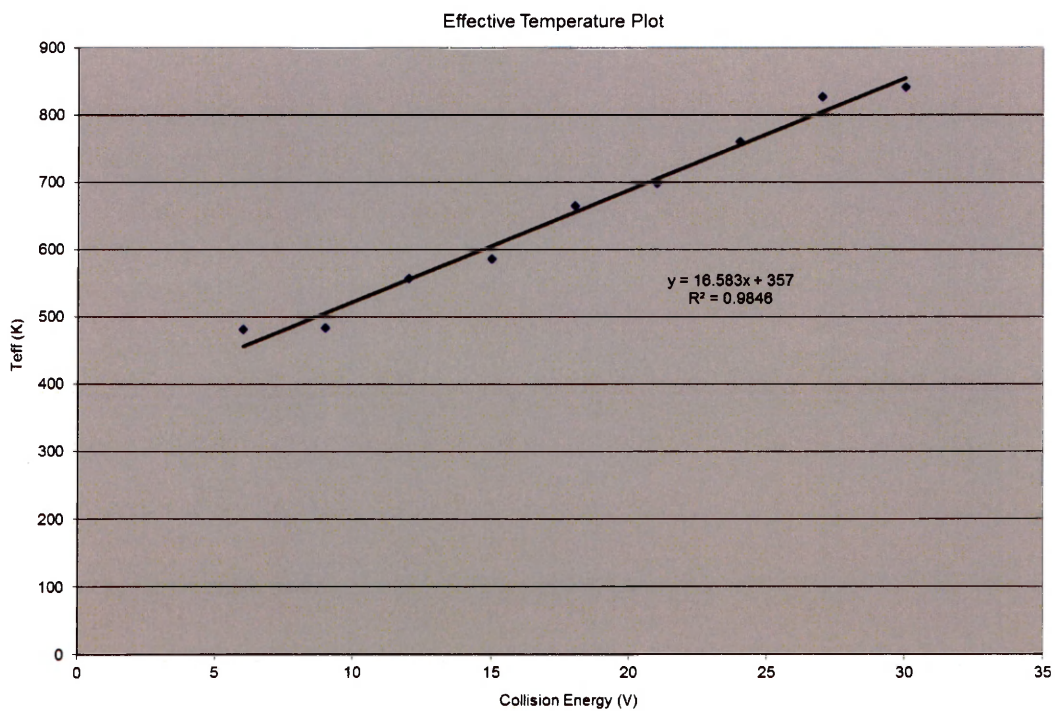*Effective Temperature Plot for Pro-Leu.*

83

Kinetic Method Plot 1 for Gly-Pro.

Effective Temperature Plot for Gly-Pro.
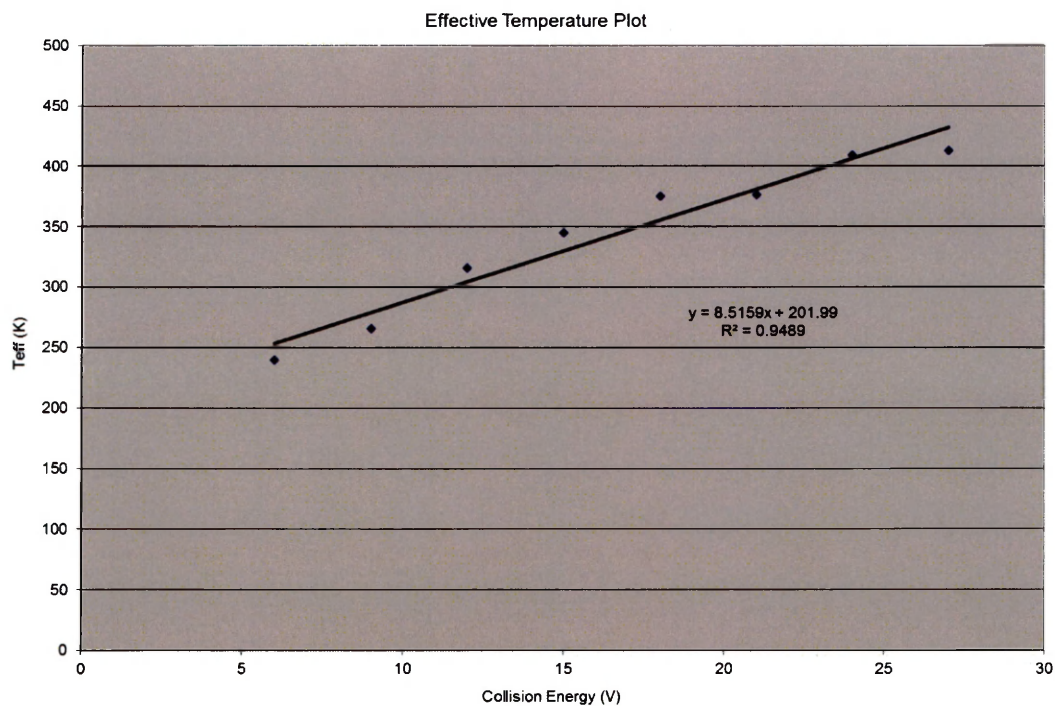
84

Kinetic Method Plot 1 for Ala-Pro.

Effective Temperature Plot for Ala-Pro.

85

Kinetic Method Plot 1 for Leu-Pro.

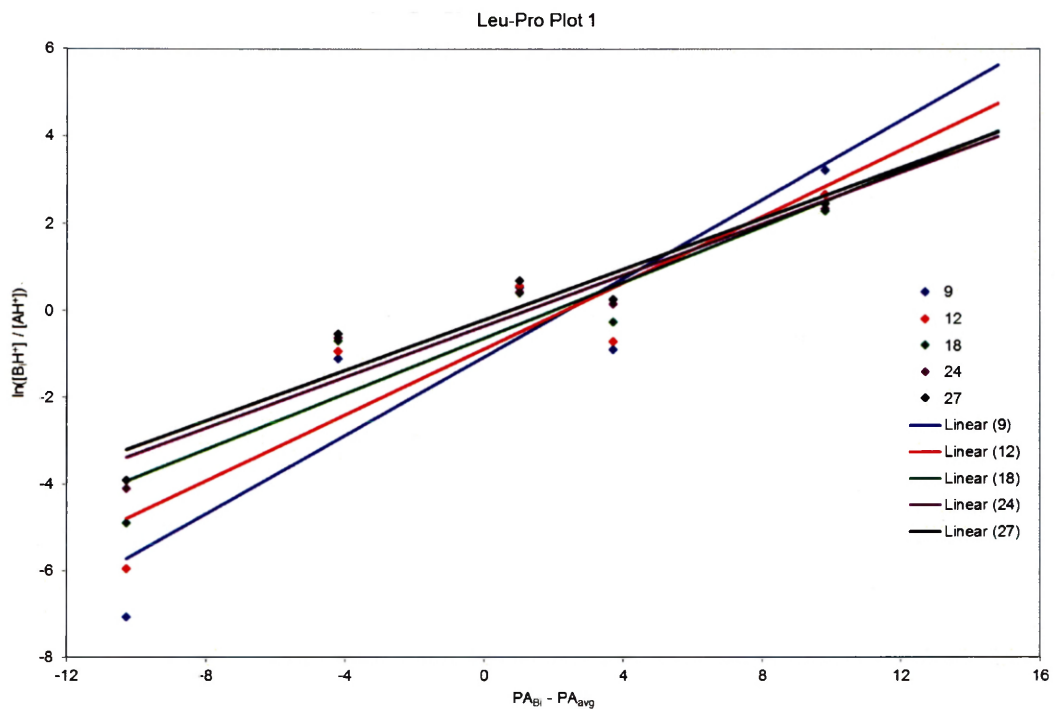*Effective Temperature Plot for Leu-Pro.*
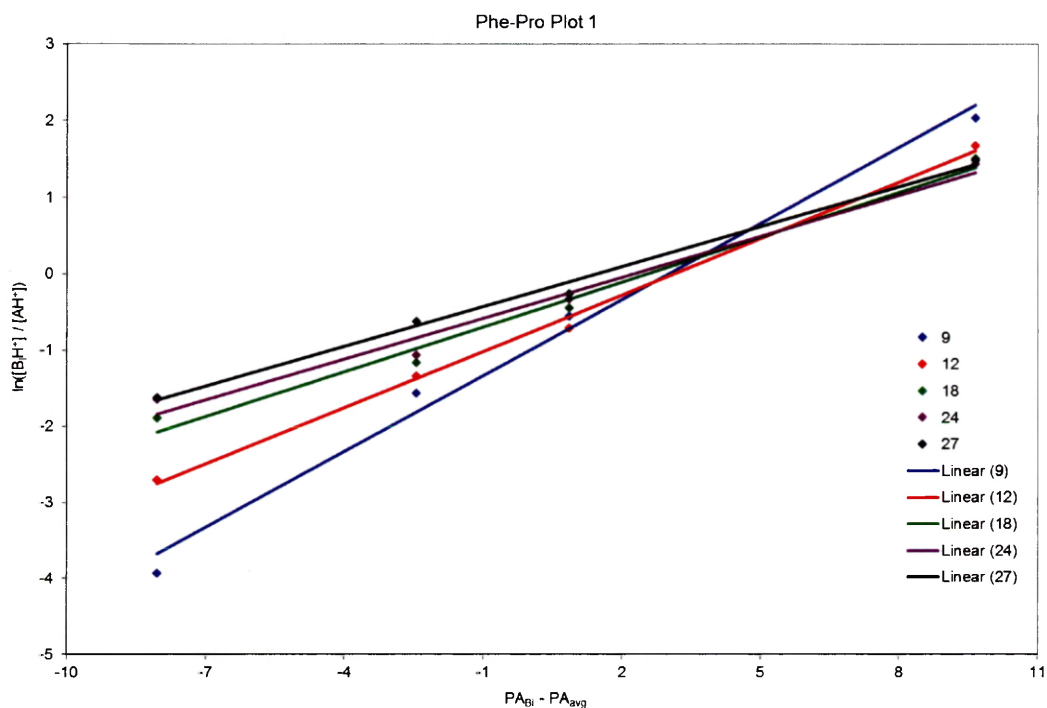
Kinetic Method Plot 1 for Phe-Pro.
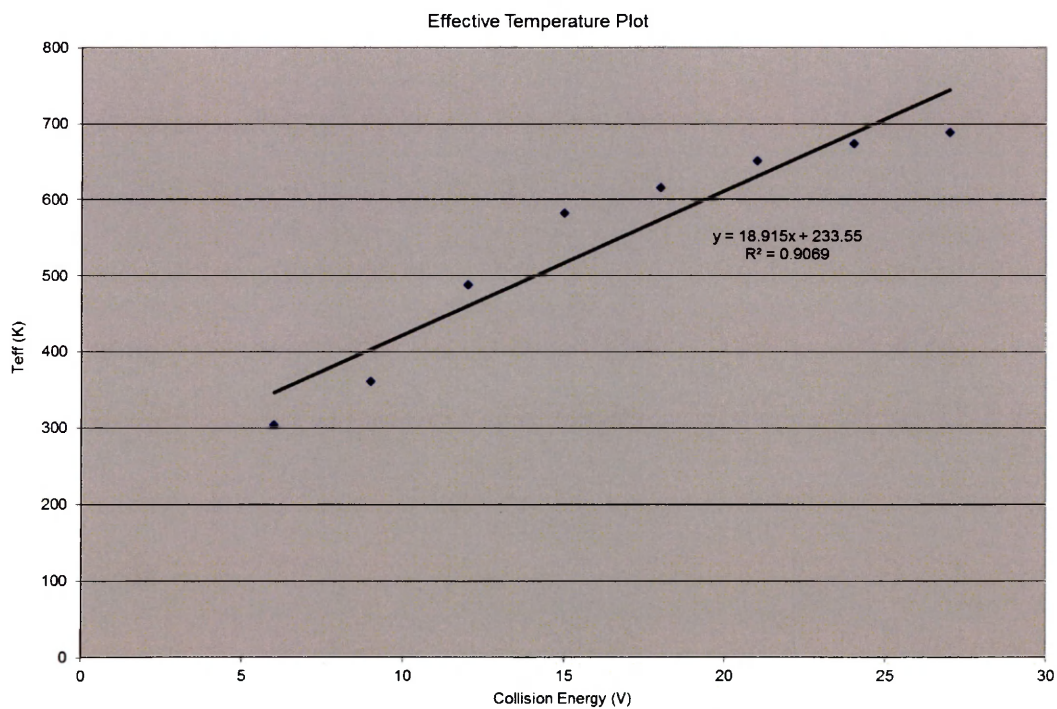
Effective Temperature Plot for Phe-Pro.
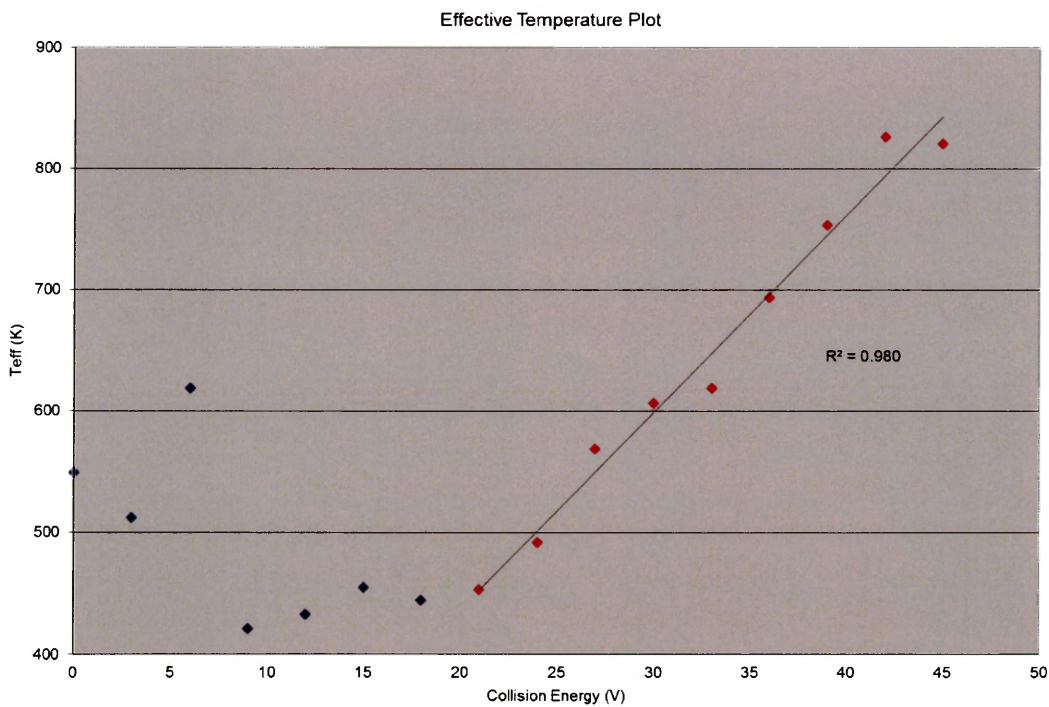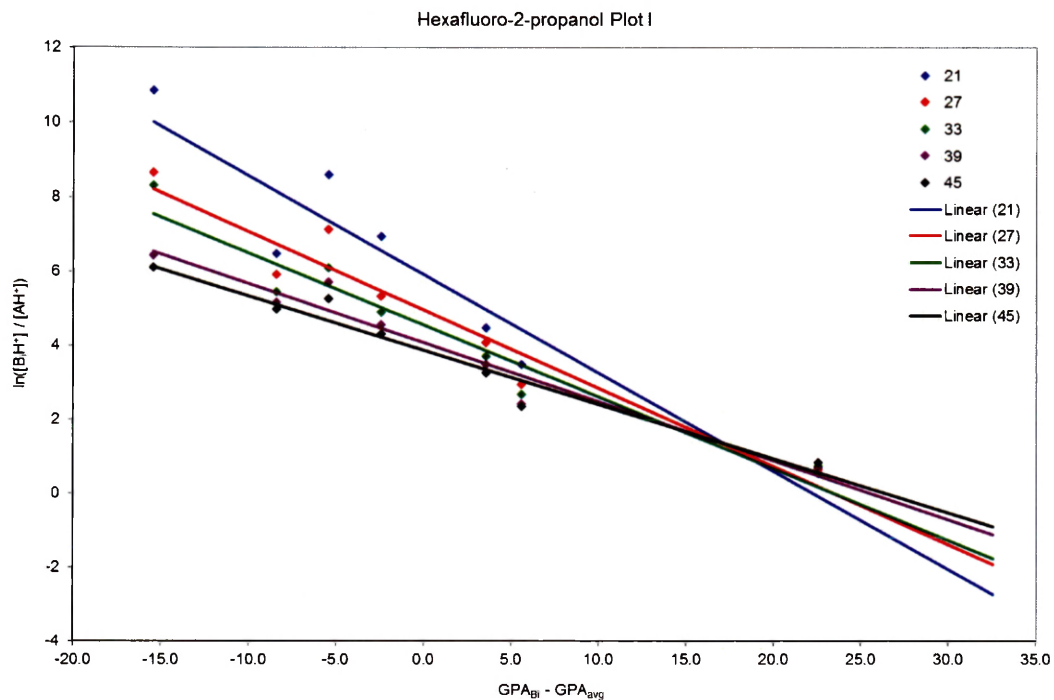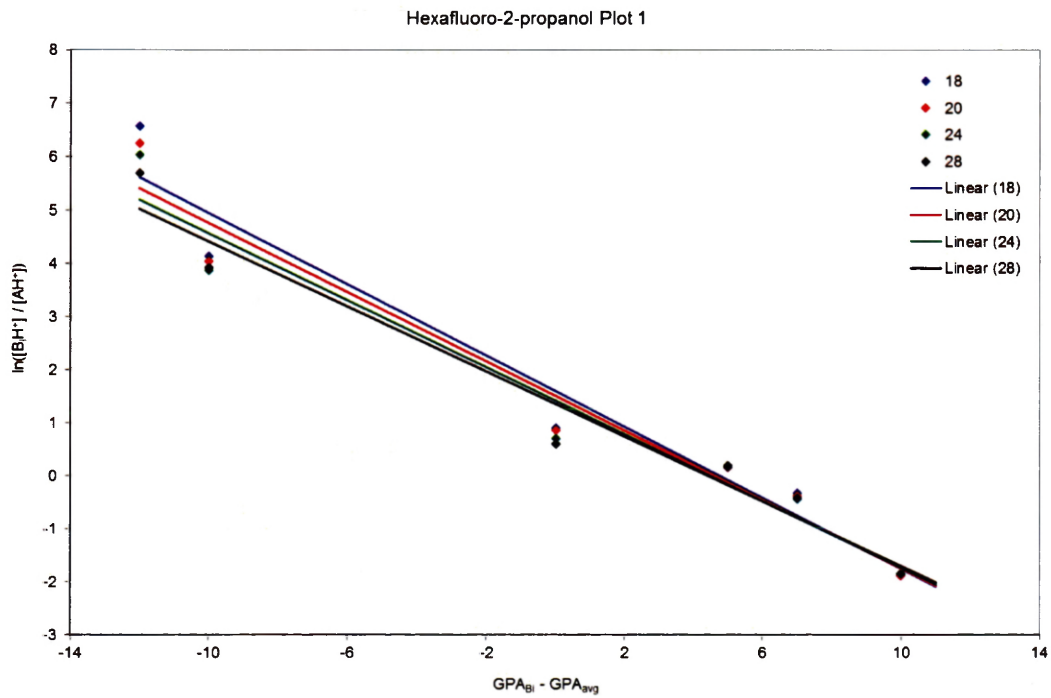
87

Kinetic Method Plot 1 for Hexafluoro-2-propanol on TSQ.

Effective Temperature Plot for Hexafluoro-2-propanol on TSQ.

88

Kinetic Method Plot 1 for Hexafluoro-2-propanol on LCQ.

Effective Temperature Plot for Hexafluoro-2-propanol on LCQ.

Kinetic Method Plot 1 for Hexafluoro-2-methyl-2-propanol on TSQ.

Effective Temperature Plot for Hexafluoro-2-methyl-2-propanol on TSQ.
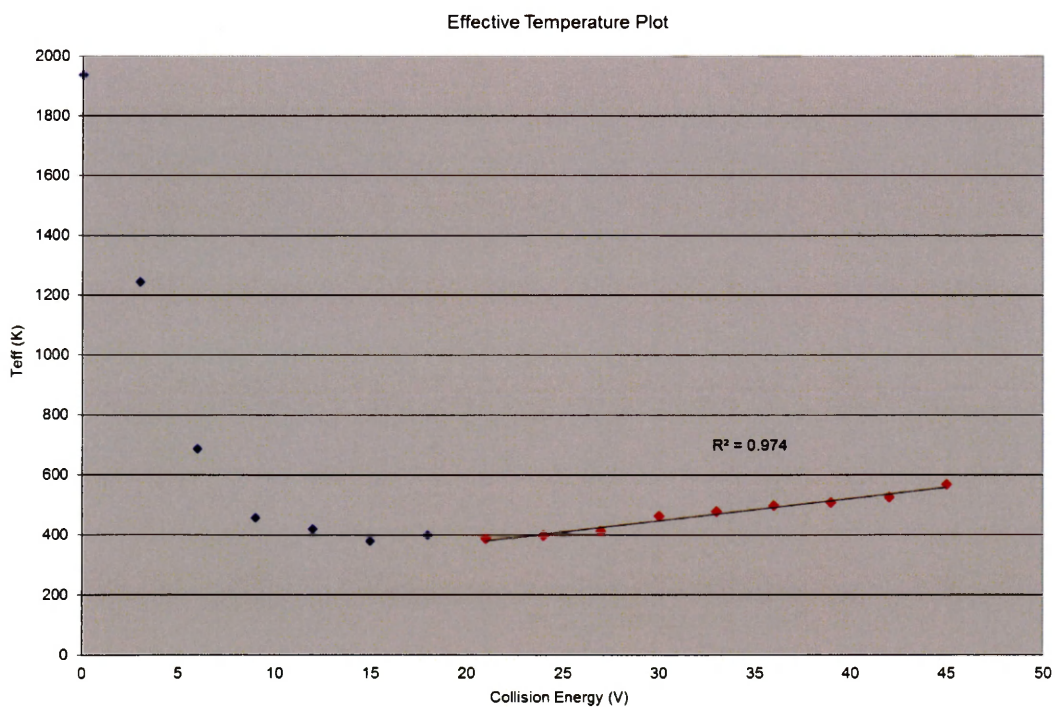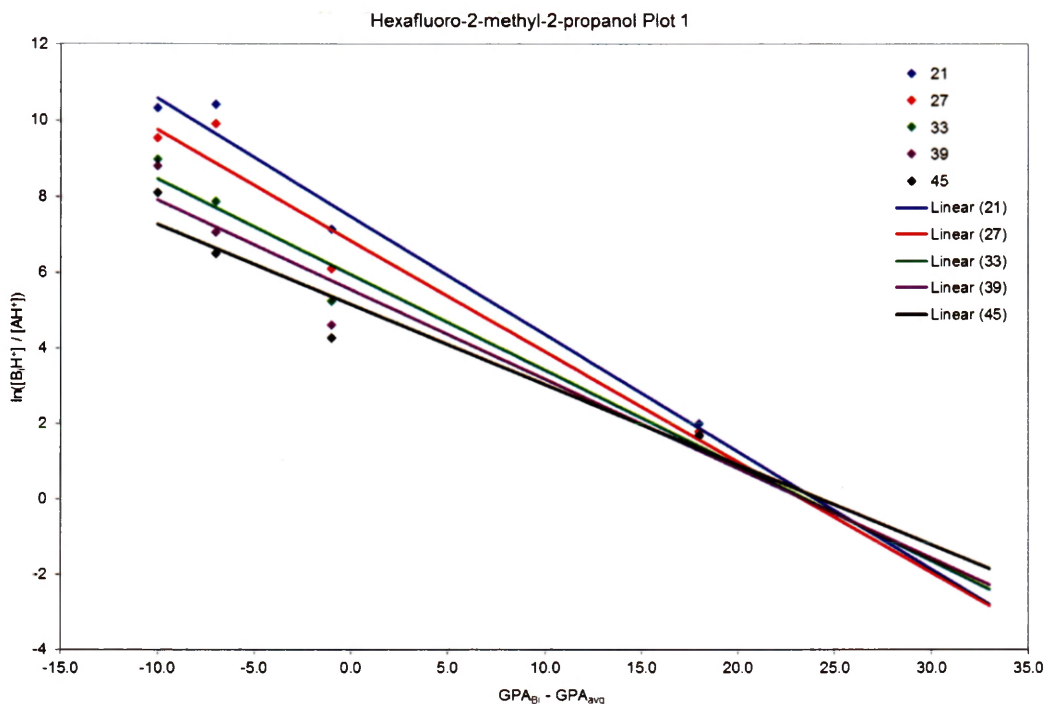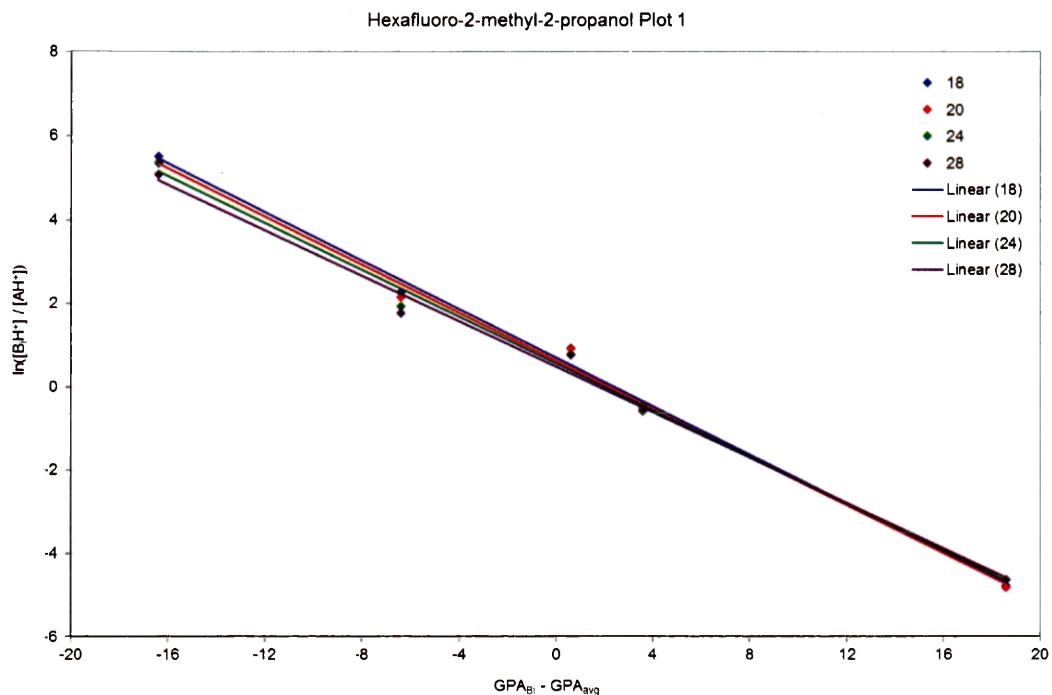
Kinetic Method Plot 1 for Hexafluoro-2-methyl-2-propanol on LCQ.
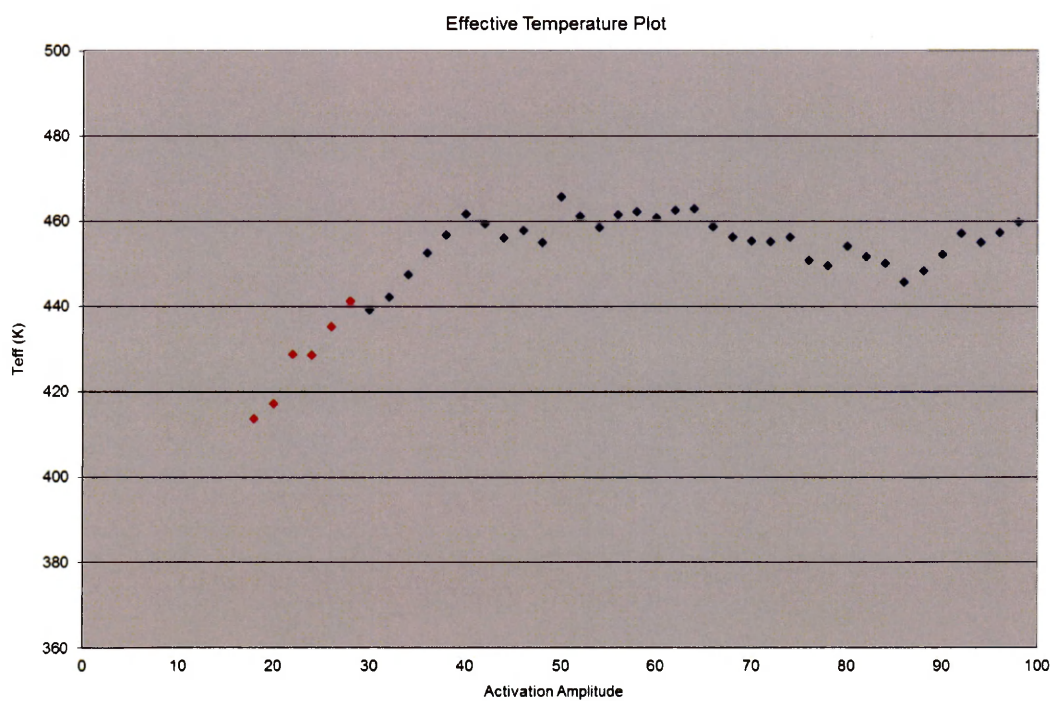
Effective Temperature Plot for Hexafluoro-2-methyl-2-propanol on LCQ.

References

(1)   Reichardt, C.; Welton, T. *Solvents and Solvent Effects in Organic Chemistry*; 4th ed.; Wiley-VCH: Germany, 2010.

(2)   Bowers, M. T. *Gas-Phase Ion Chemistry*; Academic Press: New York, 1979; Vol. 2.

(3)   Lias, S. G.; Bartmess, J. E.; Liebman, J. F.; Homes, J. F.; Levin, J. L.; Mallard, W. D. "Gas Phase Ion and Neutral Thermochemistry" *J. Phys. Chem. Ref. Data* **1988**, *17*, Suppl. 1.

(4)   Brauman, J. I.; Blair, L. K. "Gas-Phase Acidities of Amines" *J. Am. Chem. Soc.* **1971**, *93*, 3911.

(5)   Brauman, J. I.; Blair, L. K. "Gas-Phase Acidities of Alcohols" *J. Am. Chem. Soc.* **1970**, *92*, 5986.

(6)   de Hoffmann, E.; Stroobant, V. *Mass Spectrometry: Principles and Applications*; 3rd ed.; Wiley: Hoboken, 2007.

(7)   Fenn, J. B.; Mann, M.; Meng, C. K.; Wong, S. F.; Whitehouse, C. M. "Electrospray Ionization for Mass Spectrometry of Large Biomolecules" *Science* **1989**, *246*, 64.

(8)   Karas, M.; Hillenkamp, F. "Laser Desorption Ionization of Proteins with Molecular Masses Exceeding 10,000 Daltons." *Anal. Chem.* **1988**, *60*, 2299.

(9)   Nourse, B. D.; Cooks, R. G. "Proton Affinity Determinations Using the Kinetic Method in an Ion Trap Mass Spectrometer" *Int. J. Mass Spectrom. Ion Proc.* **1991**, *106*, 249.

(10)   Bartmess, J. E.; Scott, J. A.; McIver Jr., R. T. "Scale of Acidities in the Gas Phase from Methanol to Phenol" *J. Am. Chem. Soc.* **1979**, *101*, 6046.

(11)   Cooks, R. G.; Patrick, J. S.; Kotiaho, T.; McLuckey, S. A. "Thermochemical Determinations by the Kinetic Method" *Mass Spectrom. Rev.* **1994**, *18*, 287.

(12)   Cheng, X. H.; Wu, Z.; Fenselau, C. "Collision Energy Dependence of Proton Bound Dimer Dissociation: Entropy Effects, Proton Affinities and Intramolecular Hydrogen Bonding of Protonated Peptides." *J. Am. Chem. Soc.* **1993**, *115*, 4884.

(13)   Cerda, B. A.; Wesdemiotis, C. "The Relative Copper(I) Ion Affinities of Amino Acids in the Gas Phase." *J. Am. Chem. Soc.* **1995**, *117*, 9734.

(14)   Armentrout, P. B. "Entropy Measurements and the Kinetic Method: A Statistically Meaningful Approach" *J. Am. Soc. Mass Spectrom.* **2000**, *11*, 371.

(15)   Kuntz, A. F.; Boynton, A. W.; David, G. A.; Colyer, K. E.; Poutsma, J. C. "Proton Affinities of Proline Analogs Using the Kinetic Method with Full Entropy Analysis" *J. Am. Soc. Mass Spectrom.* **2002**, *13*, 72.

(16)   Schroeder, O. E.; Andriole, E. J.; Carver, K. L.; Poutsma, J. C. "The Proton Affinity of Lysine Analogs Using the Extended Kinetic Method" *J. Phys. Chem. A* **2004**, *108*, 326.

(17)   Andriole, E. J.; Colyer, K. E.; Cornell, E.; Poutsma, J. C. "Proton Affinity of Canavanine and Canaline, Oxy-analogs of Arginine and Ornithine, from the Extended Kinetic Method. " *J. Phys. Chem. A* **2006**, *110*, 11501.

(18)   Jones, C. M.; Bernier, M.; Carson, E.; Colyer, K. E.; Metz, R.; Pawlow, A.; Wischow, E.; Webb, I.; Andriole, E. J.; Poutsma, J. C. "Gas-phase Acidities of the 20 Protein Amino Acids" *Int. J. Mass Spectrom.* **2007**, *267*, 54.

(19)   Webb, I.; Muetterties, C.; Platner, C. B.; Poutsma, J. C. "Gas-Phase Acidities of Lysine Homologues and Proline Analogs from the Extended Kinetic Method" *Int. J. Mass Spectrom.* **2012**, *316-318*, 126.

(20)   Muetterties, C.; Drissi Touzani, A.; Hardee, I.; Huynh, K. T.; Poutsma, J. C. "Gas-Phase Acid-Base Properties of 1-Aminocycloalkane-1-Carboxylic Acids from the Extended Kinetic Method." *Int. J. Mass Spectrom.* **2014**, DOI: 10.1016/j.ijms.2014.07.010.

(21)   Muetterties, C.; Janiga, A.; Huynh, K. T.; Pisano, M. G.; Tripp, V. T.; Young, D. D.; Poutsma, J. C. "Gas-Phase Acid-Base Properties of Homocysteine, Homoserine, 5-Mercaptonorvaline, and 5-Hydroxynorvaline from the Extended Kinetic Method" *Int. J. Mass Spectrom.* **2014**, *369*, 71.

(22)   Raulfs, M. M.; Breci, L.; Bernier, M.; Hamdy, O.; Janiga, A.; Wysocki, V. H.; Poutsma, J. C. "Investigations of the Mechanism of the "Proline Effect" in Mass Spectrometry Peptide Fragmentation Experiments: The Pipecolic Acid Effect."" *J. Am. Soc. Mass Spectrom.* **2014**, *25*, 1705.

(23)   Arrington, J. V.; Straus, R. N.; Reynolds, P. F.; Poutsma, J. L.; Marzluff, E.; Poutsma, J. C. "Gas-Phase Hydrogen-Deuterium Exchange Behavior of Lysine Homologues" *Int. J. Mass Spectrom.* **2012**, *330-332*, 200.

(24)   Meng, C. K.; Mann, M.; Fenn, J. B. "Of Protons or Proteins." *Z. Phys. D* **1988**, *10*, 361.

(25)   Schroeder, O. E.; Wind, J. J.; Poutsma, J. C. In *52nd American Society for Mass Spectrometry Conference on Mass Spectrometry and Allied Topics* Nashville, TN, 2004.

(26)   Lias, S. G.; Bartmess, J. E.; Liebman, J. F.; Holmes, J. L.; Levin, R. D.; Mallard, W. G. *Ion Energetics Data* In *NIST Chemistry Webbook, NIST Standard Reference Database Number 69*; Mallard, W. G., Lindstrom, P. J., Eds.; National Institute of Standards and Technology: Gaithersburg, MD, 20899 (http://webbook.nist.gov), 1999.

(27)   Ervin, K. M.; Armentrout, P. B. "Systematic and Random Errors in Ion Affinities and Activation Entropies from the Extended Kinetic Method" *J. Mass Spectrom.* **2004**, *39*, 1004.

(28)   *PCModel* Serena Software, **2006**.

(29)   Frisch, M. J.; Trucks, G. W.; Schlegel, H. B.; Scuseria, G. E.; Robb, M. A.; Cheeseman, J. R.; Zakrzewski, V. G.; Montgomery Jr., J. A.; Stratmann, R. E.; Burant, J. C.; Dapprich, S.; Millam, J. M.; Daniels, A. D.; Kudin, K. N.; Strain, M. C.; Farkas, O.; Tomasi, J.; Barone, V.; Cossi, M.; Cammi, R.; Mennucci, B.; Pomelli, C.; Adamo, C.; Clifford, S.; Ochterski, J.; Petersson, G. A.; Ayala, P. Y.; Cui, Q.; Morokuma, K.; Malick, D. K.; Rabuck, A. D.; Raghavachari, K.; Foresman, J. B.; Cioslowski, J.; Ortiz, J. V.; Baboul, A. G.; Stefanov, B. B.; Liu, G.; Liashenko, A.; Piskorz, P.; Komaromi, I.; Gomperts, R.; Martin, R. L.; Fox, D. J.; Keith, T.; Al-Laham, M. A.; Peng, C. Y.; Nanayakkara, N.; Challacombe, M.; Gill, P. M. W.; Johnson, B.; Chen, W.; Wong, M. W.; Andres, J.

L.; Gonzalez, C.; Head-Gordon, M.; Replogle, E. S.; Pople, J. A. *Gaussian 98* version A.9 Gaussian, Inc, Pittsburgh, PA **1998**.

(30)   Becke, A. D. "Density Functional Thermochemistry. III. The Role of Exact Exchange." *J. Chem. Phys.* **1993**, *98*, 5648.

(31)   Lee, C.; Yang, W.; Parr, R. G. "Development of the Colle-Salvetti Correlation Energy Formula into a Functional of the Electron Density" *Phys. Rev. B.* **1988**, *37*, 785.

(32)   Stryer, L. *Biochemistry*; 3rd ed.; W. H. Freeman and Co.: New York, 1988.

(33)   Hunt, S. *Chemistry and Biochemistry of the Amino Acids*; Chapman and Hall: London, 1985.

(34)   Rubenstein, E. "Biological Effects of and Clinical Disorders Caused by Nonprotein Amino Acids" *Medicine* **2000**, *79*, 80.

(35)   Gorman, G. S.; Amster, I. J. "Gas Phase Basicity Measurements of Dipeptides that Contain Valine" *J. Am. Chem. Soc.* **1993**, *115*, 5729.

(36)   McKiernan, J. W.; Beltrame, C. E.; Cassady, C. J. "Gas-Phase Basicities of Serine and Dipeptides of Serine and Glycine" *J. Am. Soc. Mass Spectrom.* **1994**, *5*, 718.

(37)   Cassaday, C. J.; Carr, S.; Zhang, K.; Chung-Phillips, A. "Experimental and Ab Initio Studies on Protonations of Alanine and Small Peptides of Alanine and Glycine" *J. Org. Chem.* **1995**, *60*, 1704.

(38)   Ewing, N. P.; Zhang, X.; Cassady, C. J. "Determination of the Gas-Phase Basicities of Proline and its Di- and Tripeptides with Glycine: The Enhanced Basicity of Prolylproline" *J. Mass Spectrom.* **1996**, *31*, 1345.

(39)   Schwartz, B. L.; Bursey, M. M. "Some Proline Substituent Effects in the Tandem Mass Spectrum of Protonated Pentaalanine" *Biol. Mass Spectrom.* **1992**, *21*, 92.

(40)   Loo, J. A.; Edmonds, C. A.; Smith, R. D. "Tandem Mass Spectrometry of Very Large Molecules. 2. Dissociation of Multiply Charged Proline-Containing Proteins from Electrospray Ionization" *Anal. Chem.* **1993**, *65*, 425.

(41)   Vaisar, T.; Urban, J. "Probing the Proline Effect in CID of Protonated Peptides" *J. Mass Spectrom.* **1996**, *31*, 1185.

(42)   Schaaff, T. G.; Cargile, B. J.; Stephanson Jr., J. L.; A., M. S. "Ion Trap Activation of the $(M+2H)^{2+}$ and $(M+17H)^{17+}$ Ions of Human Hemoglobin b-Chain." *Anal. Chem.* **2000**, *72*, 899.

(43)   Breci, L. A.; Tabb, D. L.; Yates, J. R. I.; Wysocki, V. H. "Cleavage N-Terminal to Proline: Analsis of a Database of Peptide Tandem Mass Spectra" *Anal. Chem.* **2003**, *75*, 1963.

(44)   Grewal, R. N.; El Aribi, E. H.; Harrison, A. G.; Siu, K. W. M.; Hopkinson, A. C. "Fragmentation of Protonated Tripeptides: The Proline Effect Revisited" *J. Phys. Chem. B.* **2004**, *108*, 4899.

(45)   Harrison, A. G.; Young, A. B. "Fragmentation Reactions of Deprotonated Peptides Containing Proline. The Proline Effect" *J. Mass Spectrom.* **2005**, *40*, 1173.

(46)   Huang, Y.; Triscari, J. M.; Tseng, G. C.; Pasa-Tolic, L.; Lipton, M. S.; Smith, R. D.; Wysocki, V. H. "Statistical Characterization of the Charge State and Residue Dependence of Low-Energy CID Peptide Dissociation Patterns" *Anal. Chem.* **2005**, *77*, 5800.

(47)   Unnithan, A. G.; Myer, M. J.; Veale, C. J.; Dannell, A. S. "MS/MS of Protonated Polyproline Peptides; The Influence of N-terminal Protonation on Dissociation" *J. Am. Soc. Mass Spectrom.* **2007**, *18*, 2198.

(48)   Huang, Y.; Tseng, G. C.; Yuan, S.; Pasa-Tolic, L.; Lipton, M. S.; Smith, R. D.; Wysocki, V. H. "A Data Mining Scheme for Identifying Peptide Structural Motifs Responsible for Different MS/MS Fragmentation Intensity Patterns" *J. Proteome. Res.* **2008**, *7*, 70.

(49)   Bleiholder, C.; Suhai, S.; Harrison, A. G.; Paizs, B. "Towards Understanding the Tandem Mass Spectra of Protonated Oligopeptides. 2: The Proline Effect in Collision-induced Dissociation of Protonated Ala-Ala-Xxx-Pro-Ala (Xxx = Ala, Ser, Leu, Val, Phe, and Trp)" *J. Am. Soc. Mass Spectrom.* **2011**, *21*, 1032.

(50)   Oomens, J.; Berden, G.; Morton, T. H. "Negative Hyperconjugation versus Electronegativity: Vibrational Spectra of Free Fluorinated Alkoxide Ions in the Gas Phase" *Chem. Phys. Chem.* **2015**, *16*, 1992.

(51)   Taft, R. W.; Koppel, I. A.; Topsom, R. D.; Anvia, F. "Acidities of OH Compounds, Including Alcohols, Phenols, Carboxylic Acids, and Mineral Acids." *J. Am. Chem. Soc.* **1990**, *112*, 2047.